UNIVERSITY OF CALIFORNIA,
IRVINE

An Aza-Diels-Alder Approach to Chloroquinoline Derivatives

THESIS

submitted in partial satisfaction of the requirements
for the degree of

MASTER OF ENGINEERING

in Materials and Manufacturing Technology

by

Huiting Qin

Thesis Committee:
Professor Alon Gorodetsky, Chair
Professor Albert Fan Yee
Professor Plamen Atanassov

2020

DEDICATION

To

my parents and friends

TABLE OF CONTENTS

LIST OF FIGURES, TABLES AND SCHEMES

ACKNOWLEDGMENTS

Firstly, I would like to express my sincere gratitude to my advisor Prof. Alon Gorodetsky for the continuous support of my master's study and related research, for his patience, motivation, and immense knowledge. His guidance helped me in all the time of research and writing of this thesis. I could not have imagined having a better advisor and mentor for my master's study.

Besides my advisor, I would like to thank the rest of my thesis committee: Prof. Albert Fan Yee, Prof. Plamen Atanassov, for their insightful comments and encouragement, but also for the hard question which incented me to widen my research from various perspectives.

Also, a thank you to Dr. Anthony Burke, who introduced me to chemistry, and whose enthusiasm for the “Organic Chemistry” had a lasting effect.

Furthermore, I would like to thank my fellow lab mates in Gorodetsky’s lab: Dr. Umerani, C. Landon Mills, Ethan Peng, Erica Leung, Chengyi Xu, Atrouli Chatterjee, Preeta Pratakshya, Yujia Lu. And a thank you to Dr. Joseph W. Ziller for the X-ray data collection.

Very special gratitude goes out to Dr. Kim, who has been generously sharing his excellent experiment work and supporting my thesis. His brilliant work on chlorobenzoquinone derivatives paved the path of development for my research after a solid foundation.

Notably, this work is the basis for a paper. The authors will be: Juhwan Kim, Reina Kurakake, Huiting Qin, Mehran J. Umerani, Anthony Burke, Joseph W. Ziller, Alon A. Gorodetsky. My contribution mainly focused on the synthesis and characterization of the chloroquinoline derivatives in order to compare the alternative protocol with the established protocol for the imine synthesis. Besides that, I also compiled all of the data for benzoquinolines and polybenzoquinolines, compiled the supporting information and drafted the main text of the associated paper

ABSTRACT OF THE THESIS

An Aza- Diels- Adel Approach to Chloroquinoline Derivatives

By

Huiting Qin

Master of Engineering in MMT

University of California, Irvine, 2020

Professor Alon Gorodetsky, Irvine, Chair

Quinoline derivatives are promising materials for optoelectronic and biomedical applications. A simple and scalable aza-Diels-Alder reaction of imine, napthyl alkyne was described for the synthesis of various chloroquinoline derivatives, benzoquinolines and corresponding polybenzoquinolines. The exploitation of quinoline derivatives with different functionalities demonstrates the great potential not only for organic electronic but also for the molecular transformation for a board range of researchers.

CHAPTER 1: INTRODUCTION

Thesis overview

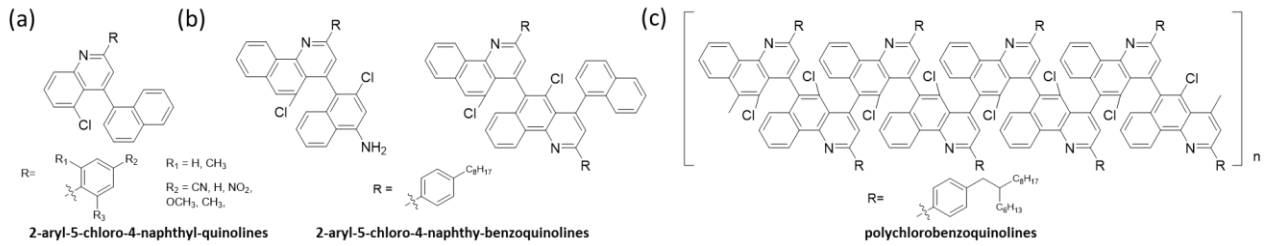

Figure 1. (a) Modular naphthyl chloroquinolines derivatives. (b) The chemical structure of napthyl chlorobenzoquinolines. (c) The chemical structure of napthyl polychlorobenzoquinolines.

Quinoline and its derivatives, including benzoquinolines, polyquinolines and polybenzoquinolines, have attracted much attention resulting from their manifold and robust optoelectrical, thermal, mechanical and biological properties [1, 3]. These attractive properties, especially those exhibited by quinoline and benzoquinoline based polymers, have demonstrated the potential to be used in the fields of optoelectronic and biomedical applications [4, 5]. However, despite their potential advantages, quinoline and benzoquinoline based polymers have suffered from both a lack of leverageable function groups and a constricted number of synthetic routes, namely the Suzuki coupling [6, 7], the Sonogashira reaction [8, 9], oxidative polymerizations [10, 11, 12], and the Friedländer synthesis [13, 14]. To overcome these limitations, our group previously reported a novel, alternate synthetic route to quinolines and benzoquinoline-based polymers via an AB-type aza-Diels-Alder (Povarov) reaction, providing facile synthetic access to a diverse array of quinoline and benzoquinoline-based polymers. [5, 16, 17] However, in our previous report, we did not have the opportunity to explore materials possessing halogen-containing

moieties. Halogen-containing quinoline derivatives can provide access to key intermediates adorned with a variety of functional groups, and to subsequently be used as substrates for a wide-ranging set of coupling reactions, including base-mediated cyclodehydrohalogenations [18], Heck coupling [19] and Suzuki-Miyaura cross-coupling reactions [20]. Therefore, in order to further increase the synthetic utility of quinoline derivatives, we consider the elucidation of the methodology to afford halogenated quinoline derivatives both necessary and worthwhile.

Herein, we report the synthesis of chloro-containing quinoline derivatives, which represent the constituent monomeric subunits of chloro-containing polybenzoquinolines. First, we demonstrate the preparation of several analogous chloro-containing quinolines featuring electron-withdrawing, electron-donating and sterically congested alkyl functionality at the 2-position of the aniline starting materials. Next, we synthesized a chloro-containing benzoquinolines and its dimer model compounds to explore the feasibility of modular syntheses of chloro-containing benzoquinolines. Finally, we apply the conditions used for the preparation of our model compound and constructed a chloro-containing polybenzoquinolines from an AB-type bifunctional monomer via an aza-Diels-Alder AB-type polymerization reaction. Our approach provides both a general and modular route to chloro-containing quinolines, benzoquinolines and polybenzoquinolines, and potentiates the synthesis of new types of halogenated quinoline derivatives.

1.1 Traditional and current applications

A. Organic electronic applications

In the 1970s, A. J. Heeger, A. G. MacDiarmid, and H. Shirakawa won a Nobel prize for their work on the exploration of conductive polymers [22]. Since then, the assumption that polymers can only be used as an insulator has been questioned. In 1990, Burroughes et al. discovered the first conjugated polymer that could be utilized in a large-area light-emitting diode; this demonstrated the possibility of light emission in the green-yellow spectrum, which contributed to later research in organic light-emitting devices (OLEDs). In 1997, Tohoku Pioneer Corporation first commercialized OLEDs, and since then OLEDs have been regarded as the next generation in flat panel displays. So far, most electronics corporations, such as Samsung, LG display, Matsushita, and Sharp, have participated in the technical competition behind OLED development. The promising stature of organic electronics like OPCs and OLEDs has, therefore, attracted significant attention. [23]

Despite the fact that scientists have diligently pursued the improvement of electroluminescent materials, increasing the efficiency and lifespan of their application is vital. The development of the rapidly growing organic electronics industry requires novel and advanced conjugated polymer semiconductors [24]. The evolution of n-typed semiconducting materials that feature outstanding electron transport properties and a range of derivatives is highly desirable as a promising material in OLEDs and organic electronic applications, quinoline is marked by its brilliant properties.

Quinoline based material has remarkable properties, such as good physical features, as well as photoelectric characteristics, their potential of application for organic electronics

has been touted for a long time. Much effort has been invested in the synthesis of quinoline materials as organic semiconductors, such as organic light emitting diodes (OLEDs), organic photovoltaics (OPVs), and organic field effect transistors [25]. It is notable that their nitrogen-doped structure can elicit even ambipolar charge transport behavior, suggesting significant potential for application in organic electronics [26]. In sum, the improvement of the rapidly growing organic electronics industry requires novel and advanced conjugated polymer semiconductors [27]. It is clear that the evolution of n-type semiconducting materials that feature outstanding electron transport properties and a range of derivatives is highly desirable.

B. Biomedical application

Owing to their widespread appearance in natural and synthetic products that exhibit remarkable biological or physical properties, quinolines and their derivatives have been branded as “privileged scaffolds”. The fact that quinoline-based materials have been widely investigated in pharmacological studies is primarily a result of their broad spectrum of biochemical activities. In the biological exploration of quinoline motifs, quinoline bases have always been regarded as “parental” compounds, with the aim being to furnish them with different functional groups for a variety of medical use. Shao et al. have recently succeeded in preparing a batch of a new and extremely promising quinoline-based material via the Friedländer heteroannulation reaction. Furthermore, Prajapati et al. have developed a new series of chloroquinoline derivatives that exhibit strong antibacterial properties, especially against several gram-positive and gram-negative microorganisms. They also touch upon research that has been conducted into the utilization of some quinoline derivatives as corrosion inhibitors, noting that some have been synthesized as novel Raf

kinase inhibitors. Many quinoline derivatives have been found to have applications as agrochemicals, while also having uses in the study of bio-organic and bio-organometallic processes; they are additionally used in manufacturing dyes, food colorants, pH indicators and other organic compounds. The broad scientific research that has been undertaken into the potential applications of quinoline-based materials is testament to their amazing properties.

1.2 Common strategies for synthesizing quinoline-based materials

As quinoline-based materials have exhibited astounding potential for use in the next generation of organic electronic, scientists have developed a variety of approaches to synthesize quinoline and benzoquinoline derivatives. More specifically, these include metal catalyzed reactions, such as the Suzuki coupling [20, 46], the Sonogashira reaction [45], and C–H Arylation [49]; oxidation reactions, such as oxidative polymerizations [10, 11, 12], and the Skraup synthesis [50]; condensation reactions, such as the Combes synthesis [51], the Friedländer synthesis [47], and the Hauser-Kraus reaction [52]; and dehydrogenation reactions [48]. The following paragraphs will illustrate the three classic routes to synthesizing quinoline-based materials.

A. Friedlander Reaction

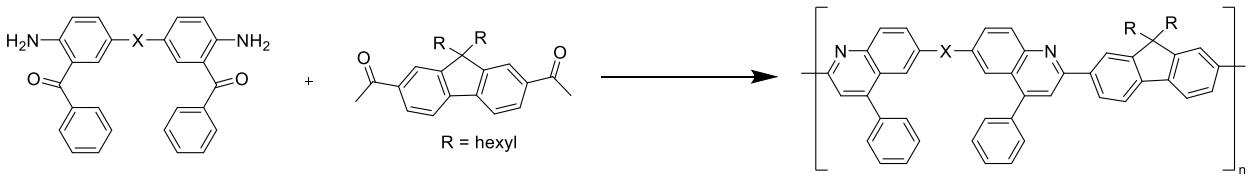

Figure 2. The synthetic route to polyquinolines via Friedlander Reaction [47].

The Friedländer synthesis combines 2-aminobenzaldehyde with ketones to produce quinoline derivatives. In 2000, Kim et al. presented the synthesis of polyquinolines via the Friedländer reaction; these particular polyquinolines possessed 9,9-di-n-hexylfluorene as its repeating units with good thermal, optical, luminescent, electrochemical, and electron-transporting properties. The synthesis of the original compounds raised a problem: substituted o-aminocarbonyl derivatives are difficult to access. Additionally, this approach does not provide sufficient access to the main chain substituents or backbone architectures, limiting the potential applications.

B. Suzuki-Miyaura Reaction

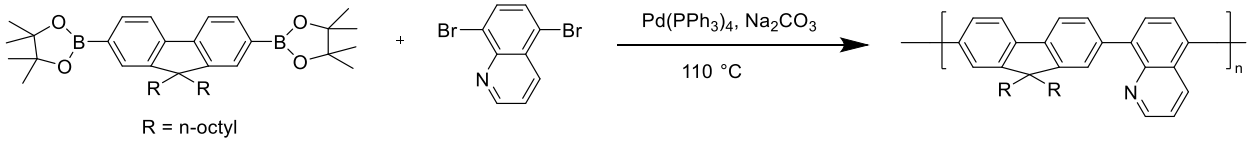

Figure 3. The synthetic route to polyquinolines via Suzuki Miyaura Reaction [46].

The Suzuki cross-coupling reaction usually utilizes a palladium catalyst and a base to couple organoboron species with a halide, resulting in a carbon-carbon single bond. In 2012, Tomar et al. developed a methodology to synthesize 5,8-linked quinoline-based copolymers via a palladium catalyzed Suzuki cross-coupling reaction. Initially, they sought to combine the distinguished electron affinity of quinoline motifs with the high quantum efficiency of fluorene. They constructed the copolymers containing 5,8-linked quinoline units with 9,9-dialkylfluorene in the main chain by reacting the model compound with dibromoquinoline in the presence of a palladium catalyst and sodium carbonate. The experiment results showed that the copolymers exhibited good thermal stability and emitted blue light well, holding potential promise for use as active materials in electronic applications.

C. The Sonogashira Reaction

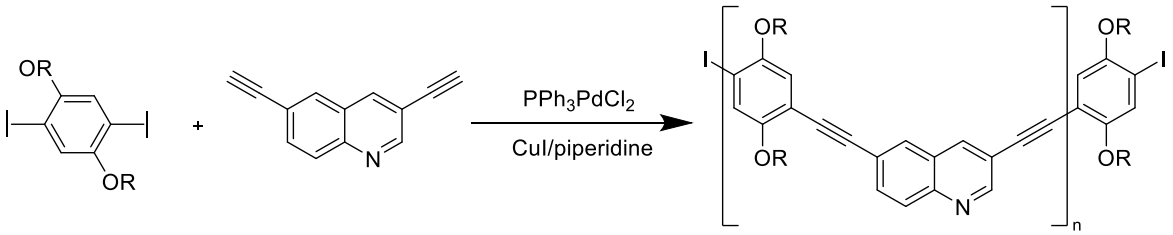

Figure 4. The synthetic route to polyquinolines via Sonogashira Reaction [45].

The Sonogashira reaction employs a palladium catalyst and a copper co-catalyst to form a carbon-carbon bond between the alkyne and an aryl or vinyl halide. In 2002, Bangcuyo et al. elucidated a synthetic route to a novel copolymer that simultaneously contained quinoline, benzene, and alkyne units via the Sonogashira reaction. The conjugated poly(aryleneethynylene)s was accessed by the reaction of 3,6-diethynylquinoline with 1,4-diiodo-2,5-bis(2-ethylhexyloxy)benzene, in the presence of a palladium catalyst and a copper co-catalyst. This polymer featured a bathochromically shifted, brilliantly yellow fluorescence when protonated; its optical properties are predominantly dependent upon the protonation and metal cation.

1.3 Our strategies for quinoline based material

For the design of our material, we sought inspiration from traditional organic electronics [30-35] and substituted benzoquinolines [36-38]. Although the potential applications of benzoquinolines materials have been explored, benzo[h]quinolines and their chloro-containing analogues have very little representation in the current literature. . Due to the near absence of the antecedent literature report, we are of the opinion that the use of quinoline derivatives as synthons has been underexplored. From this purview, we

regarded a chloro-containing quinolines and benzoquinolines, as well as their corresponding polybenzoquinolines as our envisioned construct. To achieve this product, we envisioned the stitching of polybenzoquinolines subunits from aldimine and alkyne modified monomers. Using this as our fulcrum, we anticipated leveraging our strategy of synthesizing the bifunctional monomer in order to furnish the targeted halogen -containing polybenzoquinolines.

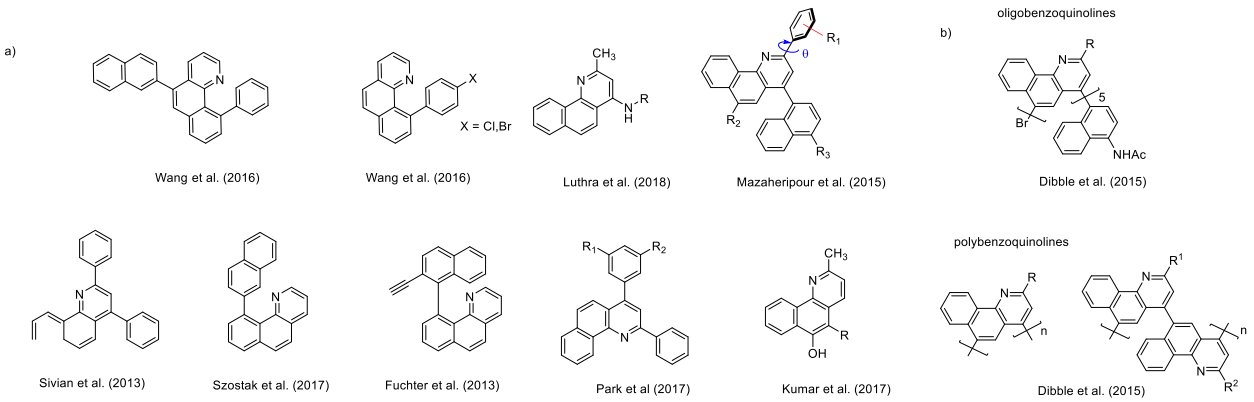

Figure 5. a) Previously reported benzoquinolines variants. b) Previously reported oligobenzoquinolines and polybenzoquinolines**.**

CHAPTER 2: Experimental Work

General information and procedures

A. Materials. All chemicals and solvents were purchased from Sigma Aldrich, Acros Organics, or Combi-Blocks; deuterated solvents for NMR spectroscopy were purchased from Cambridge Isotope Laboratories. The toluene, chloroform, and tetrahydrofuran were dried with 3 Å molecular sieves (Davison) and stored under argon. DL-α-Tocopherol methoxypolyethylene glycol succinate solution (TPGS6S-750-M [39, 40], 2% wt. solution in water) was obtained from Sigma Aldrich. The glassware was oven dried at 150 °C and cooled under argon. The reactions were performed under dry argon unless otherwise noted. During the extraction process, the brine washes and sodium bicarbonate washes consisted of biphasic extractions between the reaction mixture and a saturated aqueous solutions of sodium chloride or sodium bicarbonate.

B. Compound Purification. Flash chromatography was performed using a CombiFlash Rf200 purification system (Teledyne Isco, Inc.) according to the manufacturer's recommended protocols. When necessary, generally in the presence of acidic functional groups, the silica gel columns/cartridges were flushed with 1/9 triethylamine/hexanes (TEA/Hex) to deactivate the silica gel and then with hexanes to remove any residual triethylamine. Additional purification-relevant information and protocols are noted below as appropriate.

C. Reaction Product Characterization. All intermediates and products were characterized via ^{1}H and ^{13}C nuclear magnetic resonance (NMR) spectroscopy, as well as

high resolution mass spectrometry. The ^{1}H NMR, ^{13}C NMR were obtained on either a Bruker AVANCE400 instrument, a Bruker DRX500 instrument, a Bruker DRX500 instrument outfitted with a CryoProbe (Bruker TCI 500 MHz, 5 mm diameter tubes), or an AVANCE600 instrument. The chemical shifts were reported in ppm for both ^{1}H and ^{13}C NMR. The chemical shifts for the NMR data were referenced as follows: for samples in $CDCl_3$, the ^{1}H NMR was referenced to tetramethylsilane (TMS) at 0.00 or the residual $CHCl_3$ peak at 7.26 ppm, and the ^{13}C NMR was referenced to the residual $CHCl_3$ peak at 77.16 ppm. The data were labeled with the chemical shift, multiplicity (s = singlet, d = doublet, t = triplet, q = quartet, quint = quintet, m = multiplet, br s = broad singlet), coupling constants in Hertz, and integration values. Accurate mass measurements were obtained via electrospray ionization (ESI) high resolution mass spectrometry (HRMS) at the University of California, Irvine Mass Spectrometry Facility on a Waters LCT Premier time-of-flight instrument.

D. Polymer Characterization. The crude and purified polymers were analyzed via size exclusion chromatography with a refractive index detector (SEC-RI) by use of an Agilent Technologies 1260 Infinity Series separations module equipped with two Agilent ResiPore columns connected in series (7.5 mm x 300 mm, 3 μm particle size). The separations module was also connected to Agilent 1260 infinity dual angle light scattering, refractive index, and viscosity detectors in series. The analytical conditions were as follows: Solvent - [benzene], Flow Rate - ~ [1.0 mL/minute], Injection volume: [~ 25 – 100 μL], Sample Concentration – [~ 1.0 – 2.5 mg/mL], Temperature: [60 °C]. Molecular weights (Mn and Mw) were estimated from a calibration curve using polystyrene standards (EasiVial PS-H, Agilent).

PART 1. Modular napthyl quinoline derivatives

We began our studies by preparing a small library of napthyl quinolines via the Lewis acid-promoted aza Diels–Alder reaction (Table 1). Thus, we first synthesized aldimine precursors 1a–1f from aniline and various commercially available aldehydes via established literature protocols. [R] The reaction of 1a-1f with commercially available napthyl alkyne, in the presence of $BF_3{\cdot}OEt_2$ as the Lewis acid mediator and chloranil as the sacrificial oxidant, resulted in exclusive formation of chloroquinolines in good yield, as confirmed by ^{1}H and ^{13}C NMR spectroscopy (see Supporting Information (SI) Figures S1 to S24). Notably, we formed a series of chloroquinolines featuring varied functional motifs, including electron-withdrawing and electron-donating groups. Moreover, our current protocol accommodated sterically hindered aldimines with ortho substituents on their pendant phenyl rings (entries 6 in table 1), a new achievement for our methodology. Upon inspection, the table reveals a gradual decrease in yield for step 1, being highest for the substrates with electron withdrawing groups and declining for those with electron donating groups and final sterically hindered groups. However, in the subsequent aza-Diels-Alder step, this trend did not seem to persist, with correspond yields denoting a more complex interplay between the reactants' steric and electronics. Together, our mild and straightforward reaction condition manifested that our approach can furnish a diverse set of chlorinated quinolines from commercial reagents in facile and simple steps.

Having validated the efficiency of the condition with acetic acid and toluene, we explored the alternate protocol with PTSA and benzene for compound 1e. Moreover, the alternate protocol for the imine synthesis requires anilines to react with aldehyde on reflux, in the presence of PTSA and benzene. The protocol is straightforward and also can

afford the imine in good yield. Seeing as how the two reaction were comparable to each other and didn't result in a significant disparity in yield, we proceeded by choosing the method most convenient for the solubility of the reagents.

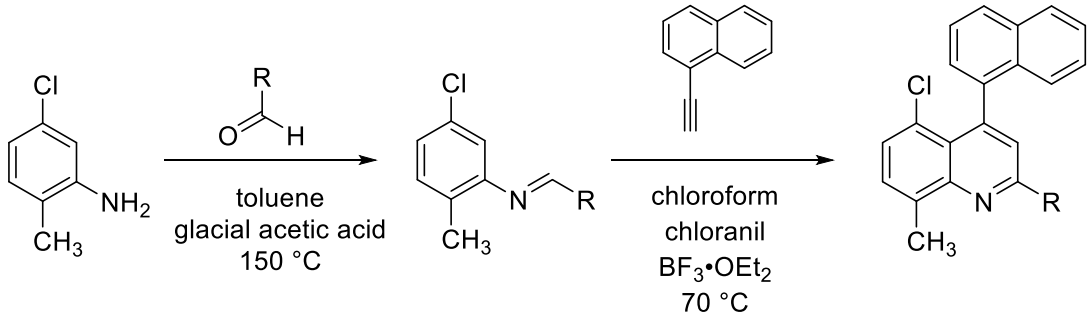

entry	compound	R	yield(%)	compound	Povarov reaction yield (%)
1	1a		95	2a	88
2	1b		91	2b	58
3	1c		92	2c	26
4	1d	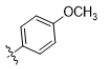	70	2d	28
5	1e		74	2e	89
6	1f	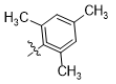	60	2f	33

Table 1. modular napthyl chloroquinoline derivative

2.1.1 Procedure

A. Representative Procedure for the Synthesis of Aldimines. Tolualdehyde (12.63 mmol), 5-chloro-2-methylanine (12.3 mmol), and acetic acid (0.35 mmol) were dissolved in toluene (30 mL) in an oven-dried round bottom flask. This flask was then fitted with a

Dean-Stark trap. The solution was then heated and allowed to proceed at reflux, with removal of water occurring via the Dean- Stark trap. After 12 hours, the mixture was cooled and the solvent was removed in vacuo to afford the crude product.

B. Representative Procedure for the Synthesis of Chloroquinolines. Molecular sieves (3 Å), chloranil (1.8 mmol), methyl imine (1.06 mmol) and naphthyl alkyne (0.914 mmol) were dissolved in chloroform (30 mL). Subsequently, $BF_3 \cdot OEt_2$ (2.7 mmol) was added to the reaction mixture and heated to 70 °C. After 24 hours, the mixture was cooled to room temperature and the solids were dissolved in 50 mL dichloromethane. Then the organic layer was washed sequentially with sodium layer bicarbonate solution (60 mL × 3), deionized water (60 mL × 3) and a brine solution (60 mL × 3). The organic layer was dried with sodium sulfate, and the solvent was removed in vacuo. The resulting residue was purified by gradient flash chromatography (1:9 ethyl acetate/hexanes to 10:90 ethyl acetate/hexanes) to afford the product.

C. Alternate Representative Procedure for the Synthesis of Aldimines. A solution of 5-chloro-2-methylaniline (100 mmol), p-tolualdehyde (110 mmol), and p-toluenesulfonic acid (5 mmol) in benzene (50 mL) was heated to reflux, while water was removed with a Dean-Stark trap. During the reaction, the solution was concentrated via removal of water through the Dean-Stark trap. The consumption of the starting materials was monitored by TLC analysis (1:9, ethyl acetate: hexanes). After the completion of the reaction, the product was precipitated in hexanes and collected by filtration to afford the product.

D. Alternate Representative Procedure for the Synthesis of Chloroquinolines. (E)-N-(5-chloro-2-methylphenyl)-1-(p-tolyl)methanimine (5 mmol) and 1-ethynylnaphthalene (6 mmol) were dissolved in toluene (25 mL) under argon. The chloranil (7.5 mmol) and

$BF_3 \cdot OEt_2$ (5.5 mmol) were added to the reaction mixture. The reaction heated to 120 °C. The reaction mixture was extracted using chloroform and sodium bicarbonate solution. The organics were dried with sodium sulfate, and the solvent was removed in vacuo. The crude product was purified by flash chromatography (1:2, dichloromethane: hexanes). After flash chromatography, the crude product was dissolved in dichloromethane then precipitated into isopropyl alcohol. The product was collected by filtration and dried under vacuum.

2.1.2 Characterization of the material

A. (E)-*N*-(5-Chloro-2-methylphenyl)-1-phenylmethanimine (1a). The product was prepared according to representative procedure A. Additional purification via recrystallization from methanol yielded the product as a burnt umber powder (13.23 g, 95 %): ^{1}H NMR (500 MHz, $CDCl_3$) δ 8.35 (s, 1H), 7.92 (dd, *J* = 7.6, 1.9 Hz, 2H), 7.55 – 7.46 (m, 3H), 7.15 (d, *J* = 8.1 z, 1H), 7.10 (dd, *J* = 8.1, 2.1 Hz, 1H), 6.94 (d, *J* = 2.1 Hz, 1H), 2.32 (s, 3H); ^{13}C NMR (126 MHz, $CDCl_3$) δ 160.5, 152.1, 136.2, 131.9, 131.8, 131.4, 130.5, 129.03, 128.95, 125.4, 118.0, 17.5 ppm; HRMS (ESI) m/z calcd. for $C_{14}H_{13}ClN$ $[M + H]^+$ 230.0737, found 230.0737.

B. (E)-4-(((5-Chloro-2-methylphenyl)imino)methyl)benzonitrile (1b). The product was prepared according to representative procedure A. Additional purification via recrystallization from methanol yielded the product as a yellow solid (8.56 g, 91 %): ^{1}H NMR (500 MHz, $CDCl_3$) δ 8.39 (s, 1H), 8.02 (d, *J* = 8.3 Hz, 2H), 7.77 (d, *J* = 8.3 Hz, 2H), 7.21 – 7.11 (m, 2H), 6.95 (d, *J* = 1.8 Hz, 1H), 2.32 (s, 3H); ^{13}C NMR (126 MHz, $CDCl_3$) δ 158.1, 151.0,

139.8, 132.7, 132.1, 131.6, 131.1, 129.3, 126.4, 118.5, 117.6, 114.8, 17.5 ppm; HRMS (ESI) m/z calcd. for $C_{15}H_{12}ClN_2$ $[M + H]^+$ 255.0689, found 255.0690.

C. (*E*)-*N*-(5-Chloro-2-methylphenyl)-1-(4-nitrophenyl)methanimine (1c). The product was prepared according to representative procedure A. Additional purification via recrystallization from methanol yielded the product as a yellow, clumpy powder (6.85 g, 92%): ^{1}H NMR (500 MHz, $CDCl_3$) δ 8.45 (s, 1H), 8.34 (d, *J* = 8.6 Hz, 2H), 8.09 (d, *J* = 8.6 Hz, 2H), 7.21 – 7.13 (m, 2H), 6.97 (d, *J* = 1.6 Hz, 1H), 2.34 (s, 3H); ^{13}C NMR (126 MHz, $CDCl_3$) δ 157.6, 150.9, 149.6, 141.4, 132.1, 131.7, 131.2, 129.7, 126.6, 124.2, 117.6, 17.5 ppm; HRMS (ESI) *m/z* calcd. for $C_{14}H_{12}ClN_2O_2$ $[M + H]^+$ 275.0587, found 275.0590.

D. (*E*)-*N*-(5-Chloro-2-methylphenyl)-1-(4-methoxyphenyl)methanimine (1d). The product was prepared according to representative procedure A. Additional purification via recrystallization from methanol yielded the product as an off-white powder (16.4 g, 70%): ^{1}H NMR (500 MHz, $CDCl_3$) δ 8.26 (s, 1H), 7.90– 7.82 (m, 2H), 7.13 (d, *J* = 8.1, 1H), 7.07 (dd, *J* = 8.1, 2.2 Hz, 1H), 7.01 – 6.97 (m, 2H), 6.91 (d, *J* = 2.2 Hz, 1H), 3.88 (s, 3H), 2.30 (s, 3H); ^{13}C NMR (126 MHz, $CDCl_3$) δ 162.5, 159.7, 152.4, 131.8, 131.3, 130.7, 130.5, 129.3, 125.0, 118.1, 114.3, 55.6, 17.5 ppm; HRMS (ESI) *m/z* calcd. for $C_{15}H_{15}ClNO$ $[M + H]^+$ 260.0842, found 260.0846.

E. (*E*)-*N*-(5-Chloro-2-methylphenyl)-1-(p-tolyl)methanimine (1e). a) The product was prepared according to representative procedure A. Additional purification via recrystallization from methanol yielded the product as an off-white powder (1.98g, 66%); b) The product was also prepared according to alternate representative procedure C. After the completion of the reaction, the product was precipitated in hexanes and collected by filtration to afford the product as an off white powder (18.16 g, 74%): ^{1}H NMR (500 MHz,

$CDCl_3$) δ 8.30 (s, 1H), 7.81 (d, *J* = 8.0 Hz, 2H), 7.29 (d, *J* = 7.9 Hz, 2H), 7.14(d, *J* = 8.1 Hz, 1H), 7.08 (dd, *J* = 8.1, 2.1 Hz, 1H), 6.92 (d, *J* = 2.0 Hz, 1H), 2.43 (s, 3H), 2.31 (s, 3H); ^{13}C NMR (125 MHz, $CDCl_3$) δ 160.3, 152.4, 142.3, 133.7, 131.9, 131.3, 130.5, 129.7, 129.0, 125.2, 118.0, 21.8, 17.5 ppm; HRMS (ESI) *m/z* calcd. for $C_{15}H_{15}ClN$ $[M + H]^+$ 244.0893, found 244.0894.

F. (*E*)-*N*-(5-Chloro-2-methylphenyl)-1-mesitylmethanimine (1f). The product was prepared according to representative procedure A. Additional purification via recrystallization from methanol yielded the product as an ivory powder (10.9 g, 60 %): ^{1}H NMR (500 MHz, $CDCl_3$) δ 8.71 (s, 1H), 7.15 (d, *J* = 8.1 Hz, 1H), 7.09 (dd, *J* = 8.1, 2.2 Hz, 1H), 6.94 (s, 2H), 6.88 (d, *J* = 2.2 Hz, 1H), 2.57 (s, 6H), 2.33 (s, 3H), 2.31 (s, 3H); ^{13}C NMR (126 MHz, $CDCl_3$) δ 160.8, 153.4, 140.4, 139.2, 132.0, 131.3, 130.3, 130.14, 130.11, 125.1, 117.9, 21.6, 21.4, 18.0 ppm; HRMS (ESI) *m/z* calcd. for $C_{17}H_{19}ClN$ $[M + H]^+$ 272.1206, found 272.1198.

G. 5-Chloro-8-methyl-4-(naphthalen-1-yl)-2-phenylquinoline (2a). The product was prepared according to representative procedure B. The product was isolated as a dark brown crystal (0.88 g, 88%). ^{1}H NMR (500 MHz, CD_2Cl_2) δ 8.31 – 8.28 (m, 2H), 8.00 – 7.91 (m, 3H), 7.61 – 7.42 (m, 7H), 7.38 – 7.27 (m, 3H), 2.96 (s, 3H); ^{13}C NMR (126 MHz, CD_2Cl_2) δ 155.1, 149.2, 147.8, 139.8, 139.3, 138.5, 133.6, 133.5, 130.3, 130.0, 129.3, 129.2, 128.6, 128.59, 128.0, 127.1, 126.7, 126.4, 126.35, 125.6, 124.9, 123.0, 19.1 ppm. HRMS (ESI) m/z calcd. for $C_{26}H_{19}ClN$ $[M + H]^+$ 380.1206, found 380.1197.

H. 4-(5-Chloro-8-methyl-4-(naphthalen-1-yl)quinolin-2-yl)benzonitrile (2b). The product was prepared according to representative procedure B. The product was isolated as a tan powder (0.40 g, 58%). ^{1}H NMR (500 MHz, CD_2Cl_2) δ 8.42 (d, *J* = 8.3 Hz, 2H), 8.01 – 7.90 (m, 3H), 7.82(d, *J* = 8.1 Hz, 2H), 7.61 – 7.56 (m, 2H), 7.49 (t, *J* = 7.5 Hz, 1H), 7.46 – 7.39

(m, 2H) 7.32 (t, *J* = 7.6 Hz, 1H), 7.25 (d, *J* = 8.5 Hz, 1H), 2.95 (s, 3H); ^{13}C NMR (126 MHz, CD_2Cl_2) 153.0, 149.2, 148.5, 143.3, 139.4, 138.7, 133.6, 133.4, 133.2, 130.4, 130.0, 128.8, 128.7, 128.5, 127.1, 126.8, 126.4, 126.3, 125.6, 125.3, 122.9, 119.3, 113.6, 110.5, 19.3 ppm; HRMS (ESI) *m/z* calcd. for $C_{27}H_{18}ClN_2$ $[M + H]^+$ 405.1158, found 405.1158.

I. 5-Chloro-8-methyl-4-(naphthalen-1-yl)-2-(4-nitrophenyl)quinoline (2c). The product was prepared according to representative procedure B. The product was isolated as a light yellow, clumpy powder (0.78 g, 26%).^{1}H NMR (500 MHz, CD_2Cl_2) δ 8.48 (d, *J* = 9.0 Hz, 2H), 8.35 (d, *J* = 9.0 Hz, 2H), 8.01 – 7.94 (m, 3 H), 7.59 (t, *J* = 7.1 Hz, 2H), 7.53 – 7.47 (m, 1H), 7.45 – 7.40 (m, 2H), 7.37 – 7.30 (m, 1H), 7.26 (d, *J* = 8.6 Hz, 1H), 2.97 (s, 3H); ^{13}C NMR (126 MHz, CD_2Cl_2) δ 152.7, 149.2, 149.1, 148.6, 145.1, 141.3, 139.4, 138.8, 133.6, 133.4, 130.5, 130.2, 128.84, 128.81, 128.71, 128.68, 127.1, 126.8, 126.5, 126.3, 125.6, 125.4, 124.5, 123.1 19.1 ppm; HRMS (ESI) *m/z* calcd. for $C_{26}H_{18}ClN_2O_2$ $[M + H]^+$ 425.1057, found 425.1055.

J. 5-Chloro-2-(4-methoxyphenyl)-8-methyl-4-(naphthalen-1-yl)quinoline (2d). The product was prepared according to representative procedure B. The product was isolated as a brown powder (0.21 g, 28%). ^{1}H NMR (500 MHz, CD_2Cl_2) δ 8.8.25 (d, *J* = 8.7 Hz, 2H), 7.95 (t, *J* = 10.1, 8.9 Hz, 1H), 7.85 (s, 1H), 7.57 (t, *J* = 8.2, 7.3 Hz, 1H), 7.53 – 7.45 (m, 2H) , 7.44 (d, *J* = 6.9 Hz, 1H), 7.36 – 7.25 (m, 1H), 7.03 (d, *J* = 8.7 Hz, 2H) 3.87 (s, 3H), 2.93 (s, 3H); ^{13}C NMR (126 MHz, CD_2Cl_2) δ 161.8, 154.8, 149.2, 147.5, 139.9, 138.2, 133.6, 133.5, 131.8, 129.9, 129.3, 128.8, 128.6, 128.52, 128.49, 127.1, 126.7, 126.4, 126.3, 125.6, 124.5, 122.5, 114.7, 55.9, 19.1ppm; HRMS (ESI) *m/z* calcd. for $C_{27}H_{21}ClNO$ $[M + H]^+$ 410.1312, found 410.1306.

K. 5-Chloro-8-methyl-4-(naphthalen-1-yl)-2-(p-tolyl)quinoline (2e). a) The product was prepared according to representative procedure B. The product was isolated as an off-white powder (1.16 g, 89%); b) The product was prepared according to the alternate representative procedure D. The product was isolated as an off white powder (1.472g, 75%): ^{1}H NMR (500 MHz, $CDCl_3$) δ 8.19 (d, *J* = 8.1 Hz, 2H), 7.94 (t, *J* = 9.2 Hz, 2H), 7.88 (s, 1H), 7.59 – 7.54 (m, 1H), 7.53 – 7.45 (m, 2H), 7.42 (d, *J* = 7.0 Hz, 1H), 7.36– 7.28 (m, 5H), 2.96 (s, 3H), 2.43 (s, 3H); ^{13}C NMR (125 MHz, $CDCl_3$) δ 154.8, 148.8, 147.3, 140.0, 139.5, 137.8, 136.2, 133.2, 133.1, 129.7, 129.5, 128.6, 128.3, 128.24, 128.21, 127.5, 126.6, 126.4, 126.1, 126.0, 125.2, 124.4, 122.4, 21.5, 18.9ppm. HRMS (ESI) *m/z* calcd. for $C_{27}H_{21}ClN$ $[M + H]^+$ 394.1363, found 394.1365.

L. 5-Chloro-2-mesityl-8-methyl-4-(naphthalen-1-yl)quinoline (2f). The product was prepared according to representative procedure B. The product was isolated as an off-white powder (1.25 g, 33 %). ^{1}H NMR (500 MHz, CD_2Cl_2) δ 7.94 (dd, *J* = 8.3, 5.1 Hz, 2H), 7.57 – 7.52 (m, 2H), 7.51 – 7.46 (m, 1H), 7.43 (dd, *J* = 7.1, 1.2 Hz, 1H), 7.39 (d, *J* = 7.6 Hz, 1H), 7.37 – 7.32 (m, 2H),7.30 (d, *J* = 8.5 Hz, 1H), 6.98 (s, 2H), 2.83 (s, 3H), 2.34 (s, 3H), 2.15 (s, 6H); ^{13}C NMR (126 MHz, CD_2Cl_2) δ 159.0, 149.3, 146.9, 139.5, 138.4, 138.3, 138.0, 136.3, 133.6, 133.4, 129.8, 129.2, 129.0, 128.7, 128.6, 128.5, 127.7, 127.1, 126.7, 126.3, 126.2, 125.6, 124.4, 21.4, 20.7, 19.2 ppm; HRMS (ESI) *m/z* calcd. for $C_{29}H_{25}ClN$ $[M + H]^+$ 422.1675, found 422.1675.

PART 2: Modular napthyl benzoquinolines

2.2.1 Procedure

After establishing our library of napthyl quinolines derivatives, we started to expand the building blocks for benzoquinolines and polymer. We first formed 2-chloro-4-nitronaphthalen-1-amine **3** in a single step from a commercially available starting material through existing literature protocol. We then reacted **3** with Isoamyl nitrite in the presence of PTSA as the catalyst, and KI as the nucleophile. We subsequently prepared **3** by using the halogenation reaction to introduce the iodinate group, producing **4**. We in turn obtained **5** by using the reductive dehalogenation reaction to reduce the nitro group to its corresponding amine. In the parallel experiment, we synthesized **6** by employing the Sonogashira reaction to form a C-C bond betwixt a protected terminal alkyne and our previously synthesized aryl lode. Subsequently, we obtained **7** by removing the TMS protecting group appended to **6** through a known literature protocol.

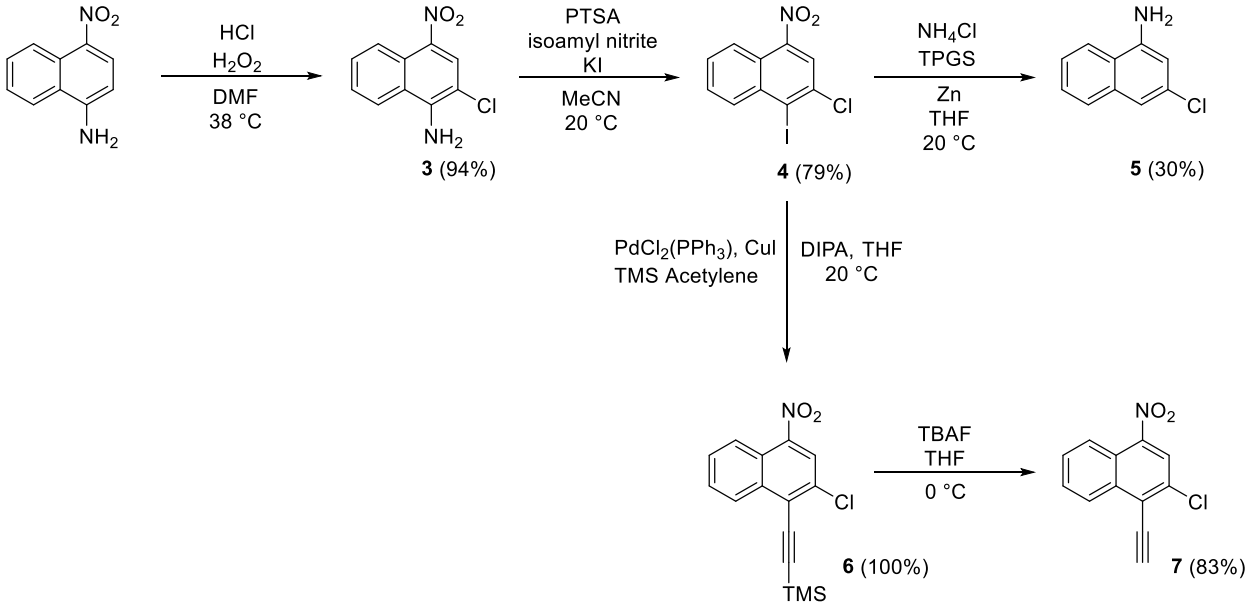

Scheme 1A. The synthetic route to the building blocks of benzoquinolines

With monomers in hand, we began to develop our route to access our desired functionalized benzoquinolines, as shown in Scheme 2. Following the preparation of **5** and **7**, we began synthesizing the aldimine precursors via the alternate protocol (see supporting information). Next, we reacted the aldimine precursor with **7**, in the presence of BF_3 OEt_2 as the Lewis acid mediator and chloranil as the oxidant, producing **8**. We then obtained **9** by preforming the reducing functionalized nitroarenes to their corresponding amine functionalities. Similarly, we in turn formed **10** by using the alternate protocol for preparing the corresponding aldimine, then reacting that aldimine with the commercially available aldehyde with BF_3 OEt_2 as the catalyst and chloranil as the oxidant. This pathway furnished the desired product **10** in moderate yields. This pathway furnished the desired product 10 in moderate yields. Overall, our approach (1) describes an efficient and accessible route and (2) obtained a functionalized benzoquinolines.

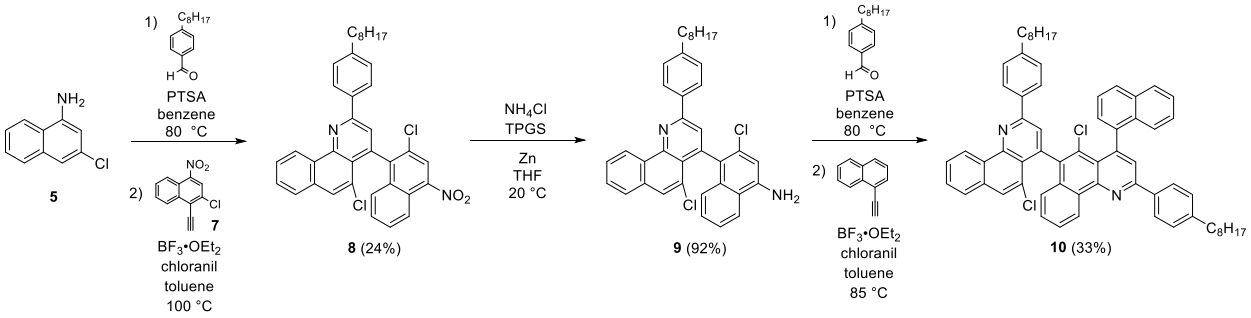

Scheme 1B. Synthetic route to the benzoquinolines.

2.2.2 Characterization of the material

M. 2-Chloro-4-nitronaphthalen-1-amine (3). 4-Nitronaphthalen-1-amine (5.64 g, 30 mmol) was dissolved in dimethylformamide (60 mL). Hydrogen chloride (2N in diethyl ether, 50 mL) was slowly added to the solution, which was stirred at room temperature. After 5 min, hydrogen peroxide (30% (w/w) in water, 3.07 mL) was slowly added to the mixture and the temperature was brought to 38 °C. After 2hr, the consumption of starting materials was monitored by TLC analysis (hexanes: ethyl acetate=2:1). The reaction mixture was cooled to room temperature and poured into sodium bicarbonate solution. The precipitate was collected by filtration and washed with water. The product was isolated as brown solid, which was used in subsequent steps without further purification (6.27 g, 94%). ^{1}H NMR (500 MHz, $CDCl_3$) δ 8.94 (d, *J* = 8.8 Hz, 1H), 8.50 (s, 1H), 7.83 (d, *J* = 8.5 Hz, 1H), 7.76 -7.71 (m, *J* = 8 Hz, 1H), 7.64 - 7.59 (m, 1H), 5.36 (s, 2H) ppm; HRMS (ESI) m/z calcd. for $C_{10}H_6ClN_2O_2$ $[M - H]^-$ 221.0118, found 221.0111.

N. 2-Chloro-1-iodo-4-nitronaphthalene (4). 2-Chloro-4-nitronaphthalen-1-amine **(3)** (3 g, 13.475 mmol) was dissolved in acetonitrile (200 mL) then PTSA (7.689 g, 40.425 mmol) was added to the solution. This solution was stirred at 0 °C for 10 min. Then isoamyl nitrite (3.157 g, 40.425 mmol) was added to the reaction solution slowly. After 10 min, potassium iodide solution (5.592 g/20 mL water) was slowly added to the reaction mixture. The reaction mixture was further stirred at 0 °C. for 20 min, then the solution was stirred for 1 hour at room temperature. The reaction mixture was poured into saturated sodium bicarbonate solution/saturated sodium thiosulfate solution. The precipitate was collected by filtration and washed with water and sodium thiosulfate solution. The crude product

was isolated as a brown solid. The crude product was purified by gradient flash chromatography (0:100 to 1:1, chloroform: hexanes) to yield a yellow powder (3.56 g, 79%). ^{1}H NMR (500 MHz, $CDCl_3$) δ 8.45 – 8.38 (m, 2H), 8.22 (s, 1H), 7.77 – 7.70 (m, 2H); ^{13}C NMR (125 MHz, $CDCl_3$) δ 137.0, 136.8, 134.5, 130.4, 129.9, 123.7, 123.4, 123.1, 111.8 ppm; HRMS (ESI) m/z calcd. for $C_{10}H_4ClINO_2$ $[M - H]^-$ 331.8975, found 331.8986.

O. 3-Chloronaphthalen-1-amine (5). 2-Chloro-1-iodo-4-nitronaphthalene **(4)** (1 g, 2.86 mmol) was dissolved in THF (11 mL) and purged with argon gas. Ammonium chloride solution (0.192 g/1 mL in water) and DL-α-Tocopherol methoxypolyethylene glycol succinate solution (TPGS-750-M, 2% wt. solution in water)[1S] (11 mL) was added to the solution. This solution was stirred at a room temperature for 5 minutes. Zinc dust (1.96 g, 28.6 mmol) was then added to the reaction solution and continuously stirred for 2 hours. The consumption of starting materials was monitored by TLC analysis (2:1 hexanes: ethyl acetate). The reaction mixture was filtered using a pad of Celite, then extracted with dichloromethane and sodium bicarbonate solution, and the organic layer was rinsed with brine. The organics were dried with sodium sulfate, and the solvent was removed *in vacuo*. The resulting product was purified by flash chromatography (Gradient - 0:100 to 3:7, ethyl acetate: hexanes) to yield a red oil (0.15 g, 30%). ^{1}H NMR (500 MHz, CD_2Cl_2) δ 7.78 (d, *J* = 8.4 Hz, 1H), 7.70 (d, *J* = 7.8 Hz, 1H), 7.52 – 7.42 (m, 2H), 7.25 (d, *J* = 1.6 Hz, 1H), 6.73 (d, *J* = 1.9 Hz, 1H), 4.34 (s, 2H); ^{13}C NMR (125 MHz, CD_2Cl_2) δ 144.5, 135.4, 132.3, 128.2, 127.6, 125.5, 122.4, 121.4, 117.4, 110.0 ppm.

P. (2-Chloro-4-nitronaphthalen-1-yl)ethynyl)trimethylsilane (6). 2-Chloro-1-iodo-4-nitronaphthalene (1 g, 2.998 mmol) was dissolved in THF/diisopropylamine (15 mL/15 mL) under argon. $PdCl_2(PPh_3)_2$ (0.104 g, 0.149 mmol) and CuI (0.057 g, 0.299 mmol) were added to the starting solution at room temperature. Trimethylsilylacetylene (0.353 g, 3.598 mmol) was then added to the reaction solution and the mixture was stirred at room temperature for 3 days. The consumption of starting materials was monitored by TLC analysis (9:1 hexanes: ethyl acetate). When all apparent starting material had been consumed, the reaction was considered complete, and the solvent was removed *in vacuo*. The product was used in subsequent steps without further purification (0.91 g, 100%). ^{1}H NMR (500 MHz, $CDCl_3$) δ 8.51 – 8.47 (m, 1H), 8.46 – 8.42 (m, 1H), 8.22 (s, 1H), 7.75 – 7.69 (m, 2H), 0.38 (s, 9H); ^{13}C NMR (125 MHz, $CDCl_3$) δ 145.9, 135.2, 133.4, 129.7, 129.2, 127.2, 126.3, 124.7, 123.6, 123.4, 111.8, 98.2, 0.2 ppm; HRMS (ESI) m/z calcd. for $C_{15}H_{14}ClNO_2SiNa$ $[M + Na]^+$ 326.0380, found 326.0367.

Q. 2-Chloro-1-ethynyl-4-nitronaphthalene (7). ((2-Chloro-4-nitronaphthalen-1-yl)ethynyl)trimethylsilane **(6)** (1.6 g, 5.23 mmol) was dissolved in THF (40 mL) and stirred at 0 °C. Tetrabutylammonium fluoride (1M in THF, 5.5 mL, 5.5 mmol) was added to the reaction mixture. After 1 hour, all starting material had been consumed, methanol (10 mL) was added to the reaction mixture to quench the reaction. The reaction mixture was extracted using chloroform and sodium bicarbonate solution. The organics were dried with sodium sulfate, and the solvent was removed *in vacuo*. The crude product was purified by flash chromatography (0:100 to 3:7 ethyl acetate: hexanes) to yield a yellow powder (1.000 g, 83%). ^{1}H NMR (500 MHz, $CDCl_3$) δ 8.52 – 8.45 (m, 2H), 8.22 (s, 1H), 7.78 – 7.71 (m, 2H),

4.04 (s, 1H); ^{13}C NMR (125 MHz, $CDCl_3$) δ 146.5, 135.4, 134.0, 129.8, 129.5, 127.0, 125.2, 124.4, 123.7, 123.3, 92.1, 77.6 ppm; HRMS (ESI) m/z calcd. for $C_{12}H_5ClNO_2$ $[M - H]^-$ 230.0009, found 230.0002.

R. 5-Chloro-4-(2-chloro-4-nitronaphthalen-1-yl)-2-(4-octylphenyl)benzo[h]quinoline (8). 3-Chloronaphthalen-1-amine (**5**) (1 g, 5.65 mmol), PTSA (0.014 g, 0.074 mmol) and 4-octylbenzaldehyde (1.244 g, 5.7 mmol) were dissolved in benzene (50 mL) and heated to reflux, while water was removed with a Dean-Stark trap. The consumption of starting materials was monitored by TLC analysis (9:1 hexanes: ethyl acetate). When all starting material had been consumed, the reaction solvent was removed *in vacuo*. The reaction mixture was dissolved in toluene (50 mL). Then chloranil (2.08 g, 8.48 mmol), 2-chloro-1-ethynyl-4-nitronaphthalene (**7**) (1.56 g, 6.78 mmol) and $BF_3{\cdot}OEt_2$ (0.962 g, 6.78 mmol) were added to the reaction mixture. The reaction was heated to 100°C for 24 hours. This reaction mixture was extracted using chloroform and sodium bicarbonate solution. The organics were dried with sodium sulfate, and the solvent was removed *in vacuo*. The crude product was purified by flash chromatography (0:100 to 1:3 chloroform: hexanes) to yield a yellow powder (0.82 g, 24%). ^{1}H NMR (500 MHz, CD_2Cl_2) δ 9.60 (d, *J* = 7.6 Hz, 1H), 8.59 (d, *J* = 8.8 Hz, 1H), 8.37 (s, 1H), 8.28 (d, *J* = 8.3 Hz, 2H), 7.88 – 7.71 (m, 6H), 7.49 (td, *J*= 6.5, 1 Hz, 1H), 7.39 (d, *J*= 8.1 Hz, 3H), 2.71 (t, *J* = 7.8 Hz, 2H), 1.67 (quint, *J*= 7.7 Hz, 2H), 1.42 – 1.21 (m, 10H), 0.88 (t, *J* = 7.0 Hz, 3H); ^{13}C NMR (125 MHz, CD_2Cl_2) δ 155.9, 148.7, 147.5, 146.2, 144.2, 143.1, 136.1, 135.3, 133.7, 131.9, 130.1, 130.0, 129.79, 129.77, 129.6, 129.2, 128.1, 127.9, 127.71, 127.69, 127.4, 126.2, 125.1, 124.0, 123.7,

122.4, 122.1,36.3, 32.4, 32.0, 30.0, 29.9, 29.8, 23.2, 14.4 ppm; HRMS (ESI) m/z calcd. for $C_{37}H_{33}Cl_2N_2O_2$ $[M + H]^+$ 607.1919, found 607.1924.

S. 3-Chloro-4-(5-chloro-2-(4-octylphenyl)benzo[h]quinolin-4-yl)naphthalen-1-amine (9). 5-Chloro-4-(2-chloro-4-nitronaphthalen-1-yl)-2-(4-octylphenyl)benzo[h]quinoline **(8)** (0.74 g, 1.222 mmol) was dissolved in THF (20 mL) and purged with argon. Ammonium chloride solution (0.82 g, 15.35 mmol/5 mL in water) and TPGS[1S]-750-M (9 mL) were added to the reaction solution. This solution was stirred at a room temperature for 5 min. Zinc dust (1.68 g, 25.7 mmol) was then added to the reaction solution and continuously stirred for 24 hours. The consumption of starting materials was monitored by TLC analysis (2:1 hexanes: ethyl acetate). The reaction mixture was filtered using a celite pad and then extracted with chloroform and sodium bicarbonate solution, and the organic layer was washed with brine. The organics were dried with sodium sulfate, and the solvent was removed *in vacuo*. The resulting product was purified by flash chromatography (0:100 to 3:7, ethyl acetate: hexanes) to yield a red oil (0.65 g, 93%). ^{1}H NMR (500 MHz, CD_2Cl_2) δ 9.58 (d, *J* = 8.7 Hz, 1H), 8.29 (d, *J* = 8.3 Hz, 2H), 7.93 (s, 1H), 7.90 (d, *J* = 8.5 Hz, 1H), 7.84 – 7.72 (m, 4H), 7.49 – 7.45 (m, 1H), 7.37 (d, *J* = 8.3 Hz, 2H), 7.32 (td, *J*= 7, 1.5 Hz, 1H), 7.17 (d, *J* = 8.5 Hz, 1H), 6.94 (s, 1H), 4.48 (s, 2H), 2.70 (t, *J* = 7.8 Hz, 2H), 1.67 (quint, *J*= 7.7 Hz, 2H), 1.45 – 1.19 (m, 10H), 0.88 (t, *J* = 7.0 Hz, 3H); ^{13}C NMR (125 MHz, CD_2Cl_2) δ 155.7, 148.6, 145.8, 145.3, 144.5, 136.5, 135.0, 133.6, 132.1, 131.7, 129.54, 129.52, 129.4, 128.5, 127.8, 127.74, 127.72, 127.3, 127.2, 126.1, 125.4, 124.1, 123.3, 122.5, 121.6, 110.1, 36.3, 32.5, 32.0, 30.0, 29.9, 29.8, 23.2, 14.4.ppm; HRMS (ESI) m/z calcd. for $C_{37}H_{34}Cl_2N_2Na$ $[M + Na]^+$ 599.1997, found 599.2004.

T. 5,5'-Dichloro-4'-(naphthalen-1-yl)-2,2'-bis(4-octylphenyl)-4,6'-bibenzo[h]quinoline (10). 3-Chloro-4-(5-chloro-2-(4-octylphenyl)benzo[h]quinolin-4-yl)naphthalen-1-amine **(9)** (1.14 g, 1.978 mmol), 4-octylbenzaldehyde (0.432 g, 1.978 mmol) and PTSA (0.005 g, 0.026 mmol) were dissolved in benzene (50 mL) and heated to reflux, while water was removed with a Dean-Stark trap. The consumption of starting materials was monitored by TLC analysis (9:1 hexanes: ethyl acetate). When all starting material has been consumed, the reaction solvent was removed *in vacuo*. Then reaction mixture was dissolved in toluene (50 mL). The chloranil (0.729 g, 2.967 mmol), 1-ethynylnaphthalene (0.361 g, 2.373 mmol) and $BF_3 \cdot OEt_2$ (0.336 g, 2.373 mmol) were added to the reaction mixture. The reaction was heated to 85 ℃ for 24 hours. This reaction mixture was extracted using chloroform and sodium bicarbonate solution. The organics were dried with sodium sulfate, and the solvent was removed *in vacuo*. The crude product was purified by flash chromatography (0:100 to 1:4 dichloromethane: hexanes) to yield a yellow powder as a mixture of atropisomers (0.60 g, 33%). ^{1}H NMR (500 MHz, CD_2Cl_2) δ 9.75 (dd, *J*= 8, 2.5 Hz, 1H), 9.54 - 9.50 (m, 1H), 8.35 (d, *J* = 7.7 Hz, 2H), 8.23 (d, *J* = 8.3 Hz, 1H), 8.19 (d, *J* = 8.3 Hz, 1H), 8.06 (d, *J* = 10.4 Hz, 1H), 7.92 - 7.66 (m, 8H), 7.59 - 7.30 (m, 10H), 7.20 (dd, , *J* = 8.2, 2.1Hz 1H), 2.70 (dt, *J* = 24.7, 7.7Hz 4H), 1.77 - 1.60 (m, 4H), 1.46 - 1.19 (m, 20H), 0.91 - 0.86 (m, 6H); ^{13}C NMR (125 MHz, CD_2Cl_2) δ 155.84, 155.81, 155.44, 155.40, 148.5, 148.3, 148.14, 148.11, 145.86, 145.83, 145.81, 145.6, 145.5, 140.4, 140.2, 138.83, 138.79, 136.54, 136.52, 136.31, 136.30, 134.5, 133.7, 133.6, 133.5, 133.3, 133.1, 131.91, 131.88, 131.6, 129.6, 129.50, 129.48, 129.36, 128.7, 128.6, 128.52, 128.50, 128.3, 127.91, 127.89, 127.80, 127.78, 127.6, 127.23, 127.22, 127.20, 126.91, 126.89, 126.85,

126.8, 126.7, 126.66, 126.40, 126.37, 126.32, 126.27, 126.08, 126.05, 125.7, 125.6, 124.1, 124.0, 123.1, 123.04, 122.82, 122.80, 122.6, 122.5, 36.34, 36.28, 32.5, 32.4, 32.00, 31.95, 30.1, 30.0, 29.92, 29.86, 29.8, 23.3, 23.2, 14.5, 14.4. ppm; HRMS (ESI) m/z calcd. for $C_{64}H_{61}Cl_2N_2$ $[M + H]^+$ 927.4212, found 927.4236.

PART 3: Polybenzoquinolines

2.3.1 Procedure

After developing our optimized methodology to synthesize benzoquinolines, we sought to feature the utility of our methodology by preparing an extended benzoquinolines macromolecule. To realize this construct, we imagined producing the polychloroquinolines through the polymerization of AB-type bifunctional monomers, which in turn were themselves generated via the Povarov reaction. To this end, we first synthesized our bifunctional AB-type monomer necessary for the polymerization reaction illustrated in Scheme 3. The design of this monomer incorporated the requisite alkyne and aldimine functional groups within a single substrate as well as an alkyl chain for enhanced solubility in aliphatic reaction mediums. By adapting the reaction conditions used to synthesize **9** (scheme 1B and 1b), we produced aryl imine **12** in 48% isolated yield. Markedly, our approach to access the monomer required modest, commercially available reagents and only a single synthetic step. We subsequently used the reaction conditions optimized for the synthesis of compounds **11** and **12** to polymerize monomer **10**. The progress of this polymerization was monitored by size exclusion chromatography with a refractive index detector (SEC-RI), as illustrated in Figure 4, and through calibration with the standard our reaction yield a weight average molecular weight (Mw) of 7,670 g/mol, a number average

molecular weight(Mn) of 7,315 g/mol, and a polydispersity index (PDI) of 1.04. . With these results we had confirmed we had indeed produced our desired polymer as well as described its attractive molecular weight and polydispersity properties.

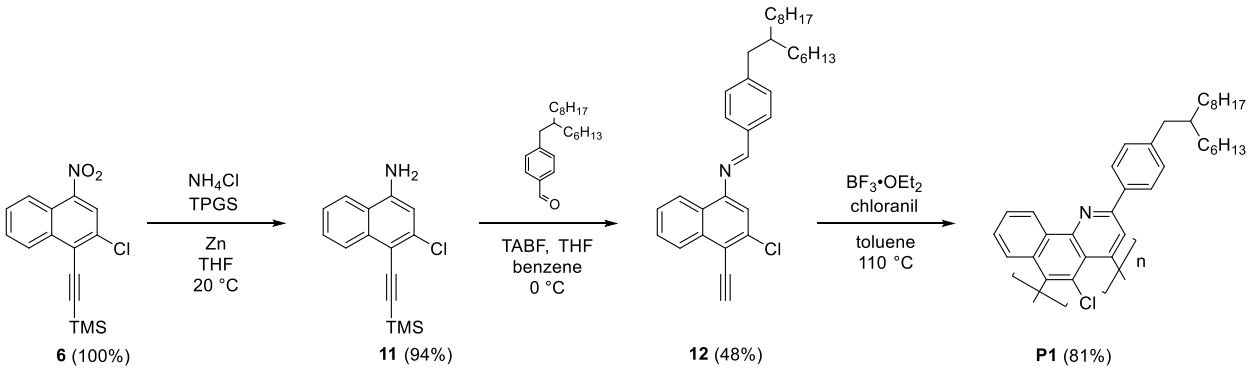

Scheme 2. Synthetic route to polybenzoquinolines

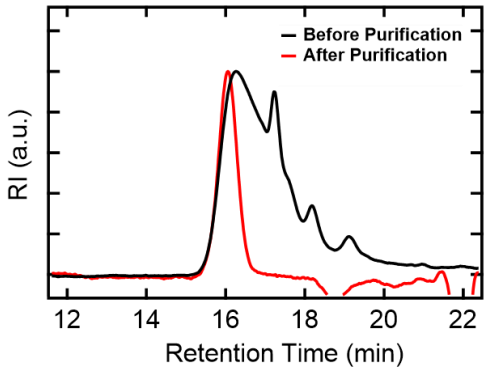

Figure 6, SEC-RI chromatograms obtained for crude polybenzoquinolines (dark solid line) and purified polybenzoquinolines (red solid line)

2.3.2 Characterization of the material

U. 3-Chloro-4-((trimethylsilyl)ethynyl)naphthalen-1-amine (11). ((2-Chloro-4-nitronaphthalen-1-yl)ethynyl)trimethylsilane **(6)** (0.91 g, 3 mmol) was dissolved in THF (15 mL) and purged with argon. TPGS-750-M[1S] (6 mL) and ammonium chloride (0.192 g,

3.6 mmol) was added to the solution. This solution was stirred at a room temperature for 5 min. Zinc dust (0.98 g, 15 mmol) was then added to the reaction solution and continuously stirred for 3 days. The consumption of starting materials was monitored by TLC analysis (2:1 hexanes: ethyl acetate). The reaction mixture was filtered through a pad of Celite and then extracted with chloroform and sodium bicarbonate solution, and the organic layer was rinsed with brine. The organics were dried with the sodium sulfate, and the solvent was removed *in vacuo*. The resulting product was purified by flash chromatography (0:100 to 1:2, ethyl acetate: hexanes) to yield a red oil (0.77 g, 94%). ^{1}H NMR (500 MHz, $CDCl_3$) δ 8.29 (d, *J* = 8.4 Hz, 1H), 7.73 (d, *J* = 8.4 Hz, 1H), 7.58 (t, *J* = 7.6 Hz, 1H), 7.47 (t, *J* = 7.6 Hz, 1H), 6.76 (s, 1H), 4.39 (s, 2H), 0.33 (s, 9H); ^{13}C NMR (125 MHz, $CDCl_3$) δ 143.8, 136.2, 135.3, 128.0, 127.2, 125.5, 121.6, 121.0, 110.1, 110.0, 102.9, 100.5, 0.4ppm; HRMS (ESI) m/z calcd. for $C_{15}H_{16}ClNSiNa$ $[M + Na]^+$ 296.0638, found 296.0648.

V. (*E*)-*N*-(3-Chloro-4-ethynylnaphthalen-1-yl)-1-(4-(2-hexyldecyl)phenyl)methanimine (12). 3-Chloro-4-((trimethylsilyl)ethynyl)naphthalen-1-amine **(11)** (1.658 g, 6.055 mmol) and 4-(2-hexyldecyl)benzaldehyde (2.01 g, 6.085 mmol) was dissolved in benzene (60 mL) and heated to reflux, while water was removed with a Dean-Stark trap. The consumption of starting materials was monitored by TLC analysis (9:1 hexanes: ethyl acetate). When all starting material has been consumed, the reaction solvent was removed *in vacuo*. Then the reaction mixture was dissolved in THF (30 mL) and stirred at 0 °C. Tetrabutylammonium fluoride (1M in THF, 6.055 mL, 6.055 mmol) was added to the reaction mixture. After 40 min, all starting material had been consumed, methanol (10 mL) was added to the reaction mixture to quench the reaction.

This reaction mixture was extracted using dichloromethane and sodium bicarbonate solution. The organics were dried with sodium sulfate, and the solvent was removed *in vacuo*. The resulting product was purified by flash chromatography using silica gel deactivated with 10 % trimethylamine in hexanes (0:100 to 3:7 ethyl acetate: hexanes) to yield a yellow powder (1.5 g, 47%). ^{1}H NMR (500 MHz, $CDCl_3$) δ 8.49 (s, 1H), 8.33 (dd, *J* = 12.8, 8.3 Hz, 2H), 7.92 (d, *J* = 8.1 Hz, 2H), 7.68 – 7.60 (m, 1H), 7.57 – 7.49 (m, 1H), 7.30 (d, *J* = 8.1 Hz, 2H), 7.06 (s, 1H), 3.82 (s, 1H), 2.62 (d, *J* = 7.1 Hz, 2H), 1.74 – 1.64 (m, 1H), 1.42 - 1.18 (m, 24H), 0.89 (t, *J* = 7.0 Hz, 6H); ^{13}C NMR (125 MHz, $CDCl_3$) δ 161.9, 151.1, 147.1, 135.9, 134.9, 133.6, 130.0, 129.3, 128.5, 127.3, 126.4, 126.0, 124.7, 115.9, 113.9, 87.5, 79.0, 40.9, 39.9, 33.4, 33.3, 32.07, 32.05, 30.1, 29.82, 29.77, 29.5, 26.70, 26.69, 22.8, 14.3. ppm; HRMS (ESI) m/z calcd. for $C_{35}H_{45}ClN$ $[M + H]^+$ 514.3241, found 514.3254.

W. Poly(5-chloro-2-(4-(2-hexyldecyl)phenyl)-4,6-dimethylbenzo[h]quinoline) (P1). (*E*)-*N*-(3-Chloro-4-ethynylnaphthalen-1-yl)-1-(4-(2-hexyldecyl)phenyl)methanimine **(12)** (1.24 g, 2.415 mmol) was dissolved in toluene and purged with argon for 5 min. The chloranil (1.187 g, 4.83 mmol) and $BF_3{\cdot}OEt_2$ (1.096 g, 7.722 mmol)) were added to the reaction mixture. The reaction mixture was stirred at 110 °C for 3 days. The mixture was then cooled to room temperature, prior to addition of phenylacetylene (1 mL, excess). The reaction mixture was further stirred at 110 °C for 24 hours and was then again cooled to room temperature. This reaction mixture was extracted using chloroform and sodium bicarbonate solution. The organics were dried with sodium sulfate, and the solvent was removed *in vacuo*. The crude product was precipitated from methanol. This crude product was further purified by size exclusion chromatography (Bio-Bead SX-1 resin) with

chloroform as the mobile phase. After evaporation of the solvent and precipitation from methanol, the brown solid was isolated by filtration (1 g, 81%). ^{1}H NMR (500 MHz, $CDCl_3$) δ 9.66 (br, 1H), 8.27 - 7.30 (br, 8H), 2.62 (br, 2H), 1.68 - 0.86 (br, 31H) ppm; SEC (vs. polystyrene standards) M_n = 7315 g mol^{-1}, M_w = 7670 g mol^{-1}, and *PDI* = 1.04.

CHAPTER 3: Summary and Conclusion

In summary, we have prepared chloro-containing quinolines, benzoquinolines and polybenzoquinolines, and our current results appear to be significant for several reasons. First, we have expanded the scope of our previously reported methodology from non-halogenated quinoline derivatives to halogenated quinoline derivatives. In addition, this current study is considered as a rare example of the synthesis of chloro-containing polybenzoquinolines via the Aza-Diels-Alde reaction. Second, our synthetic strategy accommodates various chemical functionalities at the 2 position, including electron-withdrawing, electron-donating and sterically congested alkyl functionality, and may also provide access to various chloro-containing quinoline derivatives. Third, our method uses mild conditions and simple reaction step. In particular, the benzoquinoline compounds are synthesized from napthyl amine by in-situ reaction, which is simpler than our previously reported method (two step). Finally, our findings may provide expanded opportunities for preparation of quinoline derivatives with various chemical functionalities such as peripheral substituents and a leaving group for coupling reaction, making it potentially useful for a broad range of researchers.

3.1 Future work

Graphene nanoribbons (GNRs) holds the promise for use in the next generation of semiconductor materials. Their electronic properties can be strongly influenced by the heteroatom content, while nitrogen doping could tailor the properties of GNRs to increase

their potential for use in a variety of applications [41]. Despite the fact that the researchers spent significant effort to prepare the nitrogen-doped GNRs, this highlights the problem of introducing the nitrogen into the graphene molecule at this specific location. We have developed chloro-containing polybenzoquinolines to resolve this dilemma, which also constitutes a generic class of GNR precursor. Using our aza-Diels-Alder approach, we have revealed the possibility of establishing diverse libraries of GNRs that feature varied electronic properties.

Applications

1. **Field-effect transistor (FET)**

With a high crystal quality, 2D graphene material could allow the charge carrier to travel thousands of interatomic distances without scattering. The conductivity of semiconductors is carried out by the excitation of electrons, which means that a sufficient quantity of electrons will cross over the band gap and reach the conduction band. If the semiconductor is activated by the external electric field, causing it to switch “on” and “off”, then it is called an FET [42]. However, compared with the large-scale and bilayer graphene lacking the band gap, the constrained GNRs demonstrate good semiconductor properties by inducing the band gap. Moreover, a small amount of nitrogen doping can drastically increase the conductivity of the GNRs. In order to preserve the mobility of the GNRs, it is necessary to control the nitrogen at a low doping level and explicit doping site. As they will incorporate the nitrogen at a specific site and feature different functionalities with their substitutions, our chloro-containing polybenzoquinolines will unlock the possibilities of a new generation of GNRs.

2. Lithium Ion Batteries

Due to its fascinating properties, including outstanding mechanical characteristics and high electronic performance, graphene has emerged in recent years as a particularly attractive candidate for use in lithium ion battery. However, a limitation has arisen from the low reversible capacity of pristine graphene at a high charge rate. We therefore exploited the chloro-containing polybenzoquinolines as a precursor for GNRs, which can have the potential to achieve a high reversible capacity. Earlier studies have shown that introducing nitrogen atoms into graphene can double the reversible capacity compared with untouched graphene, resulting from an enhancement of lithium ion intercalation [43].

3. Electrocatalyst for Fuel Cell Application

Generally, the Pt catalyst will be used in oxidation reactions in anodes and reduction reactions in cathodes. The scarcity of Pt catalyst, CO poisoning, and time dependent drift, however, have limited its commercial application as an electrocatalyst. Recently, nitrogen-doped GNRs have been developed as direct catalysts for fuel cell applications, or as carbon support to enhance metal catalysts. The oxygen reduction reaction (ORR) of nitrogen-doped GNRs has been the subject of much research [44]. The substitution of N atoms could introduce the unpaired electron and change the atomic charge distribution, which will determine the catalyst activation sites in oxygen reduction reactions. Nitrogen-doped GNRs will become a promising substitution for precious metal catalysts like Pt and Au, not only as a result of their commercial availability, but also due to their outstanding stability and high activity in ORR. Our approach has achieved a breakthrough in the preparation of these

nitrogen-doped GNRs, successfully synthesizing the polybenzoquinolines and realizing their nascent potential as an ORR catalyst.

BIBLIOGRAPHY

[1]. Kumar S.; Bawa S.; Gupta H. Biological activities of quinoline derivatives. Mini-Rev. Med. Chem. **2009**, 9, 1648–165410.2174/138955709791012247.

[2]. Kundal, S., Chakraborty, B., Paul, K., & Jana, U. (**2019**). Efficient two-step synthesis of structurally diverse indolo[2,3-b]quinoline derivatives. Organic & Biomolecular Chemistry, 17(9), 2321-2325.

[3]. Chung PY, e. (**2019**). Recent advances in research of natural and synthetic bioactive quinolines. - PubMed - NCBI . Retrieved 23 November 2019, from https://www.ncbi.nlm.nih.gov/pubmed/

[4]. Flores-Noria, R., Vázquez, R., Arias, E., Moggio, I., Rodríguez, M., & Ziolo, R. et al. (**2014**). Synthesis and optoelectronic properties of phenylenevinylenequinoline macromolecules. New Journal Of Chemistry, 38(3), 974.

[5]. Dibble, David & Umerani, Mehran & Mazaheripour, Amir & Park, Young & Ziller, Joseph & Gorodetsky, Alon. (**2014**). An Aza-Diels–Alder Route to Polyquinolines. Macromolecules. 48. 557–561. 10.1021/ma5020726.

[6]. Siemssen, Brent, et al. Synthesis and photophysics of new donor-acceptor copolymers based on fluorene and phenylquinolines. Molecular Crystals and Liquid Crystals 462.1 (**2006**): 159-167.

[7]. Tomar, Manisha, et al. Facile synthesis of 5, 8-linked quinoline-based copolymers. Polymer International 61.8 (**2012**): 1318-1325.

[8]. Bangcuyo, Carlito G., et al. Quinoline-containing, conjugated poly (aryleneethynylene) s: Novel metal and H+-responsive materials. Macromolecules 35.5 (**2002**): 1563-1568.

[9]. Jégou, Gwénaëlle, and Samson A. Jenekhe. Highly fluorescent poly (arylene ethynylene)s containing quinoline and 3-alkylthiophene. Macromolecules 34.23 (**2001**): 7926-7928.

[10]. Higashimura, Hideyuki, and Shiro Kobayashi. Oxidative Polymerization. Encyclopedia of Polymer Science and Technology, Feb. **2016**, pp. 1–37.

[11]. Kimyonok, Alpay & Wang, Xian-Yong & Weck, Marcus. **2006**. Electroluminescent Poly (quinoline) s and Metalloquinolates. Journal of Macromolecular Science-polymer Reviews - J MACROMOL SCI-POLYM REV. 46. 10.1080/15321790500471210

[12]. Weiqiang Fu, Lichao Dong, Jianbing Shi, Bin Tong, Zhengxu Cai, Junge Zhi, and Yuping Dong Macromolecules **2018** 51 (9), 3254-3263

[13]. Cheng, Chia-Chung, and Shou-Jen Yan. The Friedländer Synthesis of Quinolines. Organic Reactions, Aug. **1982**, pp. 37–201

[14]. Zhang, Xuejun, et al. Electroluminescence and Photophysical Properties of Polyquinolines. Macromolecules, vol. 32, no. 22, Nov. **1999**, pp. 7422–29

[15]. Umerani, M. J.; Dibble, D. J.; Wardrip, A. G.; Mazaheripour, A.; Vargas, E.; Ziller, J. W.; Gorodetsky, A. A. Synthesis of Polyquinolines Via an AA/BB-Type Aza-Diels-Alder Polymerization Reaction. J. Mater. Chem. C **2016**, 4, 4060−4066.

[16]. Dibble, David J., et al. Synthesis of Polybenzoquinolines as Precursors for Nitrogen-Doped Graphene Nanoribbons. Angewandte Chemie, vol. 127, no. 20, Mar. **2015**

[17]. Mazaheripour, Amir, et al. An Aza-Diels–Alder Approach to Crowded Benzoquinolines. Acs.Org, **2016**.

[18]. Donald L. Trepanier, Vilmars Sprancmanis, and John N. Eble. 5,6-Dihydro-4H-1,3,4-oxadiazines. V. Base-Catalyzed Cyclodehydrohalogenation of 2-(β-Chloroalkyl)carboxylic Acid Hydrazides Journal of Medicinal Chemistry **1966** 9 (5), 753-758

[19]. Singh, Radhey M., et al. Ligand Promoted and Controlled Palladium-Catalyzed Intramolecular Heck Reaction of Homoallyl Alcohols: A Facile Synthesis of Cyclopentaannulated Quinolines. Tetrahedron, vol. 68, no. 45, Nov. **2012**, pp. 9206–10.

[20]. Brad Nolt, M., et al. Controlled Derivatization of Polyhalogenated Quinolines Utilizing Selective Cross-Coupling Reactions. Tetrahedron Letters, vol. 49, no. 19, May **2008**, pp. 3137–41.

[21]. Hoeben, Freek J. M., et al. About Supramolecular Assemblies of π-Conjugated Systems. Chemical Reviews, vol. 105, no. 4, Apr. **2005**, pp. 1491–546.

[22]. Alan G. MacDiarmid, Alan J. Heeger, and Hideki Shirakawa. Science History Institute, June **2016**.

[23]. Deng, Xian-Yu. Light-Emitting Devices with Conjugated Polymers. International Journal of Molecular Sciences, vol. 12, no. 3, Mar. **2011**, pp. 1575–94.

[24]. Mitschke, Ullrich, and Peter Bäuerle. The Electroluminescence of Organic Materials. Journal of Materials Chemistry, vol. 10, no. 7, **2000**, pp. 1471–507, doi:10.1039/a908713c.

[25]. Jingquan Liu, et al. Graphene and Graphene Oxide as New Nanocarriers for Drug Delivery Applications. ResearchGate, Acta biomaterialia, 16 Aug. **2013**.

[26]. David J. Dibble., et al. Aza-Diels–Alder Approach to Diquinolineanthracene and Polydiquinolineanthracene Derivatives. Acs.Org, **2018**.

[27]. Friederich, Pascal, et al. Toward Design of Novel Materials for Organic Electronics. Advanced Materials, vol. 31, no. 26, Apr. **2019**, p. 1808256.

[28]. Prajapati, Shraddha M., et al. Recent Advances in the Synthesis of Quinolines: A Review. RSC Adv., vol. 4, no. 47, **2014**, pp. 24463–76.

[29]. Solomon, V. R., and H. Lee. Quinoline as a Privileged Scaffold in Cancer Drug Discovery. Current Medicinal Chemistry, vol. 18, no. 10, **2011**, pp. 1488–508.

[30]. Yang, Xiaolong, et al. Recent Advances of the Emitters for High Performance Deep-Blue Organic Light-Emitting Diodes. Journal of Materials Chemistry C, vol. 3, no. 5, **2015**, pp. 913–44.

[31]. Liu, Yue-Feng, et al. Recent Developments in Flexible Organic Light-Emitting Devices. Advanced Materials Technologies, vol. 4, no. 1, Oct. **2018**, p. 1800371,

[32]. National Renewable Energy Laboratory. Best Research-CellEfficiencies.https://energy.gov/eere/sunshot/downloads/research-cell-efficiency-records(accessed September **2017**).

[33]. Luo, Guoping, et al. Recent Advances in Organic Photovoltaics: Device Structure and Optical Engineering Optimization on the Nanoscale. Small, vol. 12, no. 12, Feb. **2016**, pp. 1547–71.

[34]. Dong, Huanli, et al. 25th Anniversary Article: Key Points for High-Mobility Organic Field-Effect Transistors. Advanced Materials (Deerfield Beach, Fla.), vol. 25, no. 43, **2013**, pp. 6158–83.

[35]. Choi, Dalsu, et al. Best Practices for Reporting Organic Field Effect Transistor Device Performance. Chemistry of Materials, vol. 27, no. 12, June **2015**, pp. 4167–68,

[36]. Pak, V. D., et al. Regioselective Synthesis of Benzo[g]- and Benzo[f]Quinolines by Reaction of Chalcones with Naphthalen-2-Amine. Russian Journal of Organic Chemistry, vol. 53, no. 4, Apr. **2017**, pp. 562–68.

[37]. Tarun Kumar, Vaijinath Mane, and Irishi N. N. Namboothiri. Synthesis of Aminophenanthrenes and Benzoquinolines via Hauser–Kraus Annulation of Sulfonyl Phthalide with Rauhut–Currier Adducts of Nitroalkenes. Organic Letters **2017** 19 (16), 4283-4286

[38]. Dreger, Andrij, et al. Rearrangements of N-Heterocyclic Carbenes of Pyrazole to 4-Aminoquinolines and Benzoquinolines. European Journal of Organic Chemistry, vol. 2010, no. 22, June **2010**, pp. 4296–305.

[39]. Sean M. Kelly et. al., Chemoselective Reductions of Nitroaromatics in Water at Room Temperature, Organic Letters, **2014**, 16, 98-101

[40]. Hekmatshoar, et. al., Reductive dehalogenation of arylhalides and alkylhalides with zinc in THF saturated aqueous ammonium chloride. Journal of the Chinese Chemical Society 55.3, **2008**: 616-618.

[41]. Geim, A.K. & Novoselov, K.S. The rise of graphene, Nature Materials, 6, **2007**, 183-191.

[42]. Wang, Haibo, et al. Review on Recent Progress in Nitrogen-Doped Graphene: Synthesis, Characterization, and Its Potential Applications. ACS Catalysis, vol. 2, no. 5, **2012**, pp. 781–94.

[43]. Reddy, Arava Leela Mohana, et al. Synthesis of Nitrogen-Doped Graphene Films for Lithium Battery Application. ACS Nano, vol. 4, no. 11, **2010**, pp. 6337–42.

[44]. Zhang, Lipeng, and Zhenhai Xia. Mechanisms of Oxygen Reduction Reaction on Nitrogen-Doped Graphene for Fuel Cells. The Journal of Physical Chemistry C, vol. 115, no. 22, **2011**, pp. 11170–76.

[45]. Carlito G. Bangcuyo,Mary E. Rampey-Vaughn,Lan T. Quan,S. Michael Angel,Mark D. Smith, and, and Uwe H. F. Bunz* Quinoline-Containing, Conjugated Poly(aryleneethynylene)s: Novel Metal and H+-Responsive Materials. Macromolecules, **2002** 35 (5), 1563-1568.

[46]. Tomar, Manisha, et al. Facile Synthesis of 5,8-Linked Quinoline-Based Copolymers. Polymer International, vol. 61, no. 8, Apr. **2012**, pp. 1318–25.

[47]. Jong Lae Kim,†, Jai Kyeong Kim, Hyun Nam Cho, Dong Young Kim, Chung Yup Kim, and, and Sung Il Hong*, New Polyquinoline Copolymers: Synthesis, Optical, Luminescent, and Hole-Blocking/Electron-Transporting Properties, Macromolecules **2000** 33 (16), 5880-5885.

[48]. Park, S.-R., Shin, D. H., Park, S.-M., & Suh, M. C. Benzoquinoline-based fluoranthene derivatives as electron transport materials for solution-processed red phosphorescent organic light-emitting diodes. RSC Advances, **2017**. 7(45), 28520–28526.

[49]. Jagtap, R. A., Soni, V., & Punji, B. Expeditious and Solvent-Free Nickel-Catalyzed C–H Arylation of Arenes and Indoles. ChemSusChem, **2017**. 10(10), 2242–2248.

[50]. Denmark, S. E., & Venkatraman, S. On the Mechanism of the Skraup–Doebner–Von Miller Quinoline Synthesis. The Journal of Organic Chemistry, **2006**. 71(4), 1668–1676.

[51]. Bergstrom, F. W. Heterocyclic Nitrogen Compounds. Part IIA. Hexacyclic Compounds: Pyridine, Quinoline, and Isoquinoline. Chemical Reviews, **1944**. 35(2), 77–277.

[52]. Kumar, T., Mane, V., & Namboothiri, I. N. N. Synthesis of Aminophenanthrenes and Benzoquinolines via Hauser–Kraus Annulation of Sulfonyl Phthalide with Rauhut–Currier Adducts of Nitroalkenes. Organic Letters, **2017**. 19(16), 4283–4286.

APPENDIX: Compiled ^{1}H NMR and ^{13}C NMR Spectroscopy Data

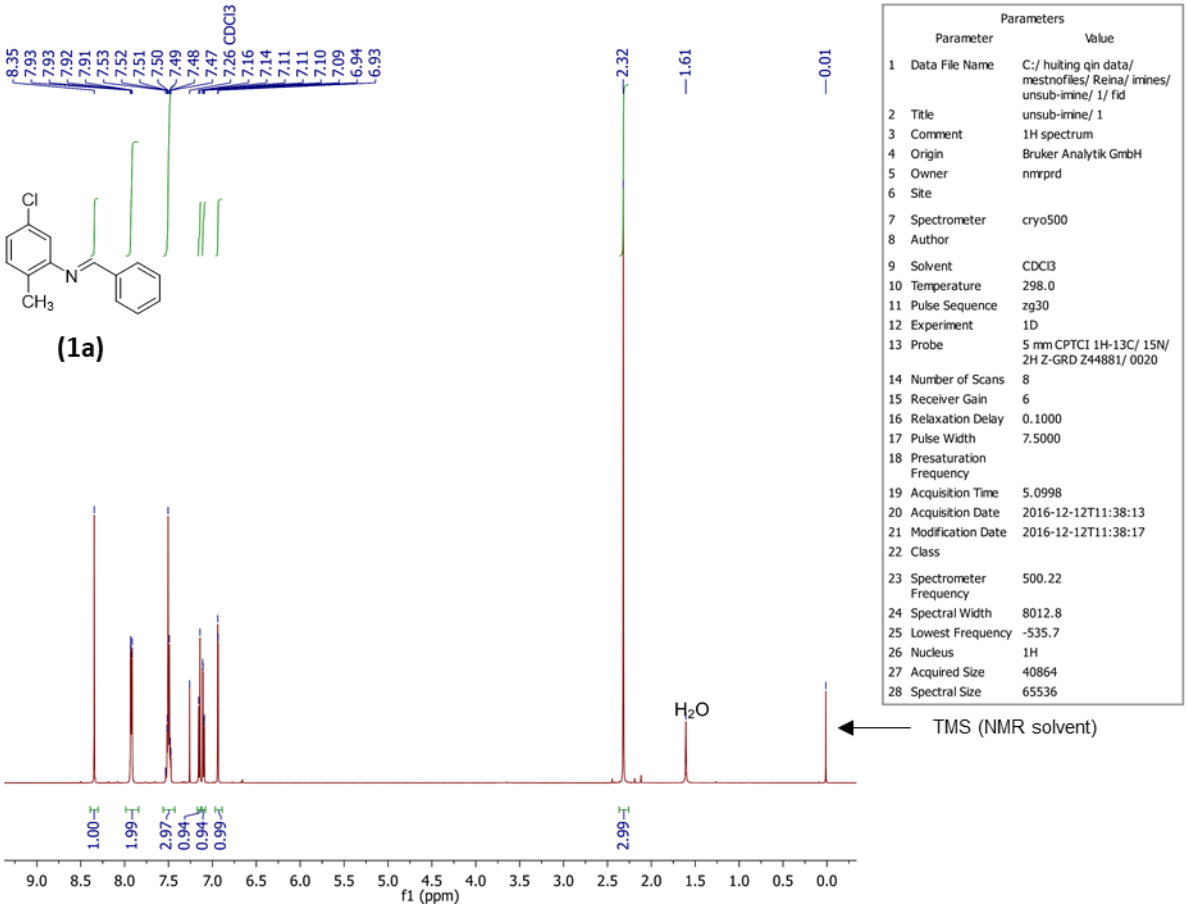

Parameters

	Parameter	Value
1	Data File Name	C:/ huiting qin data/ mestnofiles/ Reina/ imines/ unsub-imine/ 1/ fid
2	Title	unsub-imine/ 1
3	Comment	1H spectrum
4	Origin	Bruker Analytik GmbH
5	Owner	nmrprd
6	Site	
7	Spectrometer	cryo500
8	Author	
9	Solvent	CDCl3
10	Temperature	298.0
11	Pulse Sequence	zg30
12	Experiment	1D
13	Probe	5 mm CPTCI 1H-13C/ 15N/ 2H Z-GRD Z44881/ 0020
14	Number of Scans	8
15	Receiver Gain	6
16	Relaxation Delay	0.1000
17	Pulse Width	7.5000
18	Presaturation Frequency	
19	Acquisition Time	5.0998
20	Acquisition Date	2016-12-12T11:38:13
21	Modification Date	2016-12-12T11:38:17
22	Class	
23	Spectrometer Frequency	500.22
24	Spectral Width	8012.8
25	Lowest Frequency	-535.7
26	Nucleus	1H
27	Acquired Size	40864
28	Spectral Size	65536

Figure S1. The ^{1}H NMR spectrum obtained for **1a.**

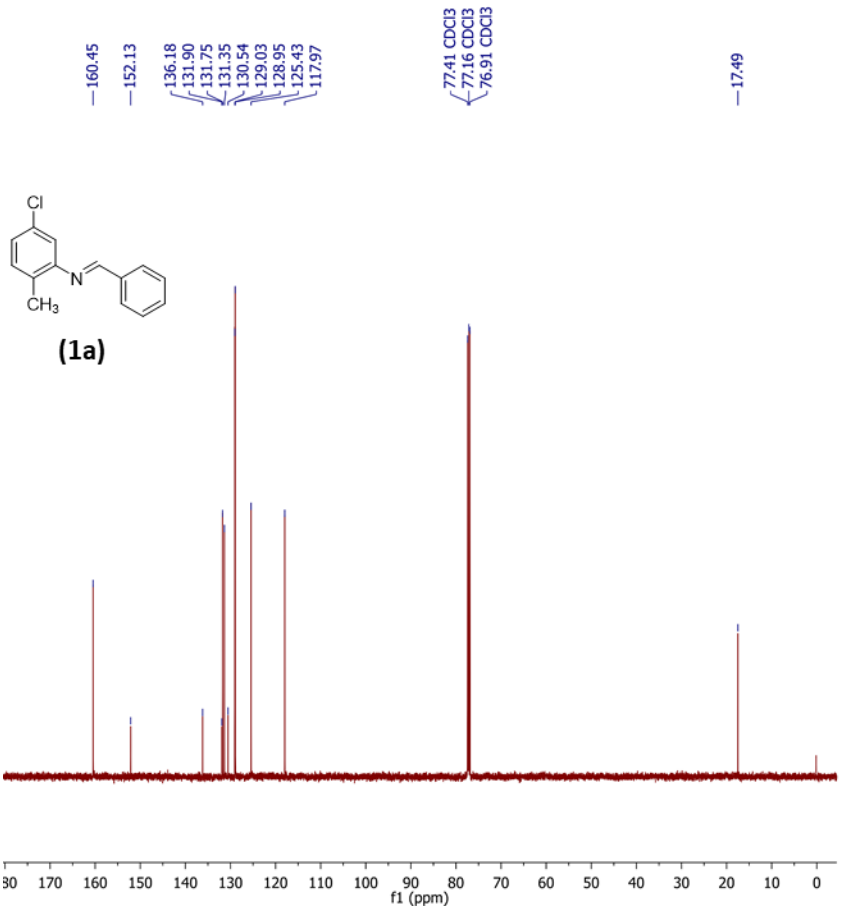

Parameters		
	Parameter	Value
1	Data File Name	C:/ huiting qin data/ mestnofiles/ Reina/ imines/ unsub-imine/ 101/ fid
2	Title	unsub-imine/ 101
3	Comment	Z-restored spin-echo 13C spectrum with 1H decoupling
4	Origin	UXNMR, Bruker Analytische Messtechnik GmbH
5	Owner	guest
6	Site	
7	Spectrometer	cryo500
8	Author	
9	Solvent	CDCl3
10	Temperature	298.0
11	Pulse Sequence	SpinEchopg30gp.prd
12	Experiment	1D
13	Probe	5 mm CPTCI 1H-13C/ 15N/ 2H Z-GRD Z44881/ 0020
14	Number of Scans	536
15	Receiver Gain	7298
16	Relaxation Delay	0.2500
17	Pulse Width	16.5500
18	Presaturation Frequency	
19	Acquisition Time	1.0813
20	Acquisition Date	2016-12-12T11:46:57
21	Modification Date	2016-12-12T11:57:52
22	Class	
23	Spectrometer Frequency	125.79
24	Spectral Width	30303.0
25	Lowest Frequency	-1315.7
26	Nucleus	13C
27	Acquired Size	32768
28	Spectral Size	65536

Figure S2. The ^{13}C NMR spectrum obtained for **1a.**

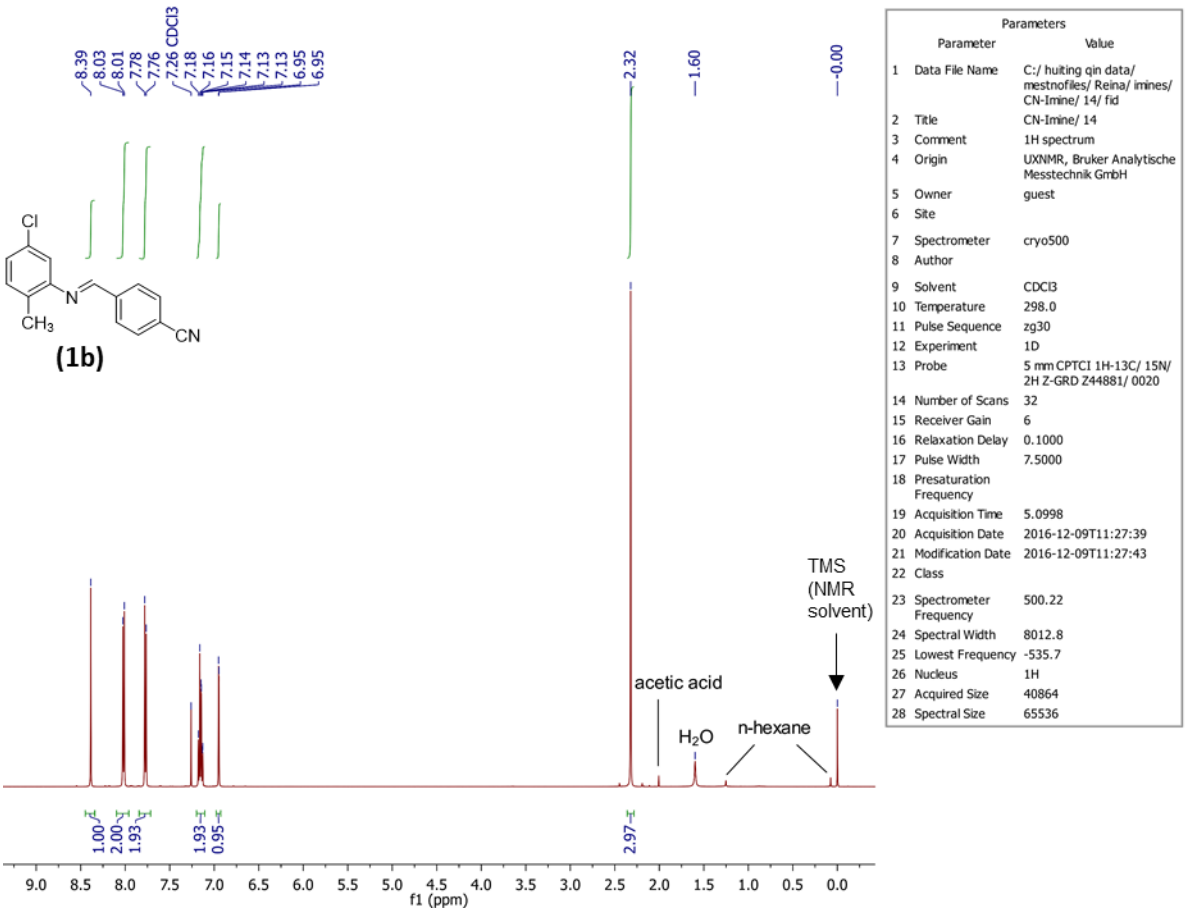

Parameters

	Parameter	Value
1	Data File Name	C:/ huiting qin data/ mestnofiles/ Reina/ imines/ CN-Imine/ 14/ fid
2	Title	CN-Imine/ 14
3	Comment	1H spectrum
4	Origin	UXNMR, Bruker Analytische Messtechnik GmbH
5	Owner	guest
6	Site	
7	Spectrometer	cryo500
8	Author	
9	Solvent	CDCl3
10	Temperature	298.0
11	Pulse Sequence	zg30
12	Experiment	1D
13	Probe	5 mm CPTCI 1H-13C/ 15N/ 2H Z-GRD Z44881/ 0020
14	Number of Scans	32
15	Receiver Gain	6
16	Relaxation Delay	0.1000
17	Pulse Width	7.5000
18	Presaturation Frequency	
19	Acquisition Time	5.0998
20	Acquisition Date	2016-12-09T11:27:39
21	Modification Date	2016-12-09T11:27:43
22	Class	
23	Spectrometer Frequency	500.22
24	Spectral Width	8012.8
25	Lowest Frequency	-535.7
26	Nucleus	1H
27	Acquired Size	40864
28	Spectral Size	65536

Figure S3. The ^{1}H NMR spectrum obtained for **1b.**

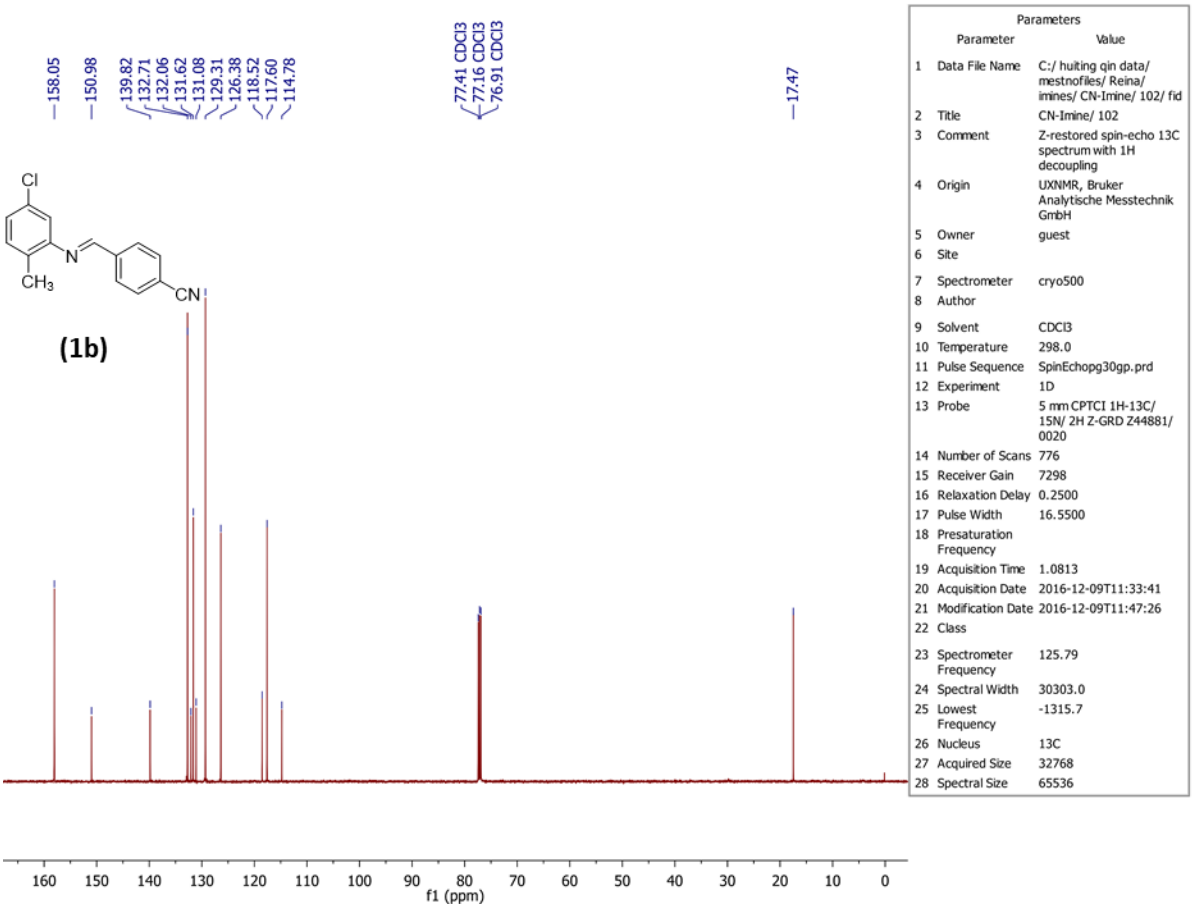

Parameters

	Parameter	Value
1	Data File Name	C:/ huiting qin data/ mestnofiles/ Reina/ imines/ CN-Imine/ 102/ fid
2	Title	CN-Imine/ 102
3	Comment	Z-restored spin-echo 13C spectrum with 1H decoupling
4	Origin	UXNMR, Bruker Analytische Messtechnik GmbH
5	Owner	guest
6	Site	
7	Spectrometer	cryo500
8	Author	
9	Solvent	CDCl3
10	Temperature	298.0
11	Pulse Sequence	SpinEchopg30gp.prd
12	Experiment	1D
13	Probe	5 mm CPTCI 1H-13C/ 15N/ 2H Z-GRD Z44881/ 0020
14	Number of Scans	776
15	Receiver Gain	7298
16	Relaxation Delay	0.2500
17	Pulse Width	16.5500
18	Presaturation Frequency	
19	Acquisition Time	1.0813
20	Acquisition Date	2016-12-09T11:33:41
21	Modification Date	2016-12-09T11:47:26
22	Class	
23	Spectrometer Frequency	125.79
24	Spectral Width	30303.0
25	Lowest Frequency	-1315.7
26	Nucleus	13C
27	Acquired Size	32768
28	Spectral Size	65536

Figure S4. The ^{13}C NMR spectrum obtained for **1b.**

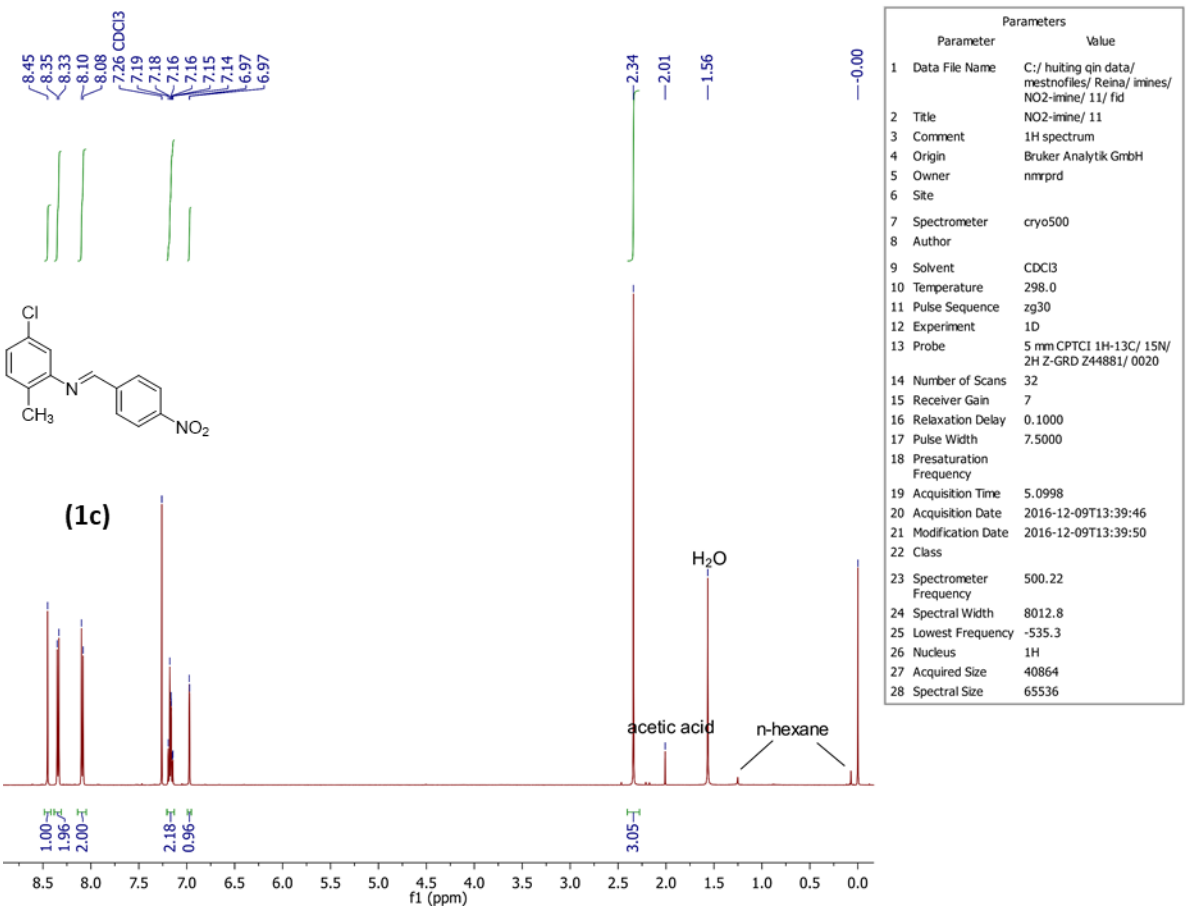

Parameters		
	Parameter	Value
1	Data File Name	C:/ huiting qin data/ mestnofiles/ Reina/ imines/ NO2-imine/ 11/ fid
2	Title	NO2-imine/ 11
3	Comment	1H spectrum
4	Origin	Bruker Analytik GmbH
5	Owner	nmrprd
6	Site	
7	Spectrometer	cryo500
8	Author	
9	Solvent	CDCl3
10	Temperature	298.0
11	Pulse Sequence	zg30
12	Experiment	1D
13	Probe	5 mm CPTCI 1H-13C/ 15N/ 2H Z-GRD Z44881/ 0020
14	Number of Scans	32
15	Receiver Gain	7
16	Relaxation Delay	0.1000
17	Pulse Width	7.5000
18	Presaturation Frequency	
19	Acquisition Time	5.0998
20	Acquisition Date	2016-12-09T13:39:46
21	Modification Date	2016-12-09T13:39:50
22	Class	
23	Spectrometer Frequency	500.22
24	Spectral Width	8012.8
25	Lowest Frequency	-535.3
26	Nucleus	1H
27	Acquired Size	40864
28	Spectral Size	65536

Figure S5. The ^{1}H NMR spectrum obtained for **1c.**

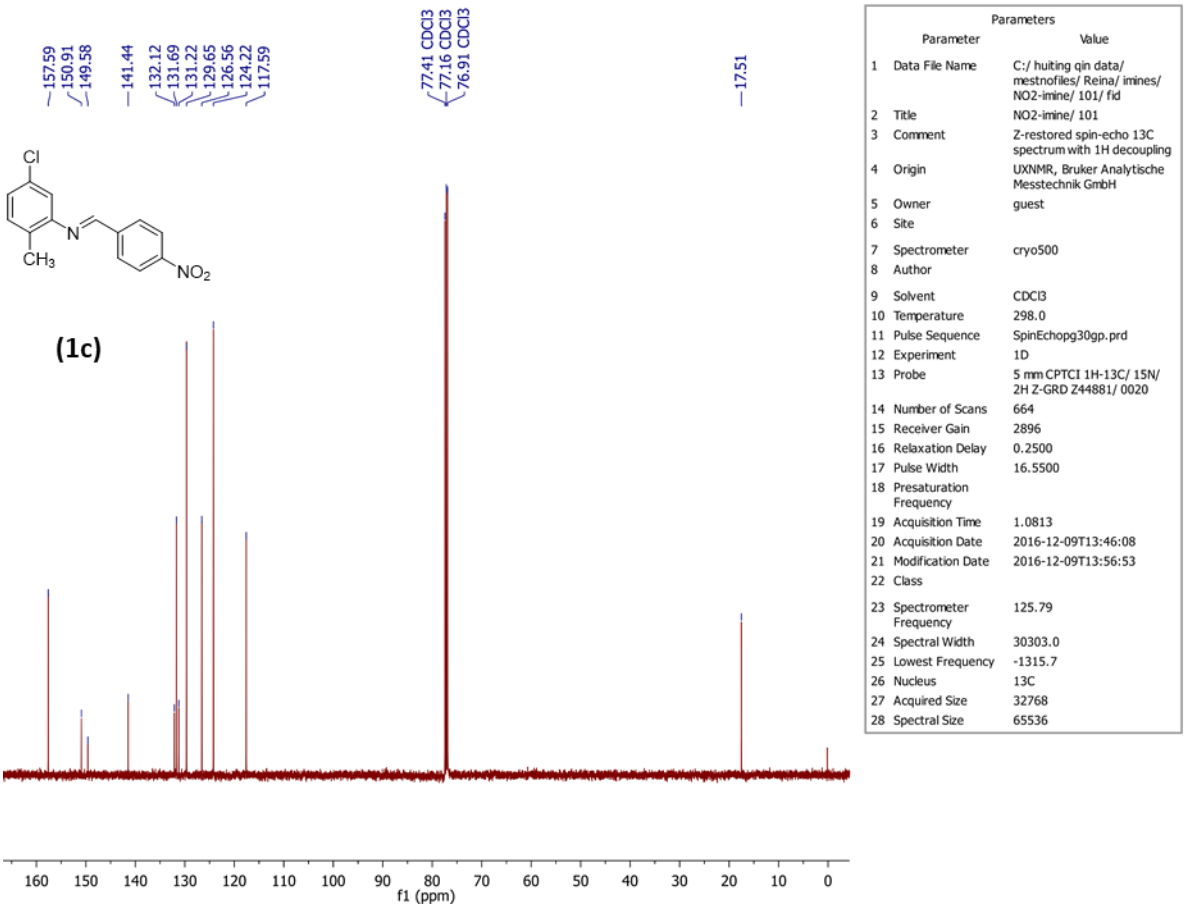

Parameters

	Parameter	Value
1	Data File Name	C:/ huiting qin data/ mestnofiles/ Reina/ imines/ NO2-imine/ 101/ fid
2	Title	NO2-imine/ 101
3	Comment	Z-restored spin-echo 13C spectrum with 1H decoupling
4	Origin	UXNMR, Bruker Analytische Messtechnik GmbH
5	Owner	guest
6	Site	
7	Spectrometer	cryo500
8	Author	
9	Solvent	CDCl3
10	Temperature	298.0
11	Pulse Sequence	SpinEchopg30gp.prd
12	Experiment	1D
13	Probe	5 mm CPTCI 1H-13C/ 15N/ 2H Z-GRD Z44881/ 0020
14	Number of Scans	664
15	Receiver Gain	2896
16	Relaxation Delay	0.2500
17	Pulse Width	16.5500
18	Presaturation Frequency	
19	Acquisition Time	1.0813
20	Acquisition Date	2016-12-09T13:46:08
21	Modification Date	2016-12-09T13:56:53
22	Class	
23	Spectrometer Frequency	125.79
24	Spectral Width	30303.0
25	Lowest Frequency	-1315.7
26	Nucleus	13C
27	Acquired Size	32768
28	Spectral Size	65536

Figure S6. The ^{13}C NMR spectrum obtained for **1c.**

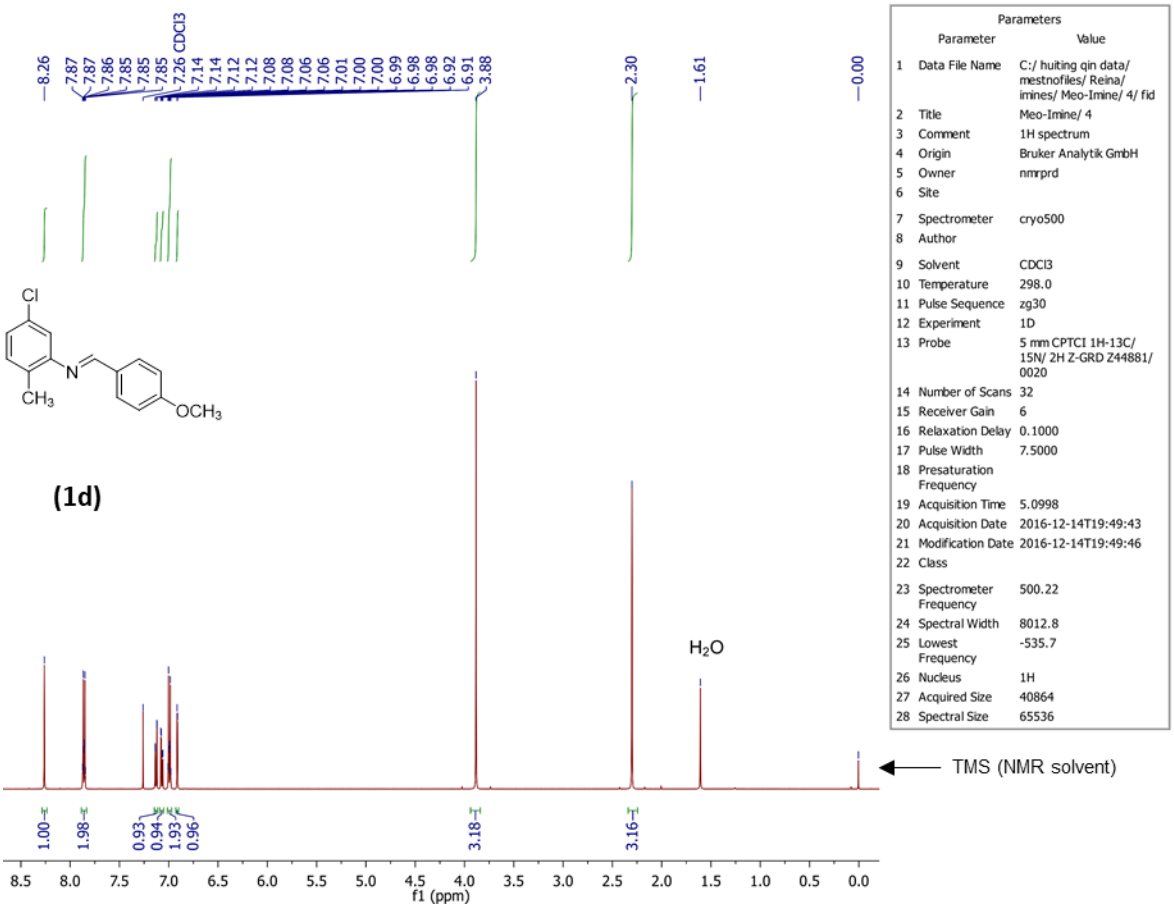

Parameters		
	Parameter	Value
1	Data File Name	C:/ huiting qin data/ mestnofiles/ Reina/ imines/ Meo-Imine/ 4/ fid
2	Title	Meo-Imine/ 4
3	Comment	1H spectrum
4	Origin	Bruker Analytik GmbH
5	Owner	nmrprd
6	Site	
7	Spectrometer	cryo500
8	Author	
9	Solvent	CDCl3
10	Temperature	298.0
11	Pulse Sequence	zg30
12	Experiment	1D
13	Probe	5 mm CPTCI 1H-13C/ 15N/ 2H Z-GRD Z44881/ 0020
14	Number of Scans	32
15	Receiver Gain	6
16	Relaxation Delay	0.1000
17	Pulse Width	7.5000
18	Presaturation Frequency	
19	Acquisition Time	5.0998
20	Acquisition Date	2016-12-14T19:49:43
21	Modification Date	2016-12-14T19:49:46
22	Class	
23	Spectrometer Frequency	500.22
24	Spectral Width	8012.8
25	Lowest Frequency	-535.7
26	Nucleus	1H
27	Acquired Size	40864
28	Spectral Size	65536

Figure S7. The ^{1}H NMR spectrum obtained for **1d.**

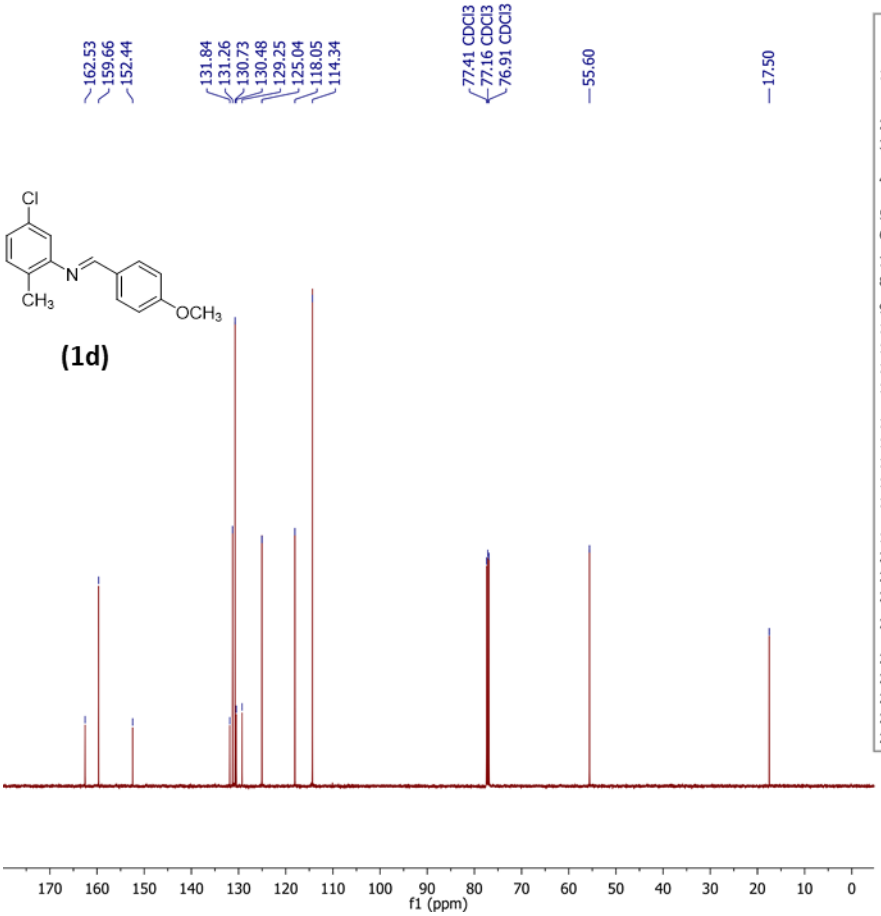

Parameters		
	Parameter	Value
1	Data File Name	C:/ huiting qin data/ mestnofiles/ Reina/ imines/ Meo-Imine/ 101/ fid
2	Title	Meo-Imine/ 101
3	Comment	Z-restored spin-echo 13C spectrum with 1H decoupling
4	Origin	UXNMR, Bruker Analytische Messtechnik GmbH
5	Owner	guest
6	Site	
7	Spectrometer	cryo500
8	Author	
9	Solvent	CDCl3
10	Temperature	298.0
11	Pulse Sequence	SpinEchopg30gp.prd
12	Experiment	1D
13	Probe	5 mm CPTCI 1H-13C/ 15N/ 2H Z-GRD Z44881/ 0020
14	Number of Scans	728
15	Receiver Gain	9195
16	Relaxation Delay	0.2500
17	Pulse Width	16.5500
18	Presaturation Frequency	
19	Acquisition Time	1.0813
20	Acquisition Date	2016-12-14T19:52:57
21	Modification Date	2016-12-14T20:08:39
22	Class	
23	Spectrometer Frequency	125.79
24	Spectral Width	30303.0
25	Lowest Frequency	-1315.7
26	Nucleus	13C
27	Acquired Size	32768
28	Spectral Size	65536

Figure S8. The ^{13}C NMR spectrum obtained for **1d.**

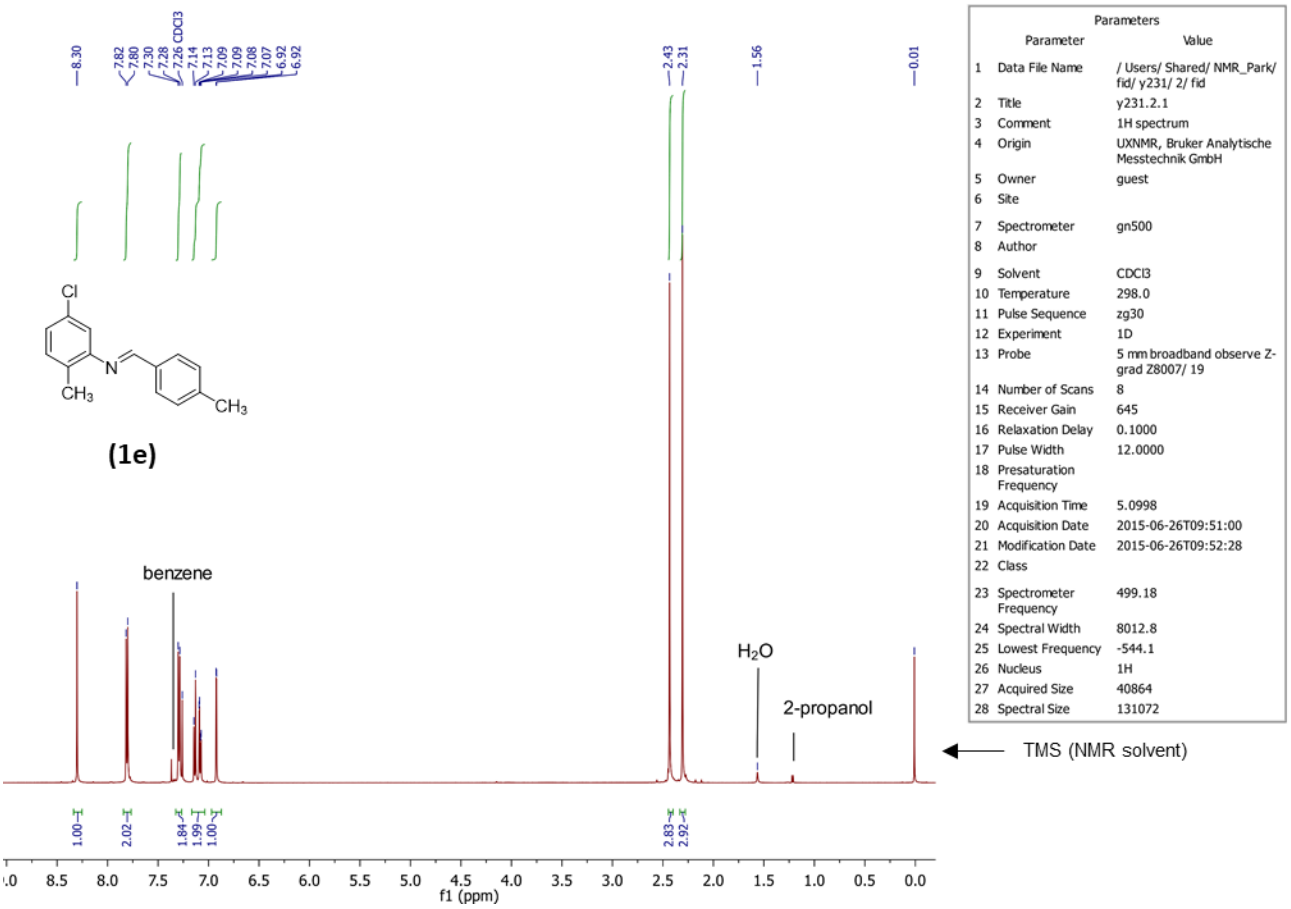

Parameters		
	Parameter	Value
1	Data File Name	/ Users/ Shared/ NMR_Park/ fid/ y231/ 2/ fid
2	Title	y231.2.1
3	Comment	1H spectrum
4	Origin	UXNMR, Bruker Analytische Messtechnik GmbH
5	Owner	guest
6	Site	
7	Spectrometer	gn500
8	Author	
9	Solvent	CDCl3
10	Temperature	298.0
11	Pulse Sequence	zg30
12	Experiment	1D
13	Probe	5 mm broadband observe Z-grad Z8007/ 19
14	Number of Scans	8
15	Receiver Gain	645
16	Relaxation Delay	0.1000
17	Pulse Width	12.0000
18	Presaturation Frequency	
19	Acquisition Time	5.0998
20	Acquisition Date	2015-06-26T09:51:00
21	Modification Date	2015-06-26T09:52:28
22	Class	
23	Spectrometer Frequency	499.18
24	Spectral Width	8012.8
25	Lowest Frequency	-544.1
26	Nucleus	1H
27	Acquired Size	40864
28	Spectral Size	131072

Figure S9. The ^{1}H NMR spectrum obtained for **1e.**

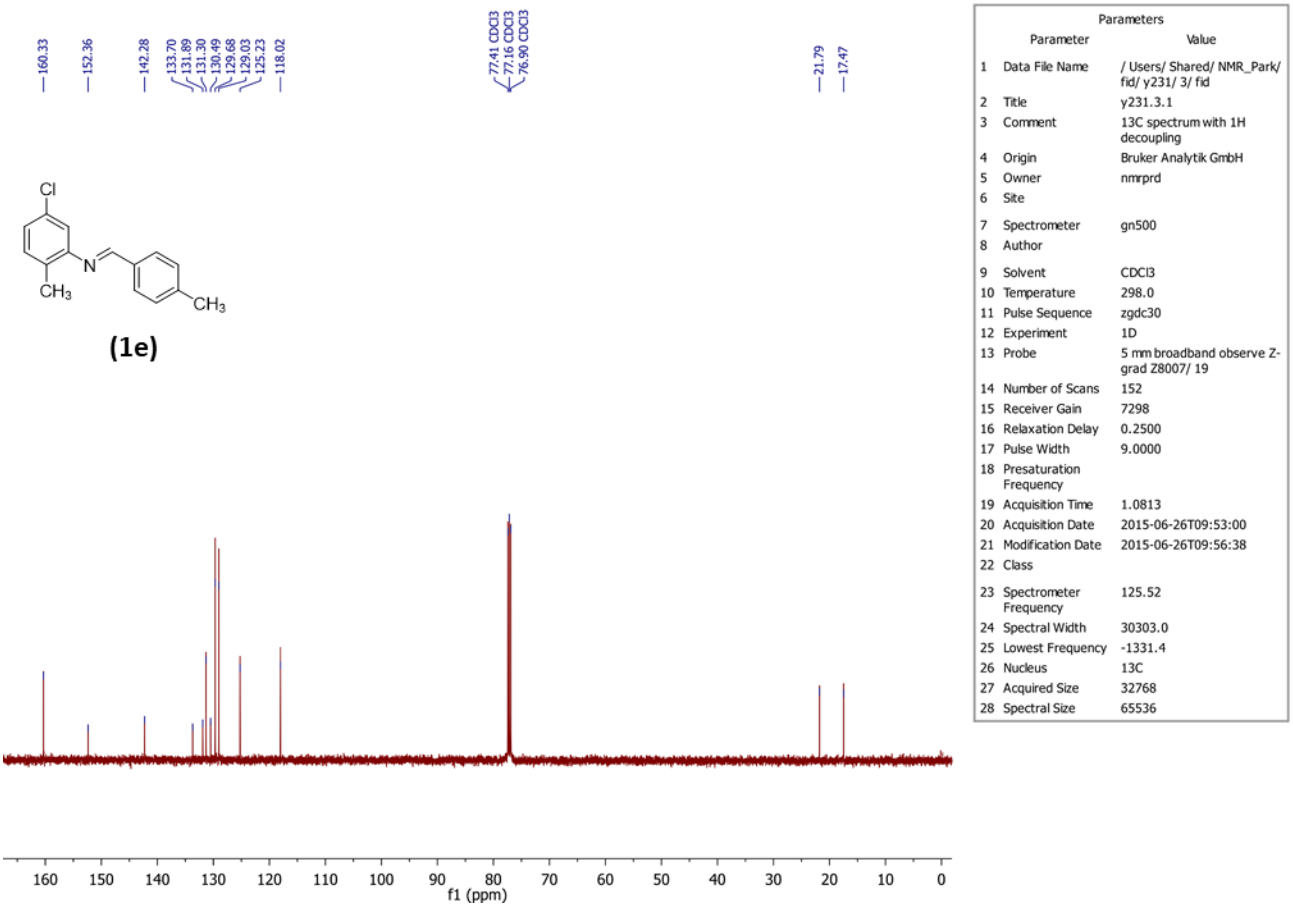

Parameters

	Parameter	Value
1	Data File Name	/ Users/ Shared/ NMR_Park/ fid/ y231/ 3/ fid
2	Title	y231.3.1
3	Comment	13C spectrum with 1H decoupling
4	Origin	Bruker Analytik GmbH
5	Owner	nmrprd
6	Site	
7	Spectrometer	gn500
8	Author	
9	Solvent	CDCl3
10	Temperature	298.0
11	Pulse Sequence	zgdc30
12	Experiment	1D
13	Probe	5 mm broadband observe Z-grad Z8007/ 19
14	Number of Scans	152
15	Receiver Gain	7298
16	Relaxation Delay	0.2500
17	Pulse Width	9.0000
18	Presaturation Frequency	
19	Acquisition Time	1.0813
20	Acquisition Date	2015-06-26T09:53:00
21	Modification Date	2015-06-26T09:56:38
22	Class	
23	Spectrometer Frequency	125.52
24	Spectral Width	30303.0
25	Lowest Frequency	-1331.4
26	Nucleus	13C
27	Acquired Size	32768
28	Spectral Size	65536

Figure S10. The ^{13}C NMR spectrum obtained for **1e.**

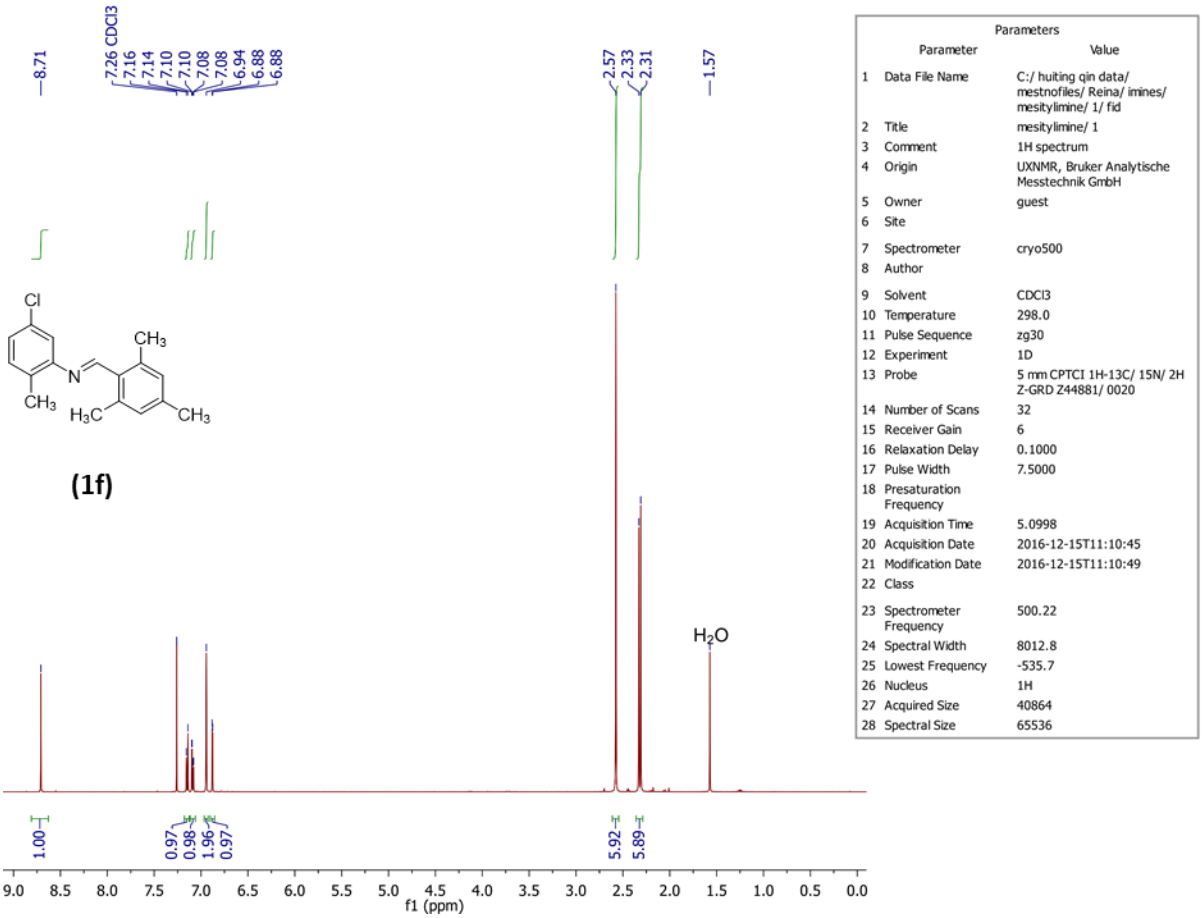

Parameters

	Parameter	Value
1	Data File Name	C:/ huiting qin data/ mestnofiles/ Reina/ imines/ mesitylimine/ 1/ fid
2	Title	mesitylimine/ 1
3	Comment	1H spectrum
4	Origin	UXNMR, Bruker Analytische Messtechnik GmbH
5	Owner	guest
6	Site	
7	Spectrometer	cryo500
8	Author	
9	Solvent	CDCl3
10	Temperature	298.0
11	Pulse Sequence	zg30
12	Experiment	1D
13	Probe	5 mm CPTCI 1H-13C/ 15N/ 2H Z-GRD Z44881/ 0020
14	Number of Scans	32
15	Receiver Gain	6
16	Relaxation Delay	0.1000
17	Pulse Width	7.5000
18	Presaturation Frequency	
19	Acquisition Time	5.0998
20	Acquisition Date	2016-12-15T11:10:45
21	Modification Date	2016-12-15T11:10:49
22	Class	
23	Spectrometer Frequency	500.22
24	Spectral Width	8012.8
25	Lowest Frequency	-535.7
26	Nucleus	1H
27	Acquired Size	40864
28	Spectral Size	65536

Figure S11. The ^{1}H NMR spectrum obtained for **1f.**

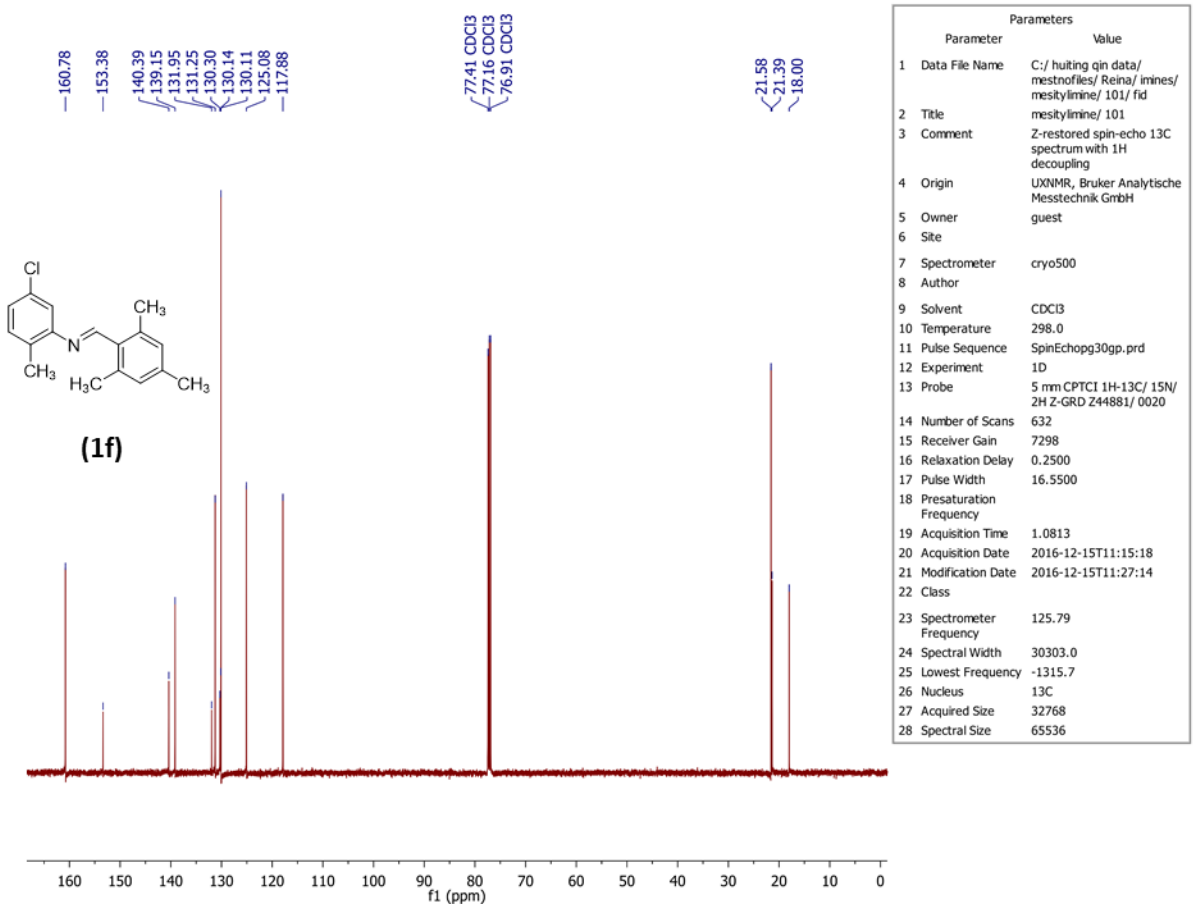

Figure S12. The ^{13}C NMR spectrum obtained for **1f.**

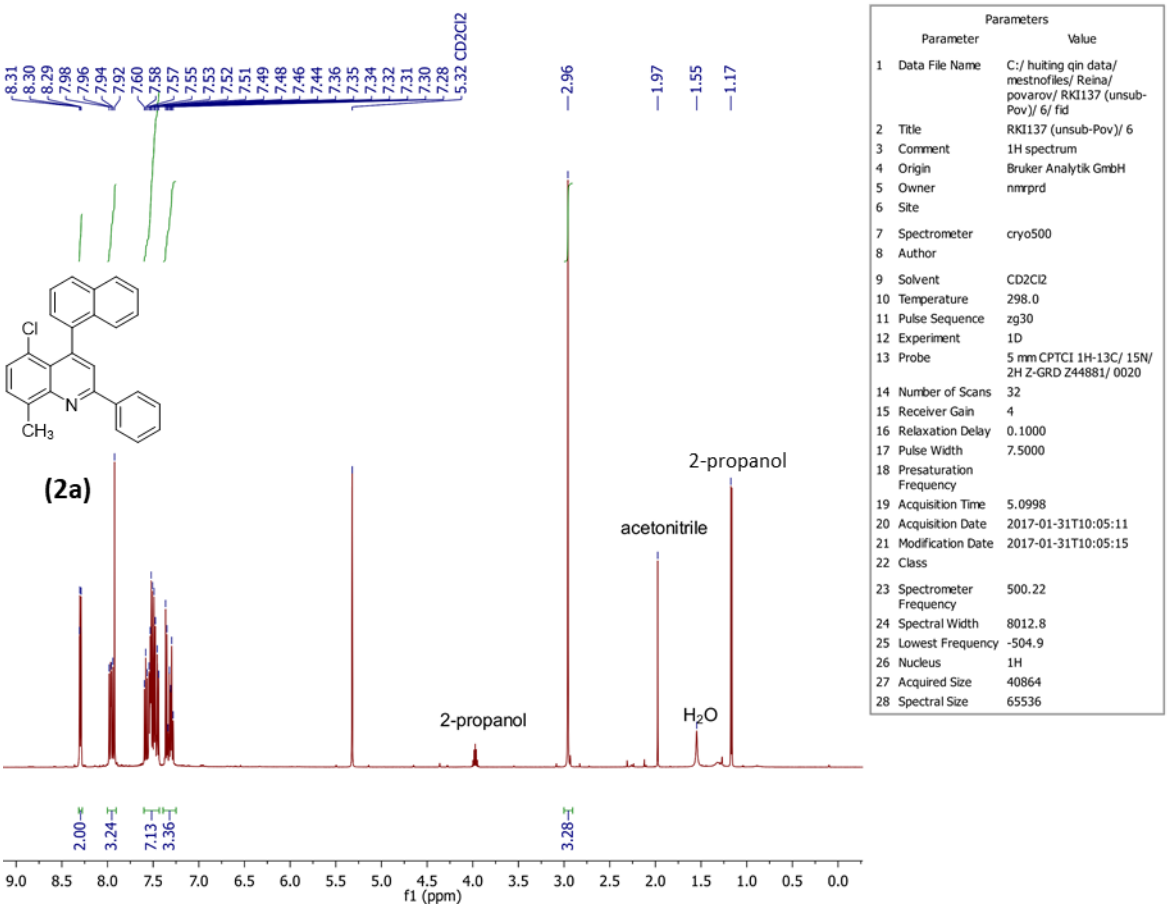

Parameters		
	Parameter	Value
1	Data File Name	C:/ huiting qin data/ mestnofiles/ Reina/ povarov/ RKI137 (unsub-Pov)/ 6/ fid
2	Title	RKI137 (unsub-Pov)/ 6
3	Comment	1H spectrum
4	Origin	Bruker Analytik GmbH
5	Owner	nmrprd
6	Site	
7	Spectrometer	cryo500
8	Author	
9	Solvent	CD2Cl2
10	Temperature	298.0
11	Pulse Sequence	zg30
12	Experiment	1D
13	Probe	5 mm CPTCI 1H-13C/ 15N/ 2H Z-GRD Z44881/ 0020
14	Number of Scans	32
15	Receiver Gain	4
16	Relaxation Delay	0.1000
17	Pulse Width	7.5000
18	Presaturation Frequency	
19	Acquisition Time	5.0998
20	Acquisition Date	2017-01-31T10:05:11
21	Modification Date	2017-01-31T10:05:15
22	Class	
23	Spectrometer Frequency	500.22
24	Spectral Width	8012.8
25	Lowest Frequency	-504.9
26	Nucleus	1H
27	Acquired Size	40864
28	Spectral Size	65536

Figure S13. The ^{1}H NMR spectrum obtained for **2a.**

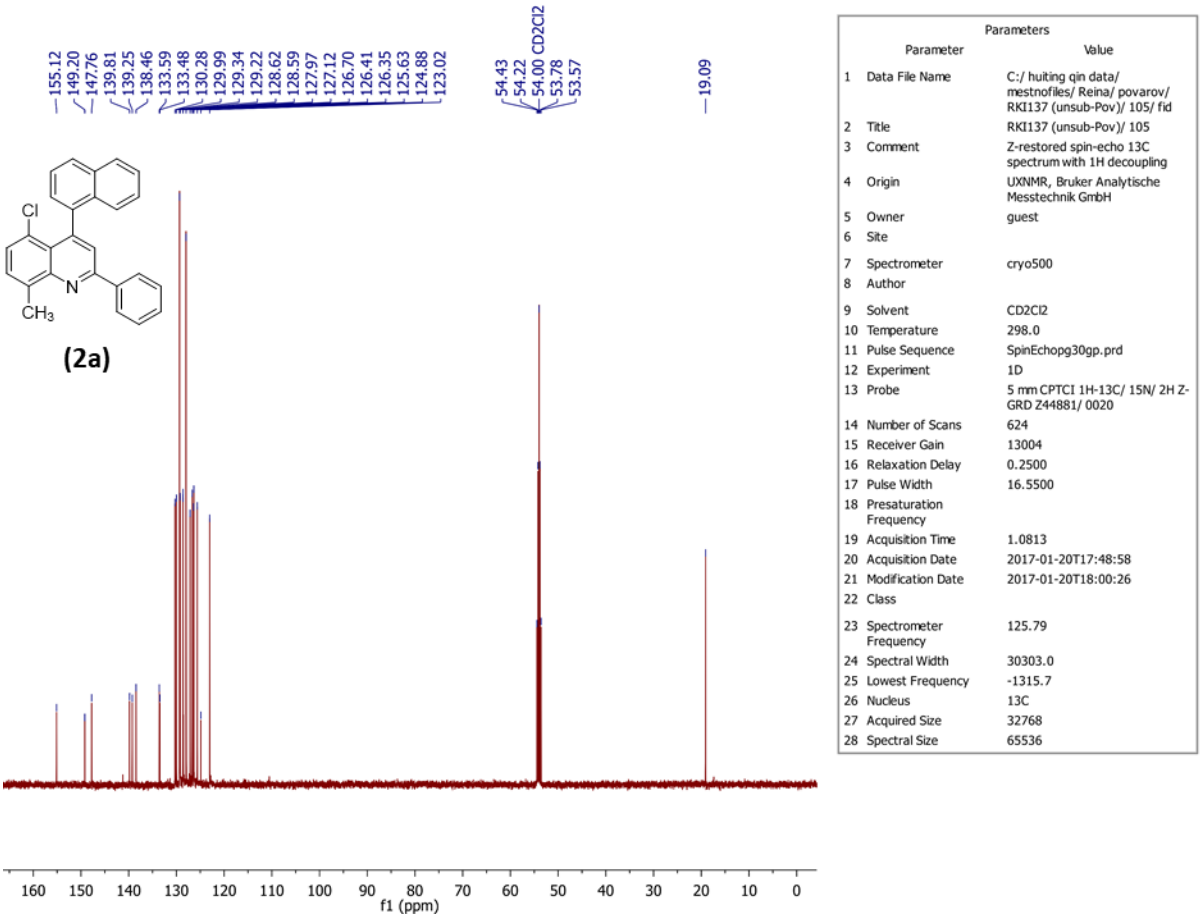

Parameters		
	Parameter	Value
1	Data File Name	C:/ huiting qin data/ mestnofiles/ Reina/ povarov/ RKI137 (unsub-Pov)/ 105/ fid
2	Title	RKI137 (unsub-Pov)/ 105
3	Comment	Z-restored spin-echo 13C spectrum with 1H decoupling
4	Origin	UXNMR, Bruker Analytische Messtechnik GmbH
5	Owner	guest
6	Site	
7	Spectrometer	cryo500
8	Author	
9	Solvent	CD2Cl2
10	Temperature	298.0
11	Pulse Sequence	SpinEchopg30gp.prd
12	Experiment	1D
13	Probe	5 mm CPTCI 1H-13C/ 15N/ 2H Z-GRD Z44881/ 0020
14	Number of Scans	624
15	Receiver Gain	13004
16	Relaxation Delay	0.2500
17	Pulse Width	16.5500
18	Presaturation Frequency	
19	Acquisition Time	1.0813
20	Acquisition Date	2017-01-20T17:48:58
21	Modification Date	2017-01-20T18:00:26
22	Class	
23	Spectrometer Frequency	125.79
24	Spectral Width	30303.0
25	Lowest Frequency	-1315.7
26	Nucleus	13C
27	Acquired Size	32768
28	Spectral Size	65536

Figure S14. The ^{13}C NMR spectrum obtained for **2a.**

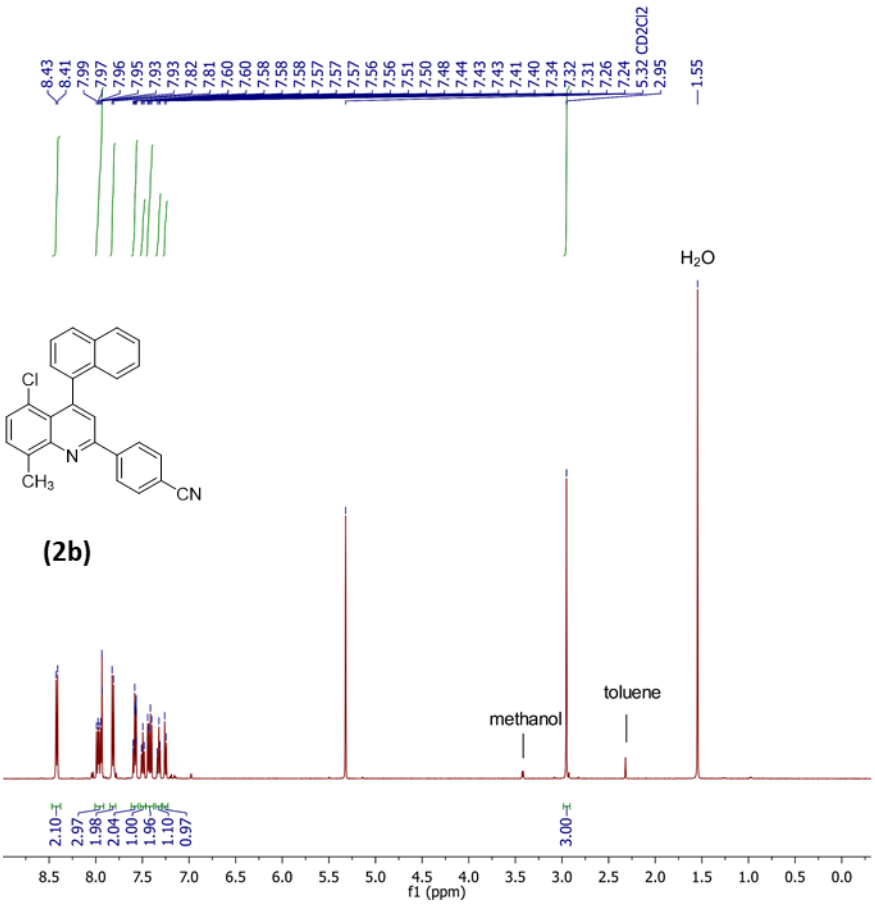

Parameters		
	Parameter	Value
1	Data File Name	C:/ huiting qin data/ mestnofiles/ Reina/ povarov/ RKI138 (CN-Pov)/ 6/ fid
2	Title	RKI138 (CN-Pov)/ 6
3	Comment	1H spectrum
4	Origin	Bruker Analytik GmbH
5	Owner	nmrprd
6	Site	
7	Spectrometer	cryo500
8	Author	
9	Solvent	CD2Cl2
10	Temperature	298.0
11	Pulse Sequence	zg30
12	Experiment	1D
13	Probe	5 mm CPTCI 1H-13C/ 15N/ 2H Z-GRD Z44881/ 0020
14	Number of Scans	16
15	Receiver Gain	4
16	Relaxation Delay	0.1000
17	Pulse Width	7.5000
18	Presaturation Frequency	
19	Acquisition Time	5.0998
20	Acquisition Date	2017-01-20T13:06:26
21	Modification Date	2019-08-26T18:46:41
22	Class	
23	Spectrometer Frequency	500.22
24	Spectral Width	8012.8
25	Lowest Frequency	-504.9
26	Nucleus	1H
27	Acquired Size	40864
28	Spectral Size	65536

Figure S15. The ^{1}H NMR spectrum obtained for **2b.**

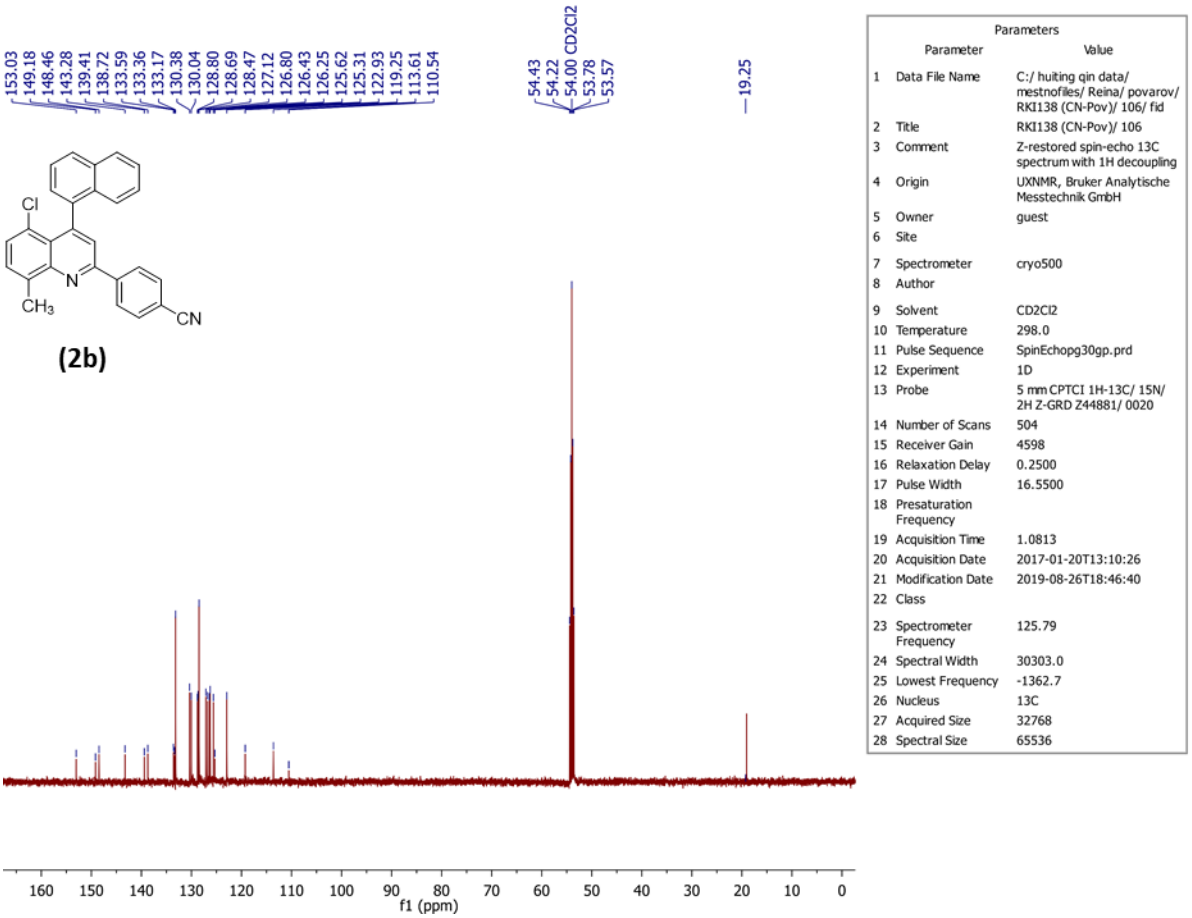

Parameters		
	Parameter	Value
1	Data File Name	C:/ huiting qin data/ mestnofiles/ Reina/ povarov/ RKI138 (CN-Pov)/ 106/ fid
2	Title	RKI138 (CN-Pov)/ 106
3	Comment	Z-restored spin-echo 13C spectrum with 1H decoupling
4	Origin	UXNMR, Bruker Analytische Messtechnik GmbH
5	Owner	guest
6	Site	
7	Spectrometer	cryo500
8	Author	
9	Solvent	CD2Cl2
10	Temperature	298.0
11	Pulse Sequence	SpinEchopg30gp.prd
12	Experiment	1D
13	Probe	5 mm CPTCI 1H-13C/ 15N/ 2H Z-GRD Z44881/ 0020
14	Number of Scans	504
15	Receiver Gain	4598
16	Relaxation Delay	0.2500
17	Pulse Width	16.5500
18	Presaturation Frequency	
19	Acquisition Time	1.0813
20	Acquisition Date	2017-01-20T13:10:26
21	Modification Date	2019-08-26T18:46:40
22	Class	
23	Spectrometer Frequency	125.79
24	Spectral Width	30303.0
25	Lowest Frequency	-1362.7
26	Nucleus	13C
27	Acquired Size	32768
28	Spectral Size	65536

Figure S16. The ^{13}C NMR spectrum obtained for **2b.**

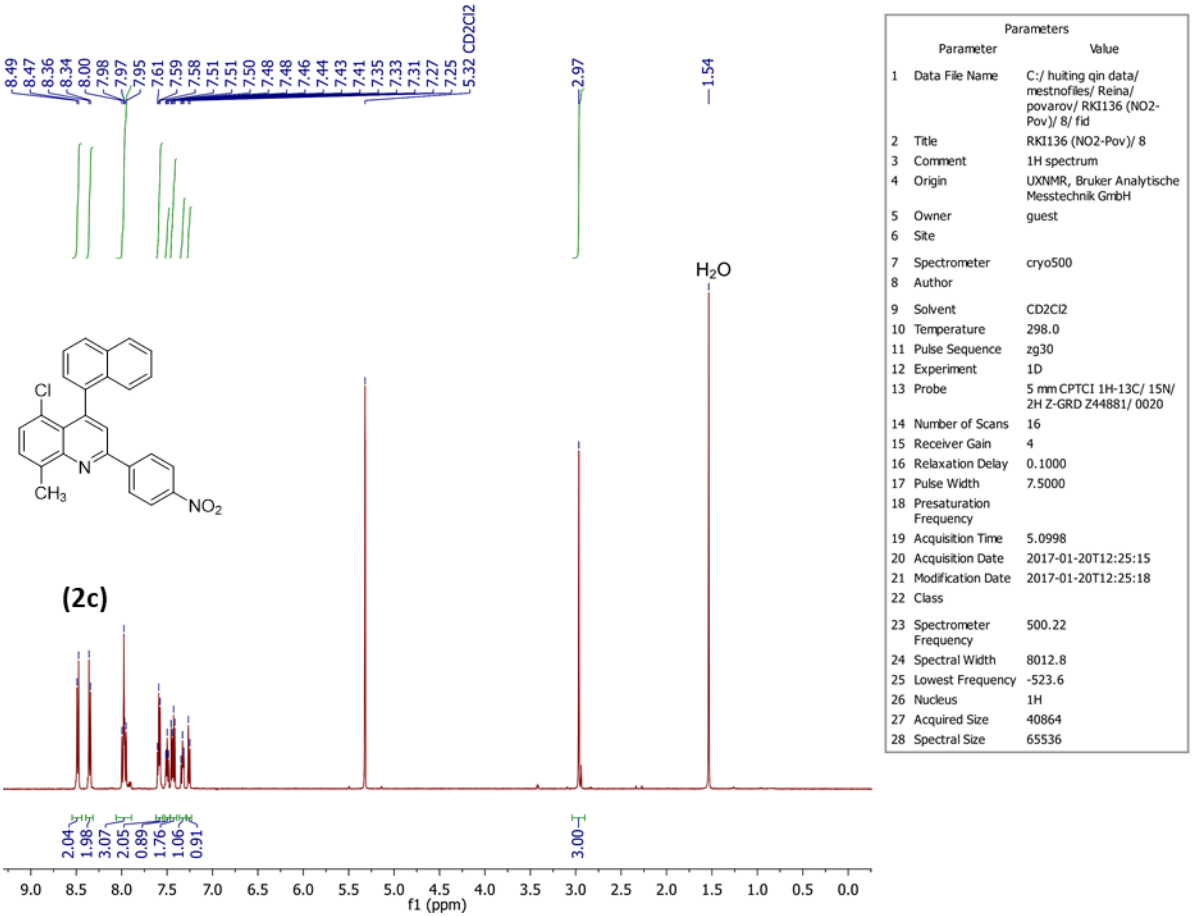

Parameters

	Parameter	Value
1	Data File Name	C:/ huiting qin data/ mestnofiles/ Reina/ povarov/ RKI136 (NO2-Pov)/ 8/ fid
2	Title	RKI136 (NO2-Pov)/ 8
3	Comment	1H spectrum
4	Origin	UXNMR, Bruker Analytische Messtechnik GmbH
5	Owner	guest
6	Site	
7	Spectrometer	cryo500
8	Author	
9	Solvent	CD2Cl2
10	Temperature	298.0
11	Pulse Sequence	zg30
12	Experiment	1D
13	Probe	5 mm CPTCI 1H-13C/ 15N/ 2H Z-GRD Z44881/ 0020
14	Number of Scans	16
15	Receiver Gain	4
16	Relaxation Delay	0.1000
17	Pulse Width	7.5000
18	Presaturation Frequency	
19	Acquisition Time	5.0998
20	Acquisition Date	2017-01-20T12:25:15
21	Modification Date	2017-01-20T12:25:18
22	Class	
23	Spectrometer Frequency	500.22
24	Spectral Width	8012.8
25	Lowest Frequency	-523.6
26	Nucleus	1H
27	Acquired Size	40864
28	Spectral Size	65536

Figure S17. The ^{1}H NMR spectrum obtained for **2c.**

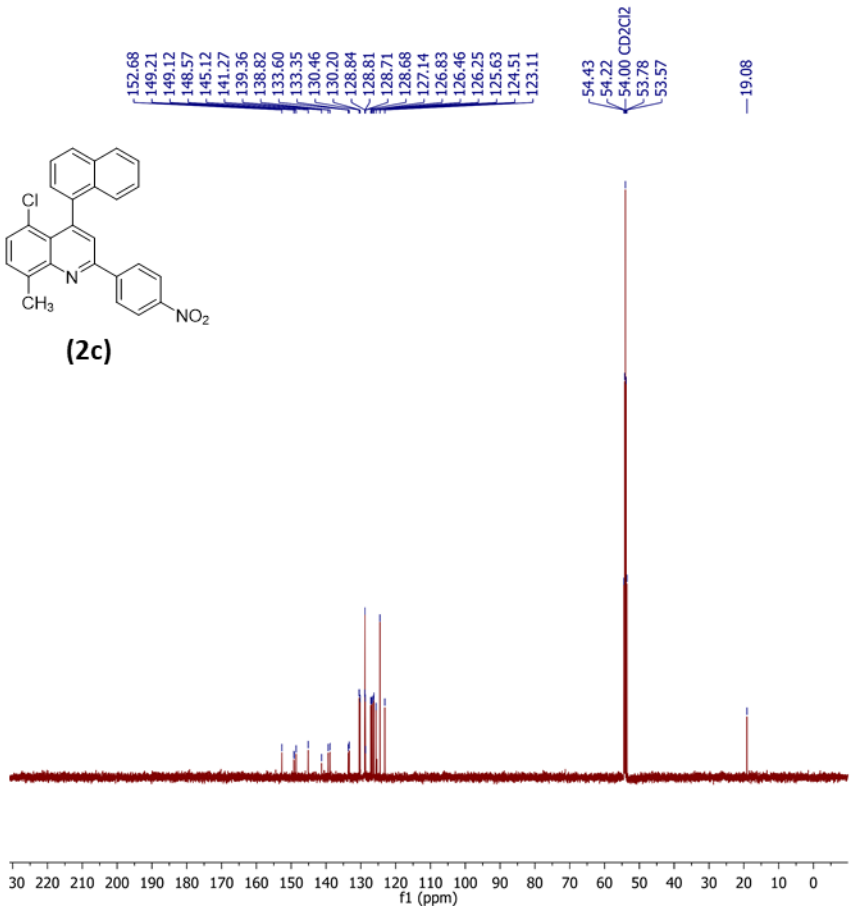

Parameters		
	Parameter	Value
1	Data File Name	C:/ huiting qin data/ mestnofiles/ Reina/ povarov/ RKI136 (NO2-Pov)/ 108/ fid
2	Title	RKI136 (NO2-Pov)/ 108
3	Comment	Z-restored spin-echo 13C spectrum with 1H decoupling
4	Origin	UXNMR, Bruker Analytische Messtechnik GmbH
5	Owner	guest
6	Site	
7	Spectrometer	cryo500
8	Author	
9	Solvent	CD2Cl2
10	Temperature	298.0
11	Pulse Sequence	SpinEchopg30gp.prd
12	Experiment	1D
13	Probe	5 mm CPTCI 1H-13C/ 15N/ 2H Z-GRD Z44881/ 0020
14	Number of Scans	552
15	Receiver Gain	7298
16	Relaxation Delay	0.2500
17	Pulse Width	16.5500
18	Presaturation Frequency	
19	Acquisition Time	1.0813
20	Acquisition Date	2017-01-20T12:29:49
21	Modification Date	2017-01-20T12:39:13
22	Class	
23	Spectrometer Frequency	125.79
24	Spectral Width	30303.0
25	Lowest Frequency	-1216.8
26	Nucleus	13C
27	Acquired Size	32768
28	Spectral Size	65536

Figure S18. The ^{13}C NMR spectrum obtained for **2c.**

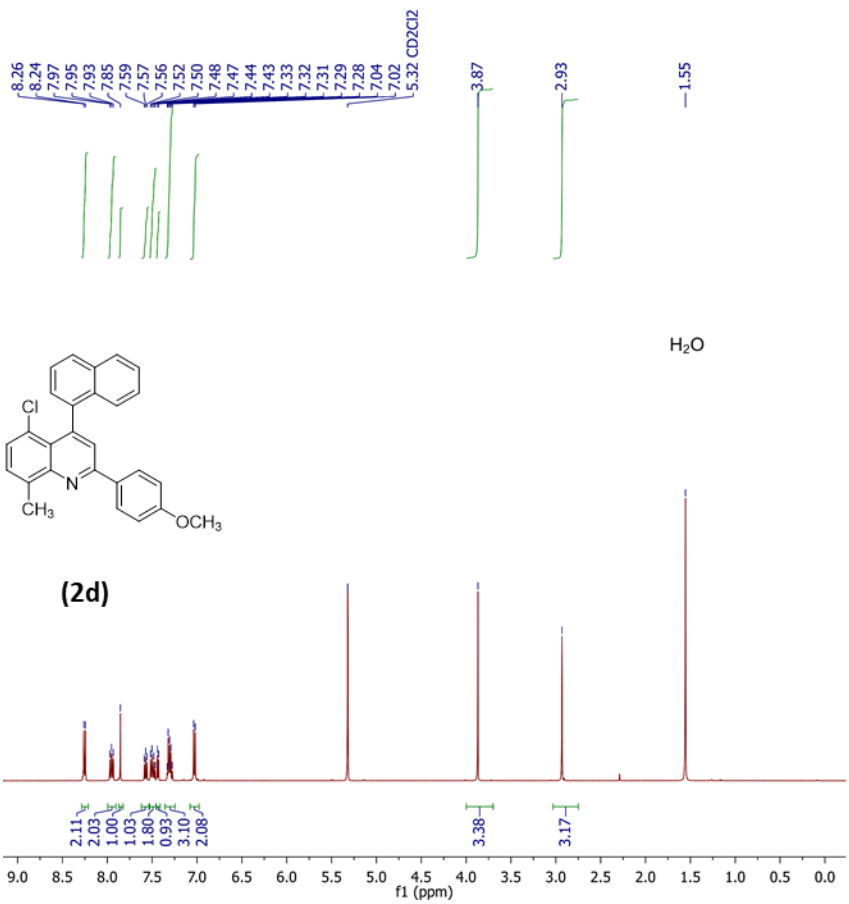

Parameters

	Parameter	Value
1	Data File Name	C:/ huiting qin data/ mestnofiles/ Reina/ povarov/ RKI139 (Meo Pov)/ 8/ fid
2	Title	RKI139 (Meo Pov)/ 8
3	Comment	1H spectrum
4	Origin	UXNMR, Bruker Analytische Messtechnik GmbH
5	Owner	guest
6	Site	
7	Spectrometer	cryo500
8	Author	
9	Solvent	CD2Cl2
10	Temperature	298.0
11	Pulse Sequence	zg30
12	Experiment	1D
13	Probe	5 mm CPTCI 1H-13C/ 15N/ 2H Z-GRD Z44881/ 0020
14	Number of Scans	32
15	Receiver Gain	4
16	Relaxation Delay	0.1000
17	Pulse Width	7.5000
18	Presaturation Frequency	
19	Acquisition Time	5.0998
20	Acquisition Date	2017-01-25T13:41:34
21	Modification Date	2017-01-25T13:41:38
22	Class	
23	Spectrometer Frequency	500.22
24	Spectral Width	8012.8
25	Lowest Frequency	-523.9
26	Nucleus	1H
27	Acquired Size	40864
28	Spectral Size	65536

Figure S19. The ^{1}H NMR spectrum obtained for **2d.**

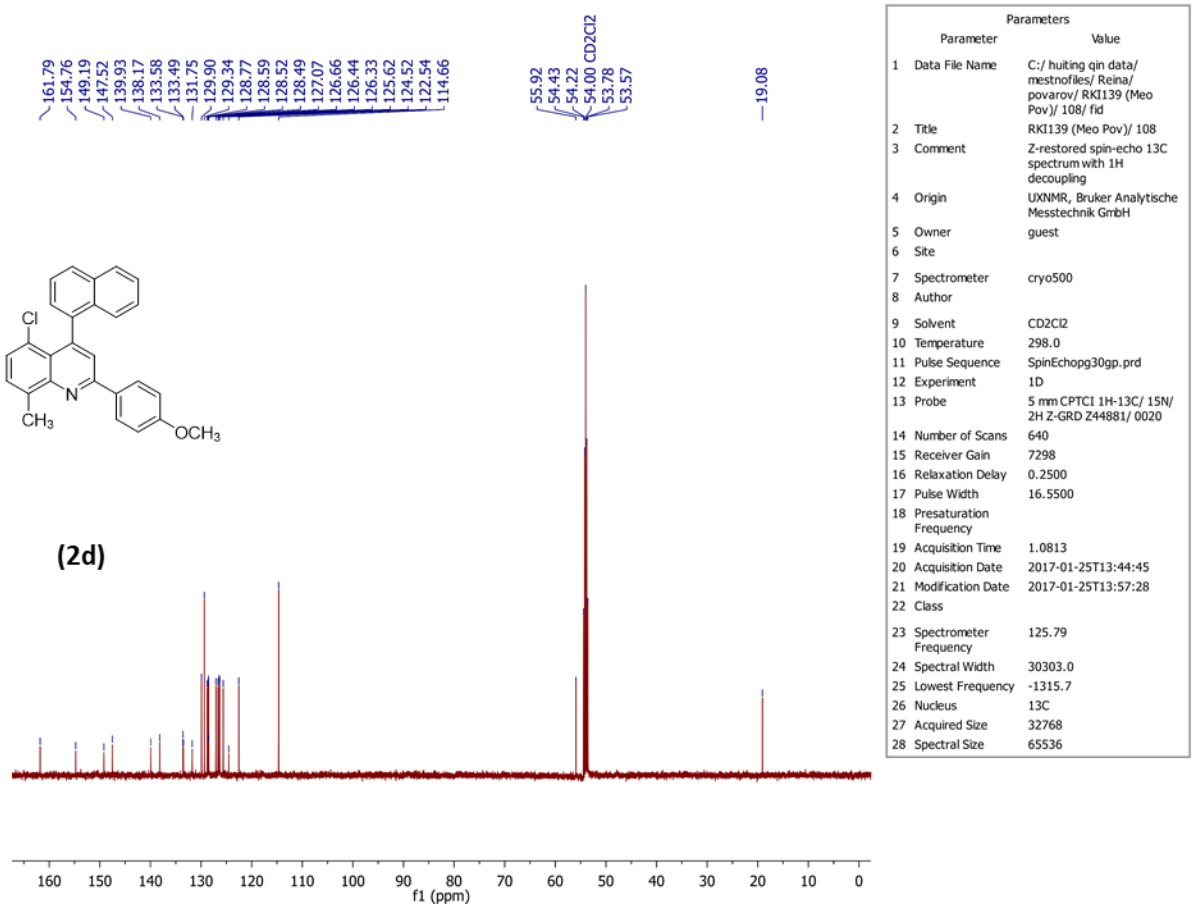

Figure S20. The ^{13}C NMR spectrum obtained for **2d.**

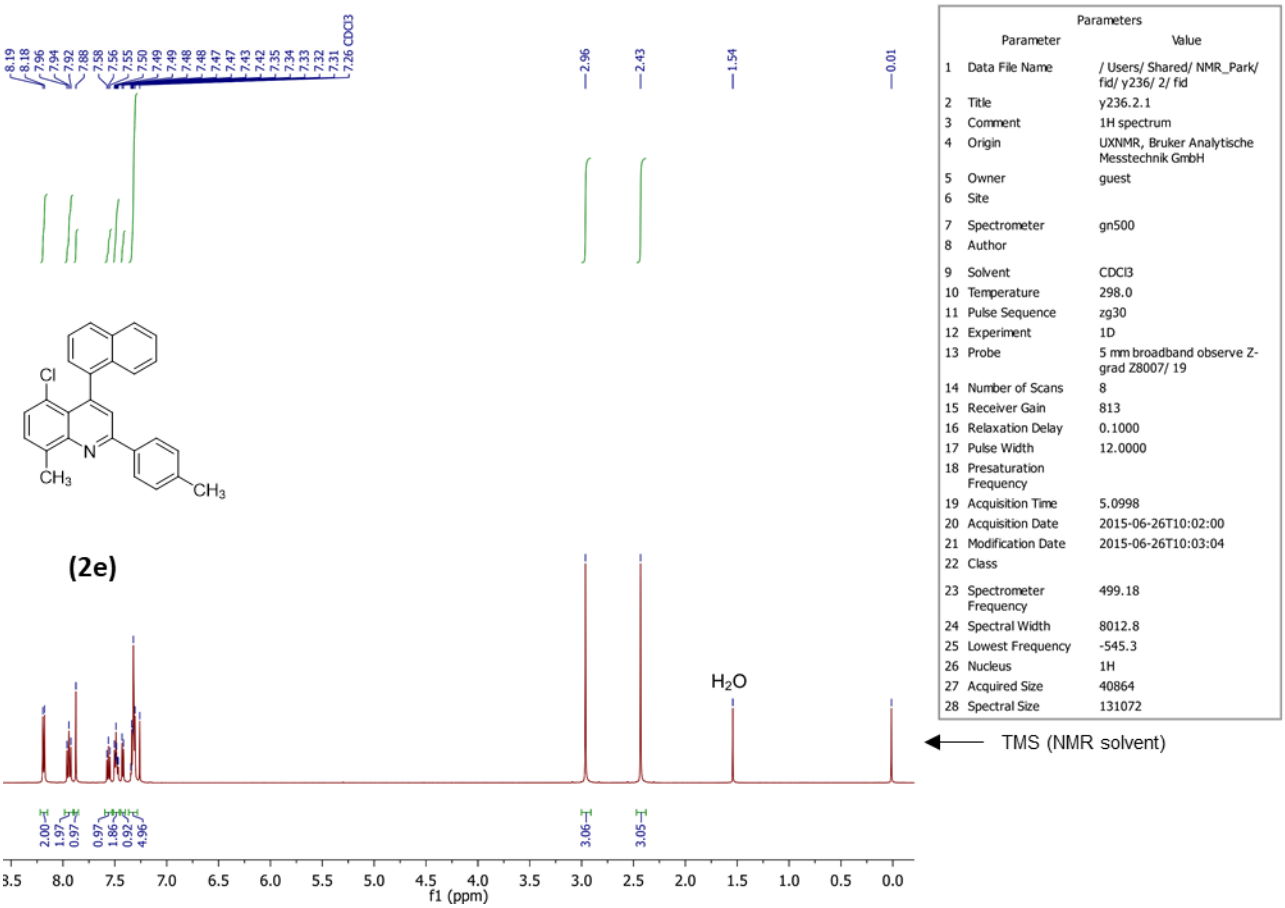

Parameters

	Parameter	Value
1	Data File Name	/ Users/ Shared/ NMR_Park/ fid/ y236/ 2/ fid
2	Title	y236.2.1
3	Comment	1H spectrum
4	Origin	UXNMR, Bruker Analytische Messtechnik GmbH
5	Owner	guest
6	Site	
7	Spectrometer	gn500
8	Author	
9	Solvent	CDCl3
10	Temperature	298.0
11	Pulse Sequence	zg30
12	Experiment	1D
13	Probe	5 mm broadband observe Z-grad Z8007/ 19
14	Number of Scans	8
15	Receiver Gain	813
16	Relaxation Delay	0.1000
17	Pulse Width	12.0000
18	Presaturation Frequency	
19	Acquisition Time	5.0998
20	Acquisition Date	2015-06-26T10:02:00
21	Modification Date	2015-06-26T10:03:04
22	Class	
23	Spectrometer Frequency	499.18
24	Spectral Width	8012.8
25	Lowest Frequency	-545.3
26	Nucleus	1H
27	Acquired Size	40864
28	Spectral Size	131072

Figure S21. The ^{1}H NMR spectrum obtained for **2e.**

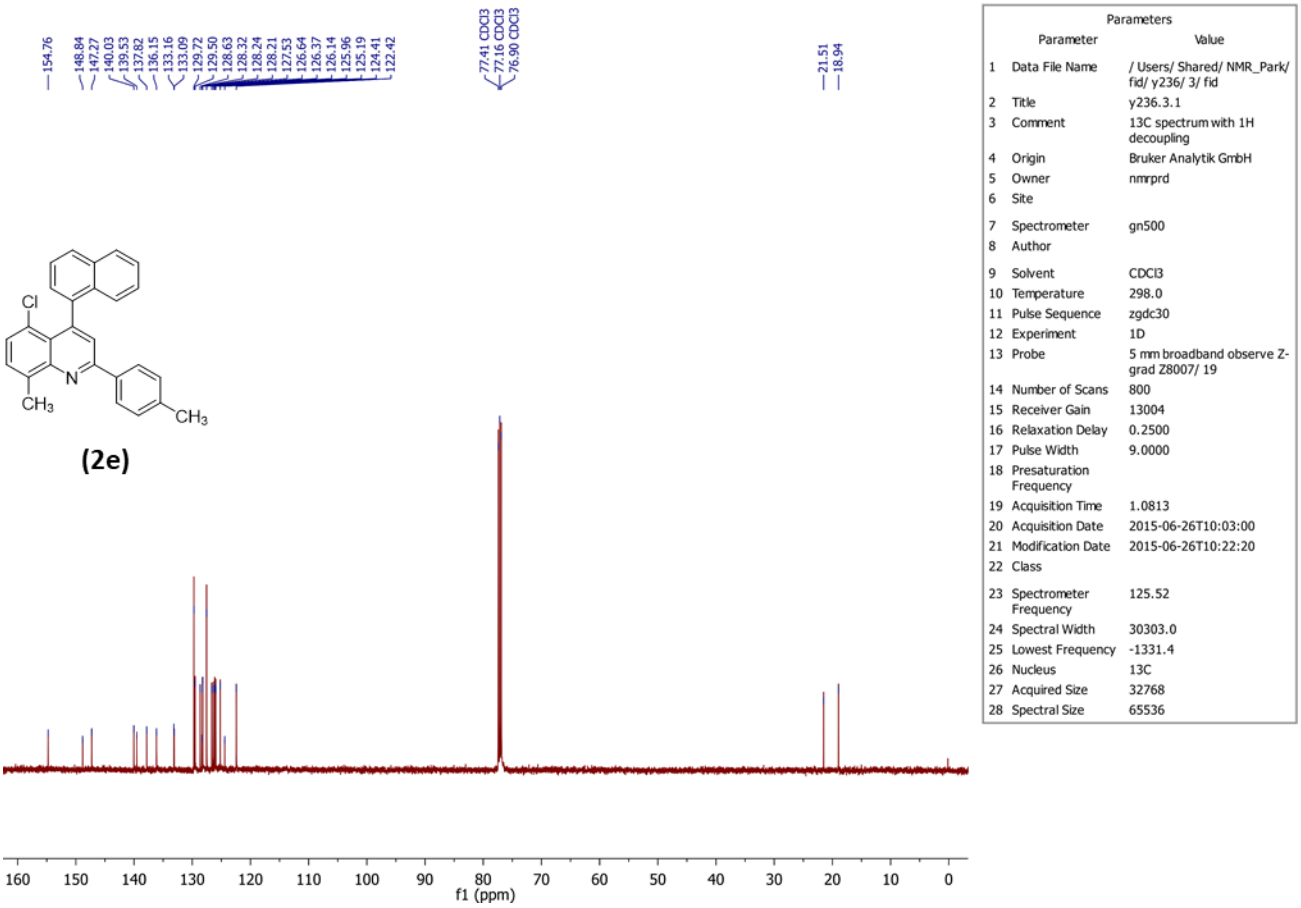

Parameters

	Parameter	Value
1	Data File Name	/ Users/ Shared/ NMR_Park/ fid/ y236/ 3/ fid
2	Title	y236.3.1
3	Comment	13C spectrum with 1H decoupling
4	Origin	Bruker Analytik GmbH
5	Owner	nmrprd
6	Site	
7	Spectrometer	gn500
8	Author	
9	Solvent	CDCl3
10	Temperature	298.0
11	Pulse Sequence	zgdc30
12	Experiment	1D
13	Probe	5 mm broadband observe Z-grad Z8007/ 19
14	Number of Scans	800
15	Receiver Gain	13004
16	Relaxation Delay	0.2500
17	Pulse Width	9.0000
18	Presaturation Frequency	
19	Acquisition Time	1.0813
20	Acquisition Date	2015-06-26T10:03:00
21	Modification Date	2015-06-26T10:22:20
22	Class	
23	Spectrometer Frequency	125.52
24	Spectral Width	30303.0
25	Lowest Frequency	-1331.4
26	Nucleus	13C
27	Acquired Size	32768
28	Spectral Size	65536

Figure S22. The ^{13}C NMR spectrum obtained for **2e.**

.

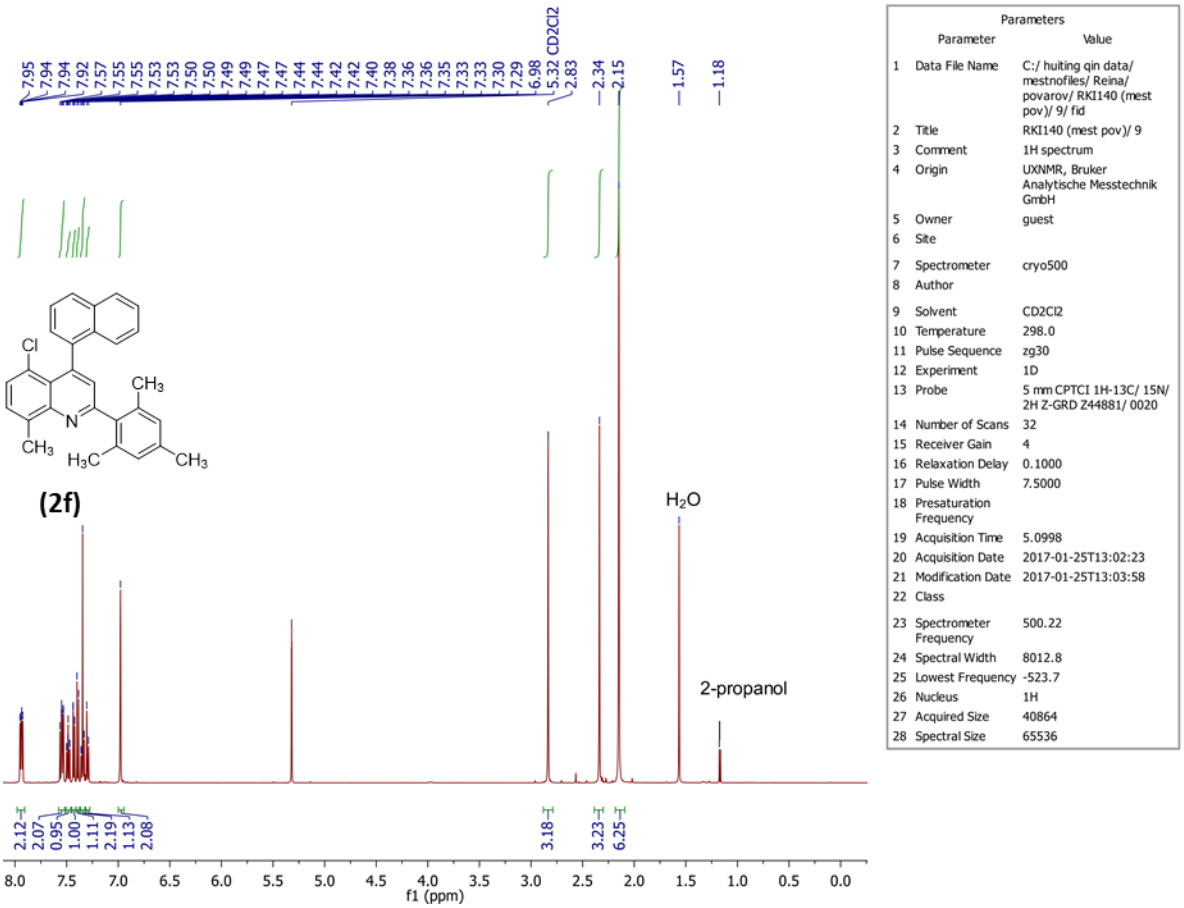

Parameters		
	Parameter	Value
1	Data File Name	C:/ huiting qin data/ mestnofiles/ Reina/ povarov/ RKI140 (mest pov)/ 9/ fid
2	Title	RKI140 (mest pov)/ 9
3	Comment	1H spectrum
4	Origin	UXNMR, Bruker Analytische Messtechnik GmbH
5	Owner	guest
6	Site	
7	Spectrometer	cryo500
8	Author	
9	Solvent	CD2Cl2
10	Temperature	298.0
11	Pulse Sequence	zg30
12	Experiment	1D
13	Probe	5 mm CPTCI 1H-13C/ 15N/ 2H Z-GRD Z44881/ 0020
14	Number of Scans	32
15	Receiver Gain	4
16	Relaxation Delay	0.1000
17	Pulse Width	7.5000
18	Presaturation Frequency	
19	Acquisition Time	5.0998
20	Acquisition Date	2017-01-25T13:02:23
21	Modification Date	2017-01-25T13:03:58
22	Class	
23	Spectrometer Frequency	500.22
24	Spectral Width	8012.8
25	Lowest Frequency	-523.7
26	Nucleus	1H
27	Acquired Size	40864
28	Spectral Size	65536

Figure S23. The ^{1}H NMR spectrum obtained for **2f.**

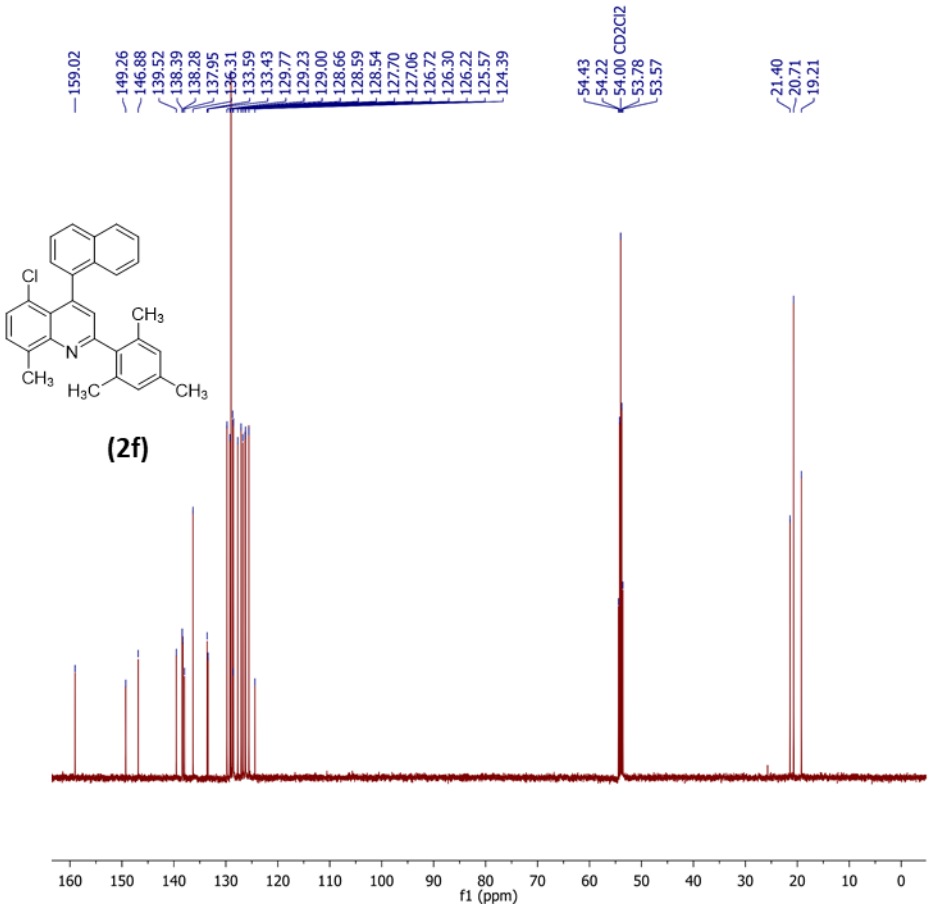

Parameters		
	Parameter	Value
1	Data File Name	C:/ huiting qin data/ mestnofiles/ Reina/ povarov/ RKI140 (mest pov)/ 109/ fid
2	Title	RKI140 (mest pov)/ 109
3	Comment	Z-restored spin-echo 13C spectrum with 1H decoupling
4	Origin	UXNMR, Bruker Analytische Messtechnik GmbH
5	Owner	guest
6	Site	
7	Spectrometer	cryo500
8	Author	
9	Solvent	CD2Cl2
10	Temperature	298.0
11	Pulse Sequence	SpinEchopg30gp.prd
12	Experiment	1D
13	Probe	5 mm CPTCI 1H-13C/ 15N/ 2H Z-GRD Z44881/ 0020
14	Number of Scans	624
15	Receiver Gain	3649
16	Relaxation Delay	0.2500
17	Pulse Width	16.5500
18	Presaturation Frequency	
19	Acquisition Time	1.0813
20	Acquisition Date	2017-01-25T13:08:31
21	Modification Date	2017-01-25T13:19:22
22	Class	
23	Spectrometer Frequency	125.79
24	Spectral Width	30303.0
25	Lowest Frequency	-1315.7
26	Nucleus	13C
27	Acquired Size	32768
28	Spectral Size	65536

Figure S24. The ^{13}C NMR spectrum obtained for **2f.**

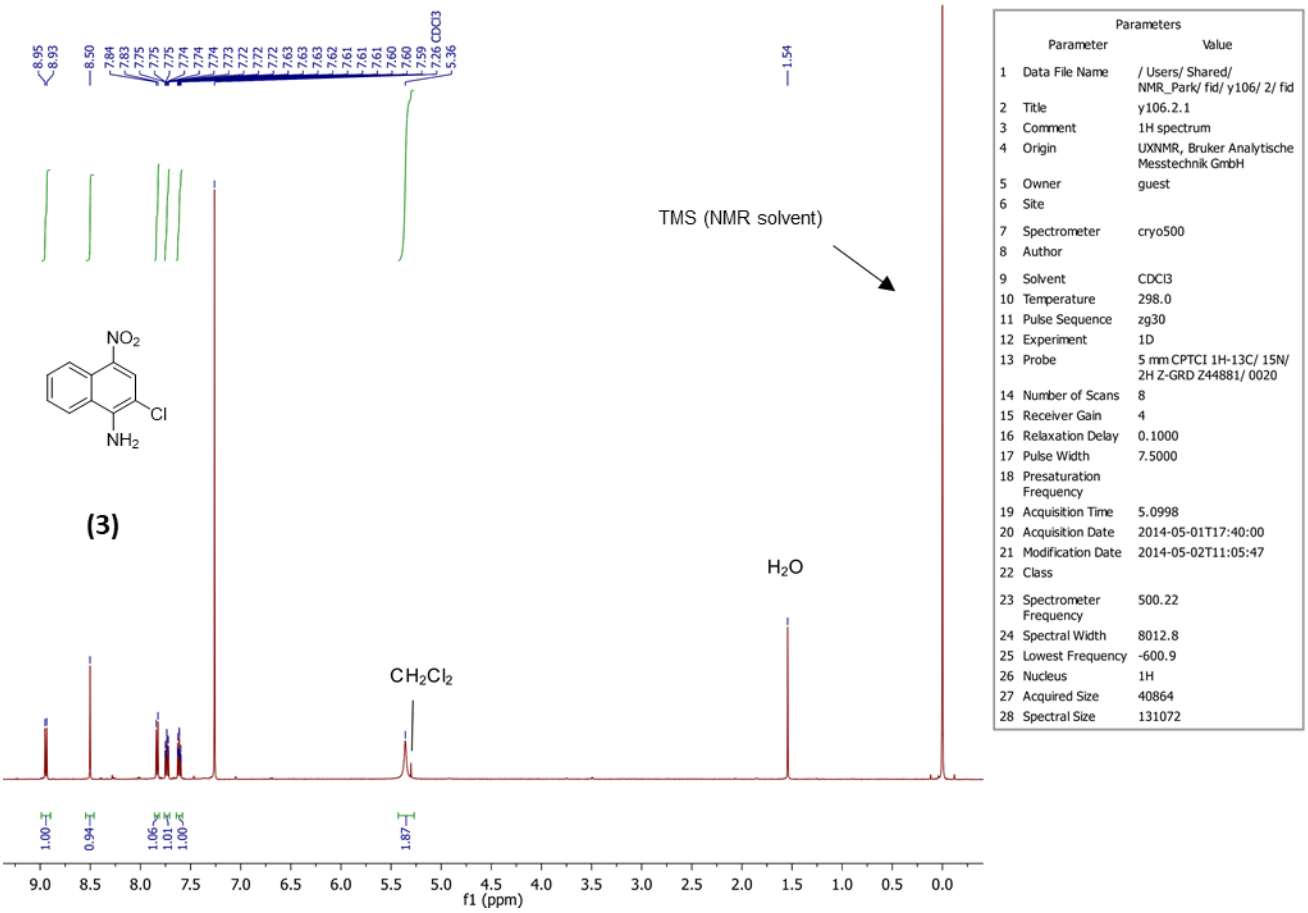

Parameters		
	Parameter	Value
1	Data File Name	/ Users/ Shared/ NMR_Park/ fid/ y106/ 2/ fid
2	Title	y106.2.1
3	Comment	1H spectrum
4	Origin	UXNMR, Bruker Analytische Messtechnik GmbH
5	Owner	guest
6	Site	
7	Spectrometer	cryo500
8	Author	
9	Solvent	CDCl3
10	Temperature	298.0
11	Pulse Sequence	zg30
12	Experiment	1D
13	Probe	5 mm CPTCI 1H-13C/ 15N/ 2H Z-GRD Z44881/ 0020
14	Number of Scans	8
15	Receiver Gain	4
16	Relaxation Delay	0.1000
17	Pulse Width	7.5000
18	Presaturation Frequency	
19	Acquisition Time	5.0998
20	Acquisition Date	2014-05-01T17:40:00
21	Modification Date	2014-05-02T11:05:47
22	Class	
23	Spectrometer Frequency	500.22
24	Spectral Width	8012.8
25	Lowest Frequency	-600.9
26	Nucleus	1H
27	Acquired Size	40864
28	Spectral Size	131072

Figure S25. The ^{1}H NMR spectrum obtained for **3.**

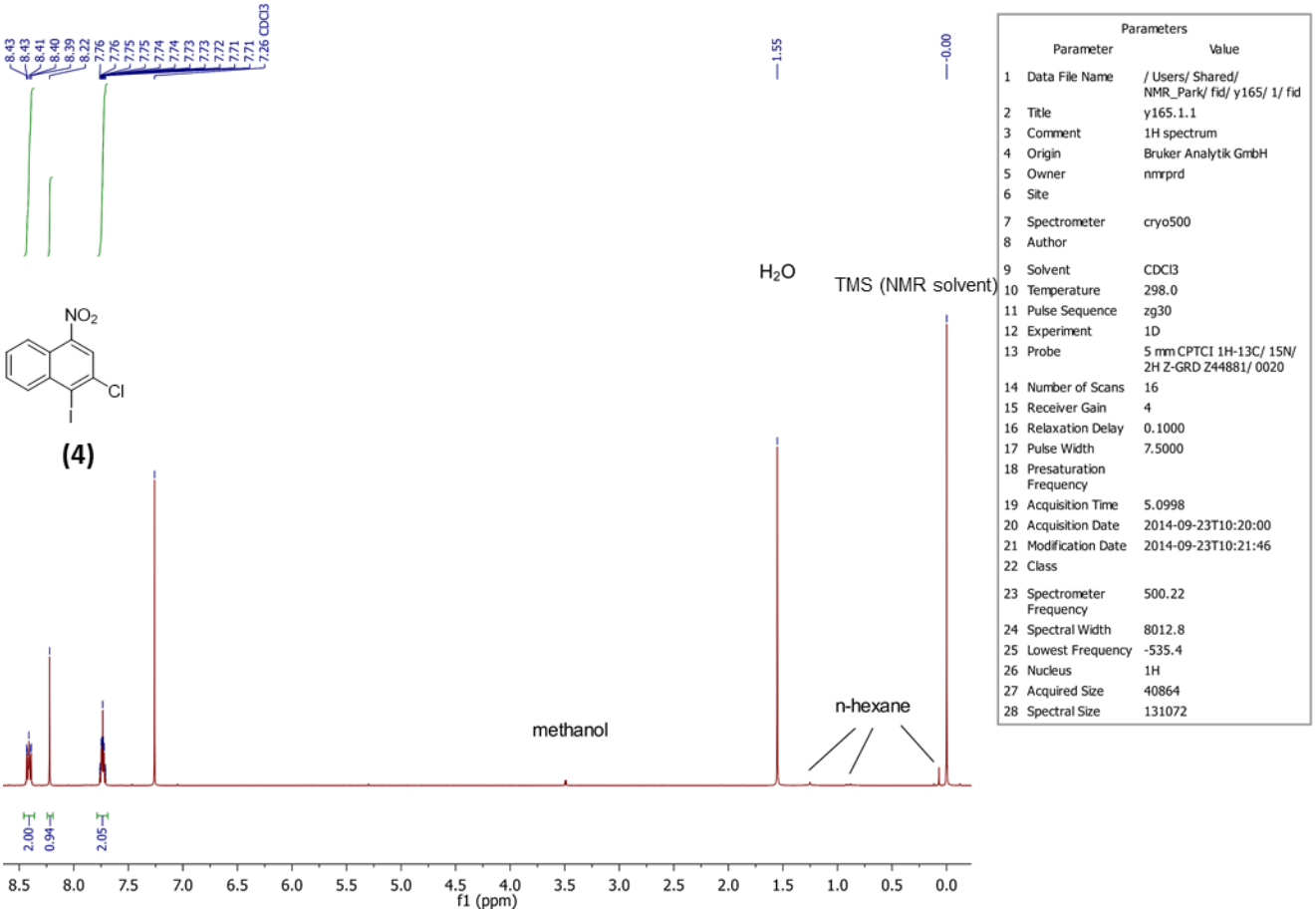

Parameters		
	Parameter	Value
1	Data File Name	/ Users/ Shared/ NMR_Park/ fid/ y165/ 1/ fid
2	Title	y165.1.1
3	Comment	1H spectrum
4	Origin	Bruker Analytik GmbH
5	Owner	nmrprd
6	Site	
7	Spectrometer	cryo500
8	Author	
9	Solvent	CDCl3
10	Temperature	298.0
11	Pulse Sequence	zg30
12	Experiment	1D
13	Probe	5 mm CPTCI 1H-13C/ 15N/ 2H Z-GRD Z44881/ 0020
14	Number of Scans	16
15	Receiver Gain	4
16	Relaxation Delay	0.1000
17	Pulse Width	7.5000
18	Presaturation Frequency	
19	Acquisition Time	5.0998
20	Acquisition Date	2014-09-23T10:20:00
21	Modification Date	2014-09-23T10:21:46
22	Class	
23	Spectrometer Frequency	500.22
24	Spectral Width	8012.8
25	Lowest Frequency	-535.4
26	Nucleus	1H
27	Acquired Size	40864
28	Spectral Size	131072

Figure S26. The ^{1}H NMR spectrum obtained for **4.**

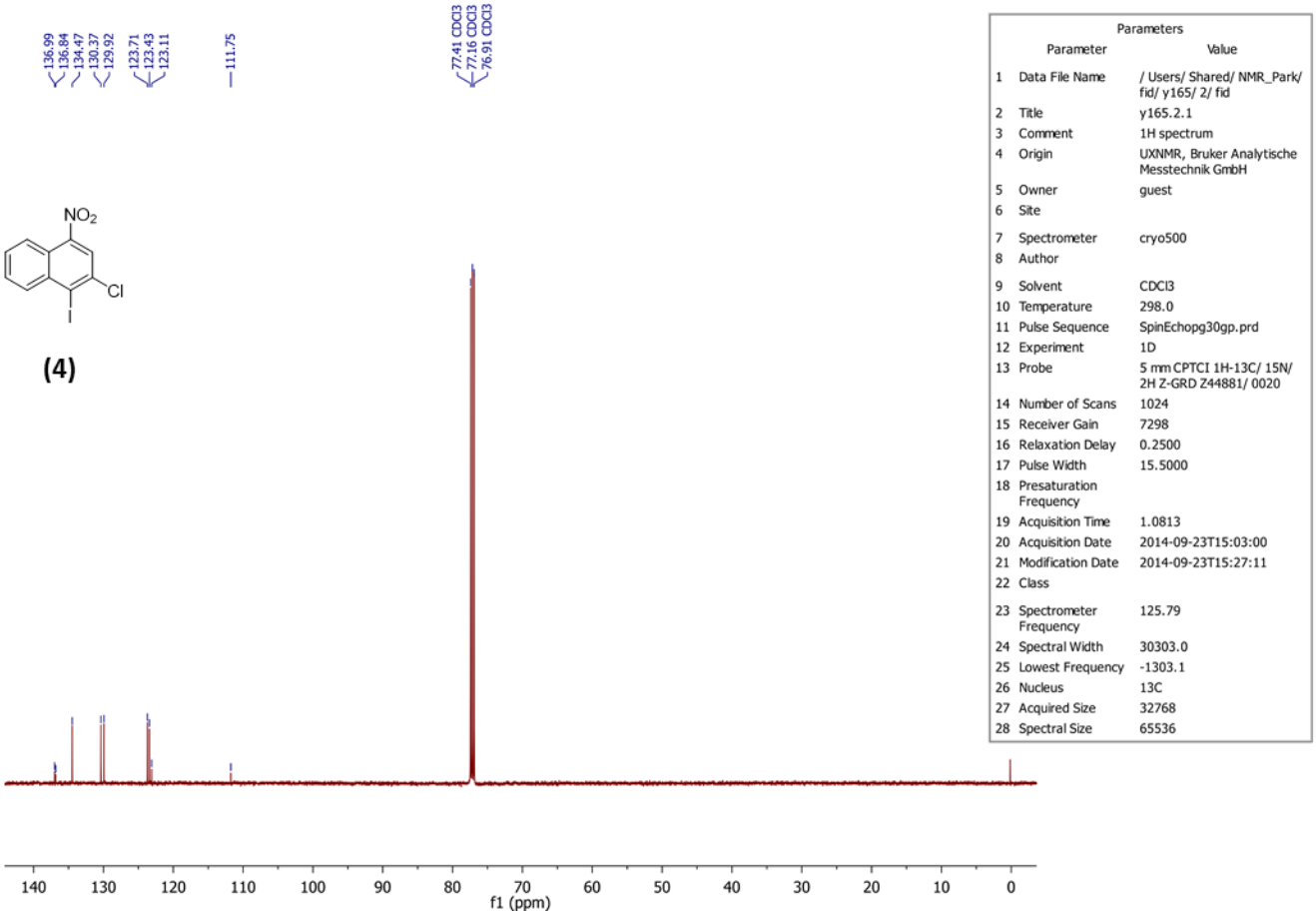

Parameters

	Parameter	Value
1	Data File Name	/ Users/ Shared/ NMR_Park/ fid/ y165/ 2/ fid
2	Title	y165.2.1
3	Comment	1H spectrum
4	Origin	UXNMR, Bruker Analytische Messtechnik GmbH
5	Owner	guest
6	Site	
7	Spectrometer	cryo500
8	Author	
9	Solvent	CDCl3
10	Temperature	298.0
11	Pulse Sequence	SpinEchopg30gp.prd
12	Experiment	1D
13	Probe	5 mm CPTCI 1H-13C/ 15N/ 2H Z-GRD Z44881/ 0020
14	Number of Scans	1024
15	Receiver Gain	7298
16	Relaxation Delay	0.2500
17	Pulse Width	15.5000
18	Presaturation Frequency	
19	Acquisition Time	1.0813
20	Acquisition Date	2014-09-23T15:03:00
21	Modification Date	2014-09-23T15:27:11
22	Class	
23	Spectrometer Frequency	125.79
24	Spectral Width	30303.0
25	Lowest Frequency	-1303.1
26	Nucleus	13C
27	Acquired Size	32768
28	Spectral Size	65536

Figure S27. The ^{13}C NMR spectrum obtained for **4.**

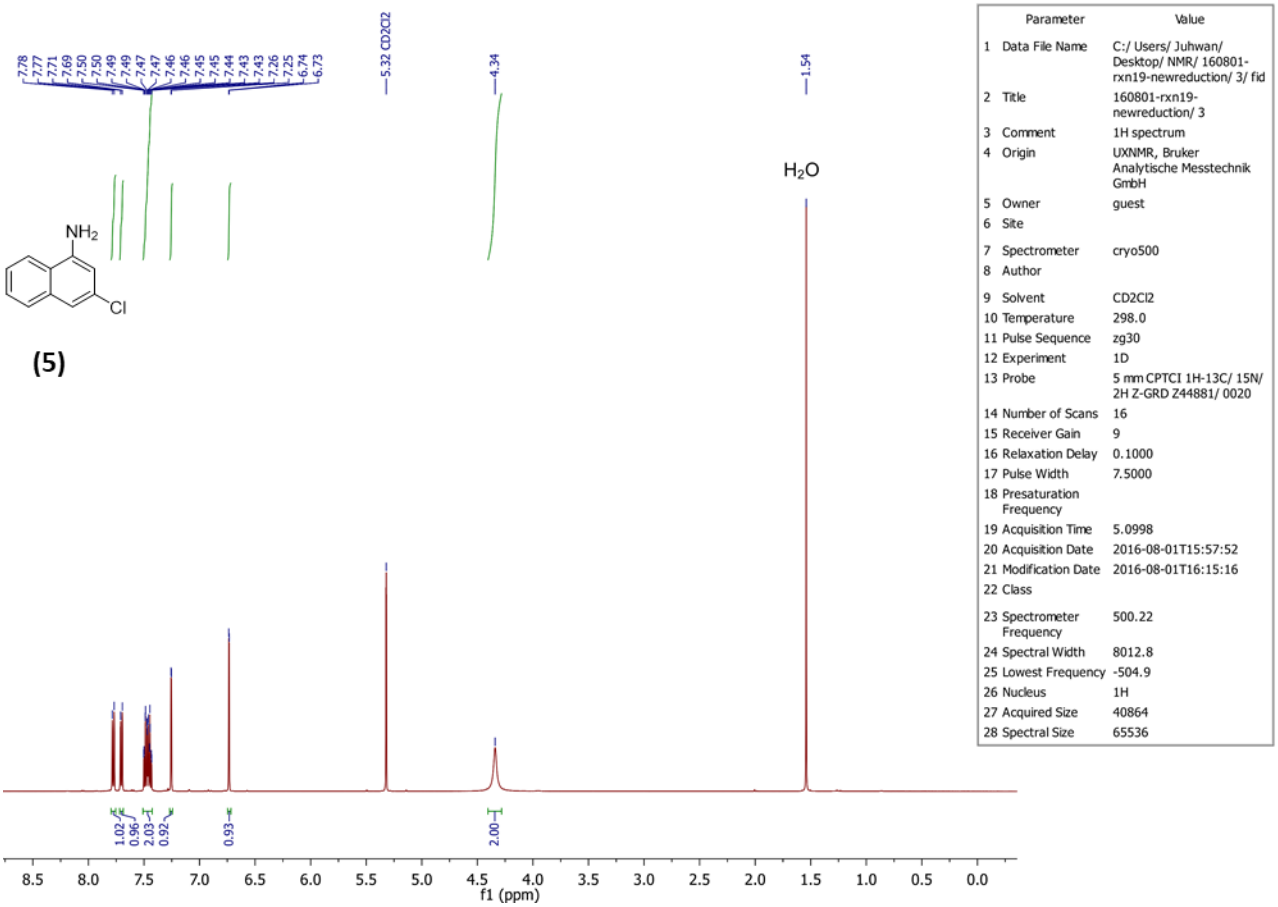

	Parameter	Value
1	Data File Name	C:/ Users/ Juhwan/ Desktop/ NMR/ 160801-rxn19-newreduction/ 3/ fid
2	Title	160801-rxn19-newreduction/ 3
3	Comment	1H spectrum
4	Origin	UXNMR, Bruker Analytische Messtechnik GmbH
5	Owner	guest
6	Site	
7	Spectrometer	cryo500
8	Author	
9	Solvent	CD2Cl2
10	Temperature	298.0
11	Pulse Sequence	zg30
12	Experiment	1D
13	Probe	5 mm CPTCI 1H-13C/ 15N/ 2H Z-GRD Z44881/ 0020
14	Number of Scans	16
15	Receiver Gain	9
16	Relaxation Delay	0.1000
17	Pulse Width	7.5000
18	Presaturation Frequency	
19	Acquisition Time	5.0998
20	Acquisition Date	2016-08-01T15:57:52
21	Modification Date	2016-08-01T16:15:16
22	Class	
23	Spectrometer Frequency	500.22
24	Spectral Width	8012.8
25	Lowest Frequency	-504.9
26	Nucleus	1H
27	Acquired Size	40864
28	Spectral Size	65536

Figure S28. The ^{1}H NMR spectrum obtained for **5.**

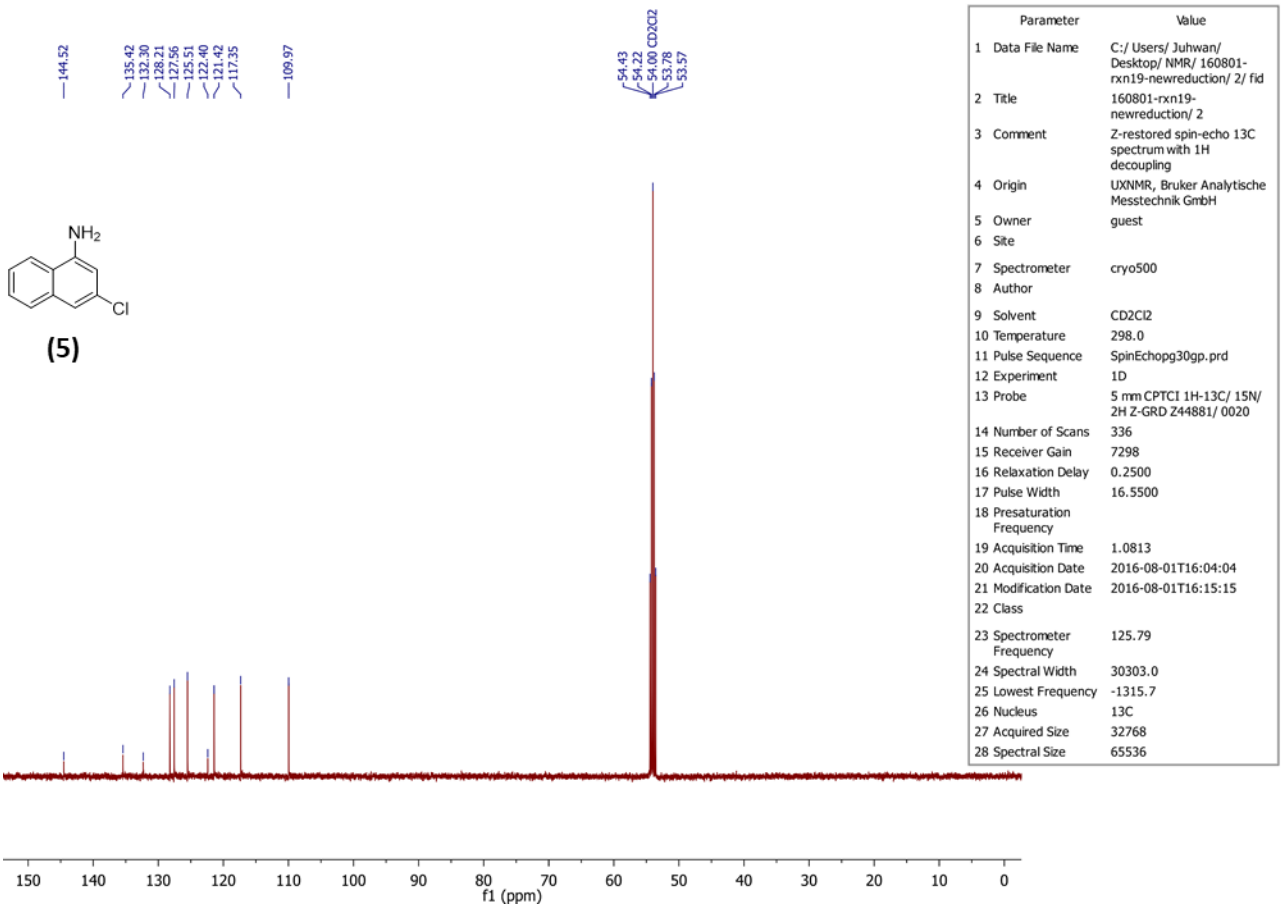

	Parameter	Value
1	Data File Name	C:/ Users/ Juhwan/ Desktop/ NMR/ 160801-rxn19-newreduction/ 2/ fid
2	Title	160801-rxn19-newreduction/ 2
3	Comment	Z-restored spin-echo 13C spectrum with 1H decoupling
4	Origin	UXNMR, Bruker Analytische Messtechnik GmbH
5	Owner	guest
6	Site	
7	Spectrometer	cryo500
8	Author	
9	Solvent	CD2Cl2
10	Temperature	298.0
11	Pulse Sequence	SpinEchopg30gp.prd
12	Experiment	1D
13	Probe	5 mm CPTCI 1H-13C/ 15N/ 2H Z-GRD Z44881/ 0020
14	Number of Scans	336
15	Receiver Gain	7298
16	Relaxation Delay	0.2500
17	Pulse Width	16.5500
18	Presaturation Frequency	
19	Acquisition Time	1.0813
20	Acquisition Date	2016-08-01T16:04:04
21	Modification Date	2016-08-01T16:15:15
22	Class	
23	Spectrometer Frequency	125.79
24	Spectral Width	30303.0
25	Lowest Frequency	-1315.7
26	Nucleus	13C
27	Acquired Size	32768
28	Spectral Size	65536

Figure S29. The ^{13}C NMR spectrum obtained for **5.**

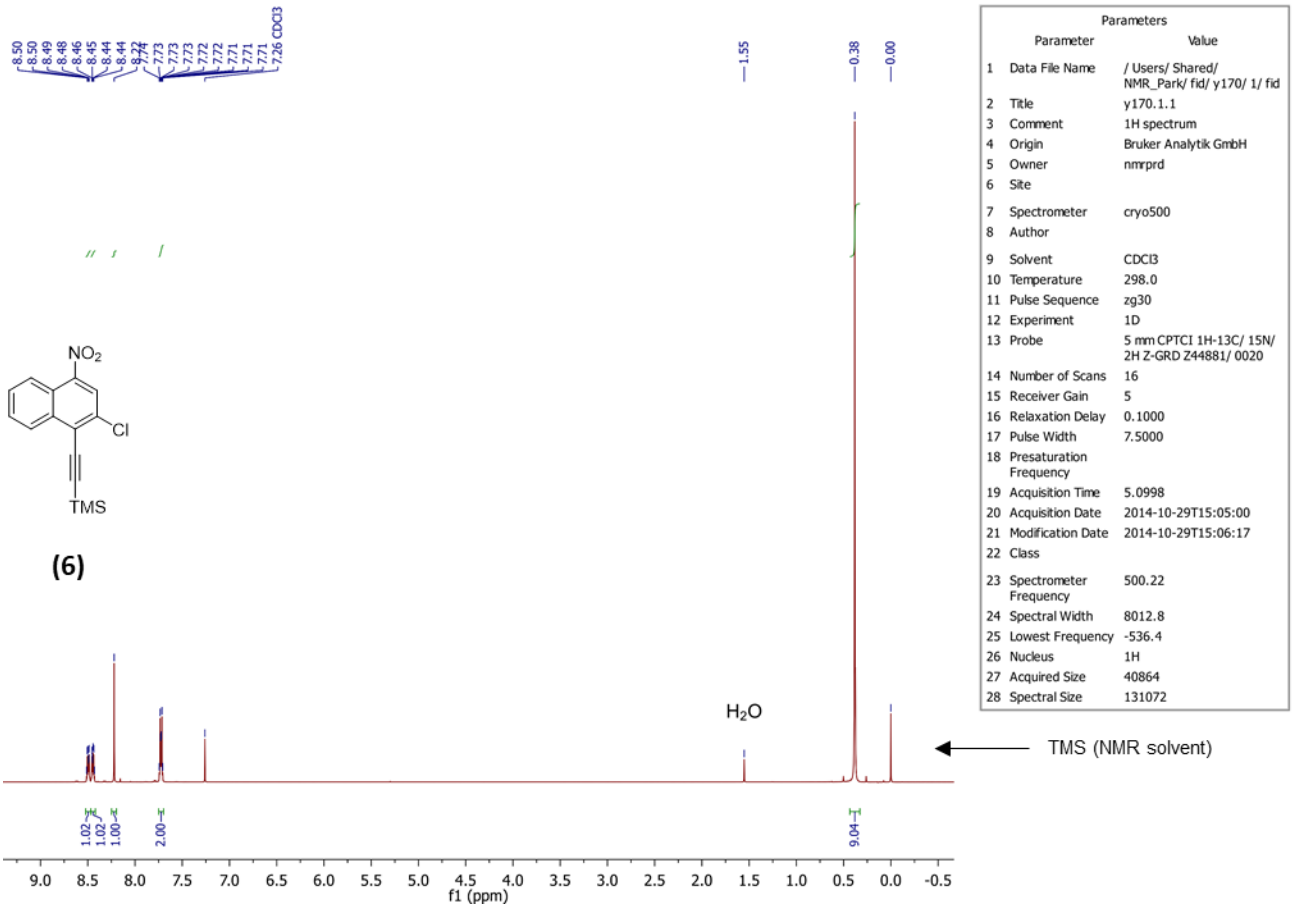

Parameters

	Parameter	Value
1	Data File Name	/ Users/ Shared/ NMR_Park/ fid/ y170/ 1/ fid
2	Title	y170.1.1
3	Comment	1H spectrum
4	Origin	Bruker Analytik GmbH
5	Owner	nmrprd
6	Site	
7	Spectrometer	cryo500
8	Author	
9	Solvent	CDCl3
10	Temperature	298.0
11	Pulse Sequence	zg30
12	Experiment	1D
13	Probe	5 mm CPTCI 1H-13C/ 15N/ 2H Z-GRD Z44881/ 0020
14	Number of Scans	16
15	Receiver Gain	5
16	Relaxation Delay	0.1000
17	Pulse Width	7.5000
18	Presaturation Frequency	
19	Acquisition Time	5.0998
20	Acquisition Date	2014-10-29T15:05:00
21	Modification Date	2014-10-29T15:06:17
22	Class	
23	Spectrometer Frequency	500.22
24	Spectral Width	8012.8
25	Lowest Frequency	-536.4
26	Nucleus	1H
27	Acquired Size	40864
28	Spectral Size	131072

Figure S30. The ^{1}H NMR spectrum obtained for **6.**

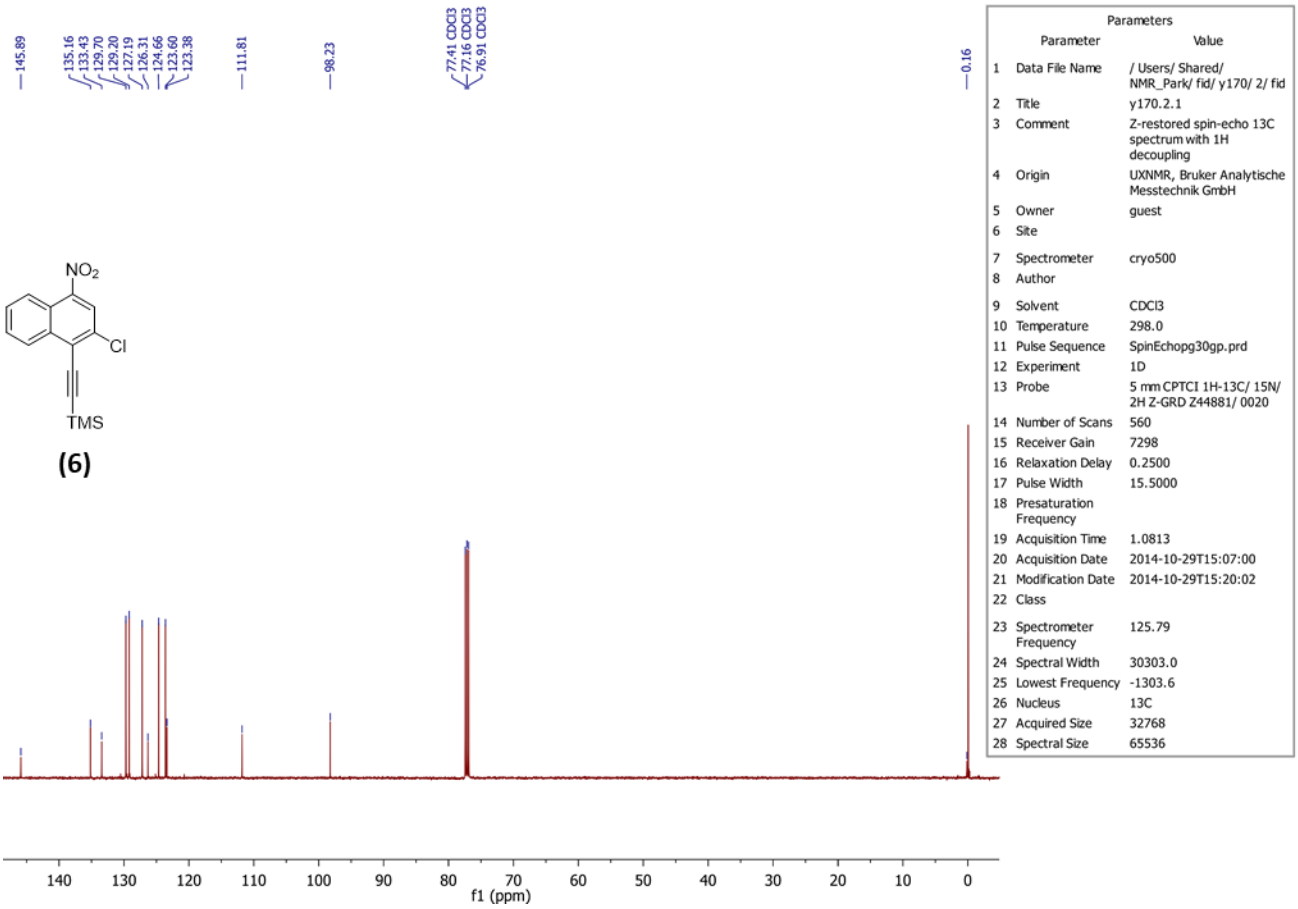

Parameters		
	Parameter	Value
1	Data File Name	/ Users/ Shared/ NMR_Park/ fid/ y170/ 2/ fid
2	Title	y170.2.1
3	Comment	Z-restored spin-echo 13C spectrum with 1H decoupling
4	Origin	UXNMR, Bruker Analytische Messtechnik GmbH
5	Owner	guest
6	Site	
7	Spectrometer	cryo500
8	Author	
9	Solvent	CDCl3
10	Temperature	298.0
11	Pulse Sequence	SpinEchopg30gp.prd
12	Experiment	1D
13	Probe	5 mm CPTCI 1H-13C/ 15N/ 2H Z-GRD Z44881/ 0020
14	Number of Scans	560
15	Receiver Gain	7298
16	Relaxation Delay	0.2500
17	Pulse Width	15.5000
18	Presaturation Frequency	
19	Acquisition Time	1.0813
20	Acquisition Date	2014-10-29T15:07:00
21	Modification Date	2014-10-29T15:20:02
22	Class	
23	Spectrometer Frequency	125.79
24	Spectral Width	30303.0
25	Lowest Frequency	-1303.6
26	Nucleus	13C
27	Acquired Size	32768
28	Spectral Size	65536

Figure S31. The ^{13}C NMR spectrum obtained for **6.**

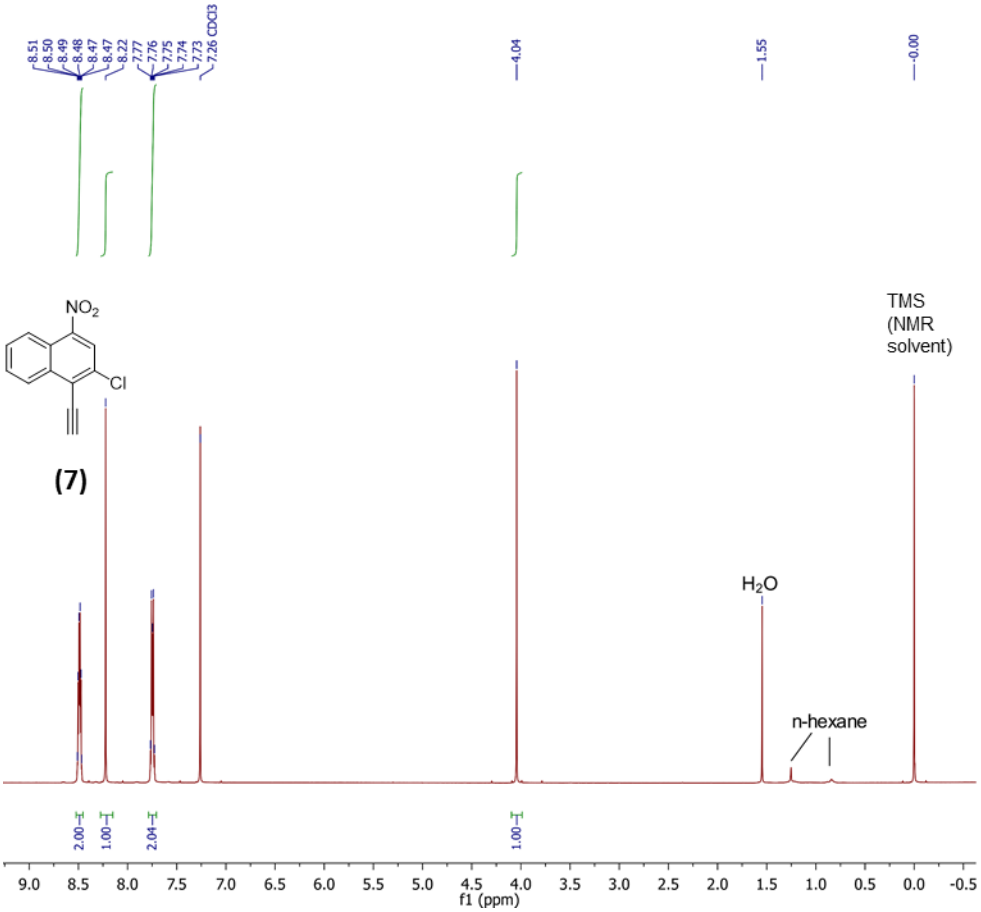

	Parameter	Value
1	Data File Name	C:/ Users/ Juhwan/ Desktop/ NMR/ 160815-noTMS/ 1/ fid
2	Title	160815-noTMS/ 1
3	Comment	1H spectrum
4	Origin	UXNMR, Bruker Analytische Messtechnik GmbH
5	Owner	guest
6	Site	
7	Spectrometer	cryo500
8	Author	
9	Solvent	CDCl3
10	Temperature	298.0
11	Pulse Sequence	zg30
12	Experiment	1D
13	Probe	5 mm CPTCI 1H-13C/ 15N/ 2H Z-GRD Z44881/ 0020
14	Number of Scans	32
15	Receiver Gain	6
16	Relaxation Delay	0.1000
17	Pulse Width	7.5000
18	Presaturation Frequency	
19	Acquisition Time	5.0998
20	Acquisition Date	2016-08-15T18:52:48
21	Modification Date	2016-08-15T20:54:45
22	Class	
23	Spectrometer Frequency	500.22
24	Spectral Width	8012.8
25	Lowest Frequency	-535.9
26	Nucleus	1H
27	Acquired Size	40864
28	Spectral Size	131072

Figure S32. The ^{1}H NMR spectrum obtained for **7.**

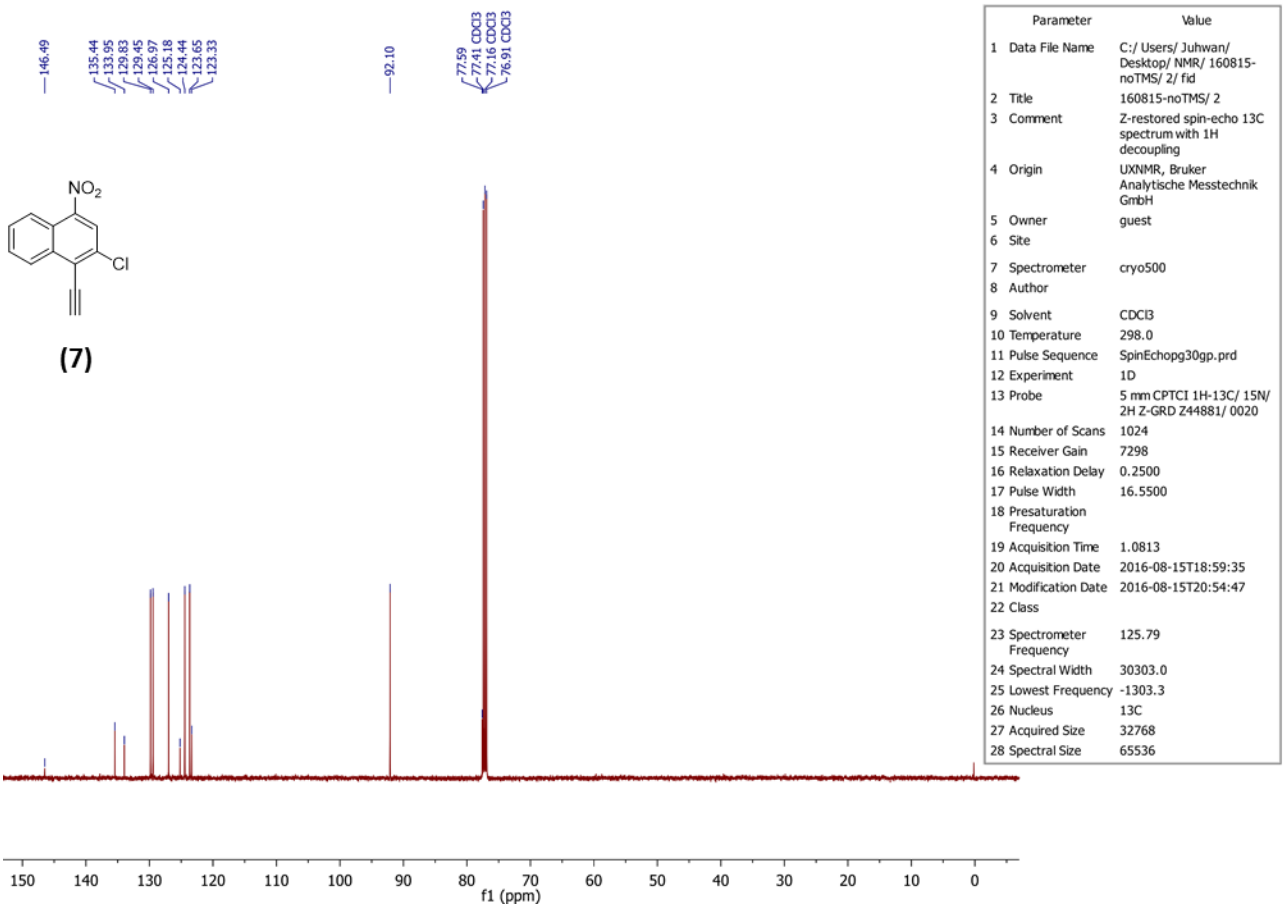

	Parameter	Value
1	Data File Name	C:/ Users/ Juhwan/ Desktop/ NMR/ 160815-noTMS/ 2/ fid
2	Title	160815-noTMS/ 2
3	Comment	Z-restored spin-echo 13C spectrum with 1H decoupling
4	Origin	UXNMR, Bruker Analytische Messtechnik GmbH
5	Owner	guest
6	Site	
7	Spectrometer	cryo500
8	Author	
9	Solvent	CDCl3
10	Temperature	298.0
11	Pulse Sequence	SpinEchopg30gp.prd
12	Experiment	1D
13	Probe	5 mm CPTCI 1H-13C/ 15N/ 2H Z-GRD Z44881/ 0020
14	Number of Scans	1024
15	Receiver Gain	7298
16	Relaxation Delay	0.2500
17	Pulse Width	16.5500
18	Presaturation Frequency	
19	Acquisition Time	1.0813
20	Acquisition Date	2016-08-15T18:59:35
21	Modification Date	2016-08-15T20:54:47
22	Class	
23	Spectrometer Frequency	125.79
24	Spectral Width	30303.0
25	Lowest Frequency	-1303.3
26	Nucleus	13C
27	Acquired Size	32768
28	Spectral Size	65536

Figure S33. The ^{13}C NMR spectrum obtained for **7.**

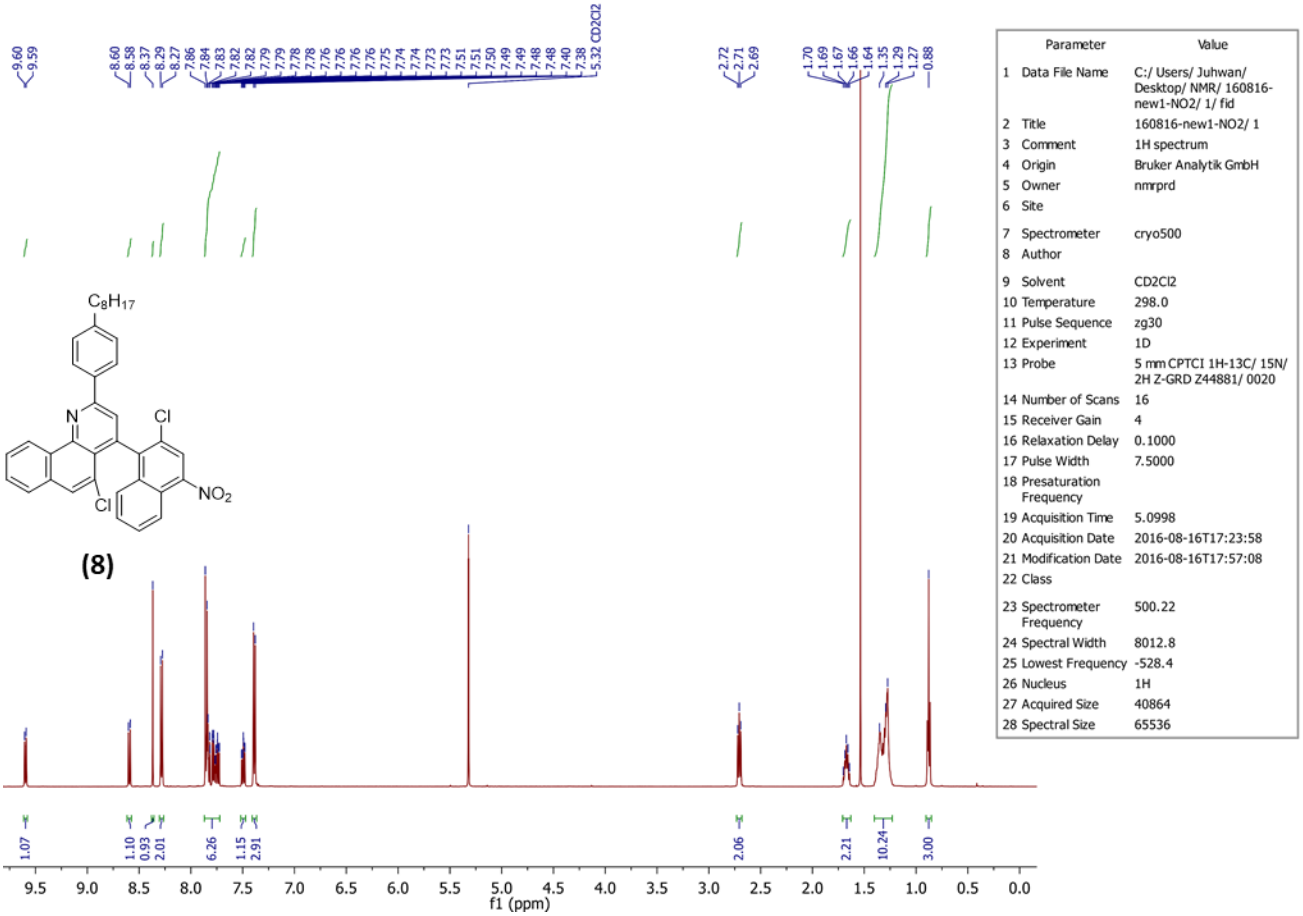

	Parameter	Value
1	Data File Name	C:/ Users/ Juhwan/ Desktop/ NMR/ 160816-new1-NO2/ 1/ fid
2	Title	160816-new1-NO2/ 1
3	Comment	1H spectrum
4	Origin	Bruker Analytik GmbH
5	Owner	nmrprd
6	Site	
7	Spectrometer	cryo500
8	Author	
9	Solvent	CD2Cl2
10	Temperature	298.0
11	Pulse Sequence	zg30
12	Experiment	1D
13	Probe	5 mm CPTCI 1H-13C/ 15N/ 2H Z-GRD Z44881/ 0020
14	Number of Scans	16
15	Receiver Gain	4
16	Relaxation Delay	0.1000
17	Pulse Width	7.5000
18	Presaturation Frequency	
19	Acquisition Time	5.0998
20	Acquisition Date	2016-08-16T17:23:58
21	Modification Date	2016-08-16T17:57:08
22	Class	
23	Spectrometer Frequency	500.22
24	Spectral Width	8012.8
25	Lowest Frequency	-528.4
26	Nucleus	1H
27	Acquired Size	40864
28	Spectral Size	65536

Figure S34. The ^{1}H NMR spectrum obtained for **8.**

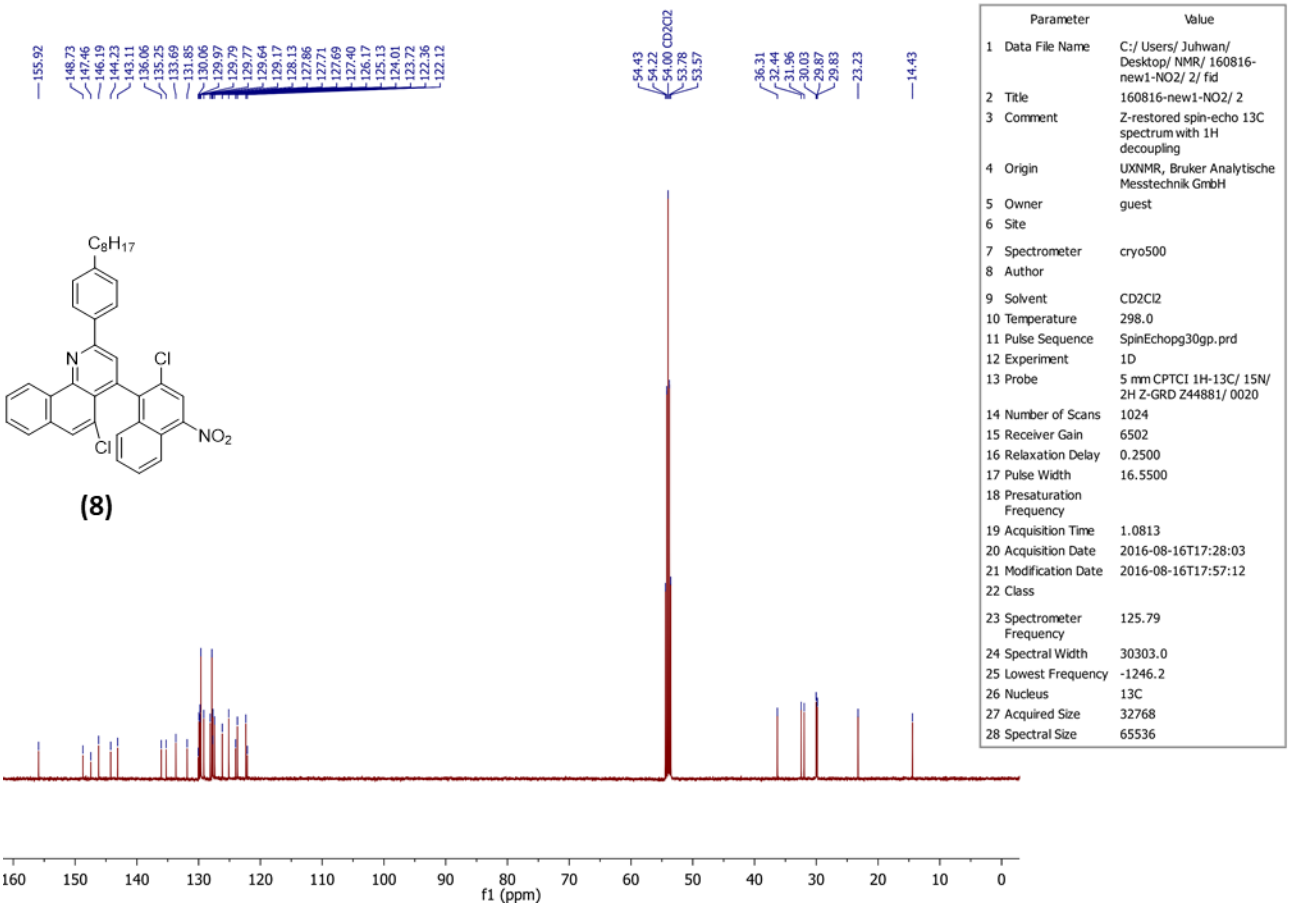

Figure S35. The ^{13}C NMR spectrum obtained for **8.**

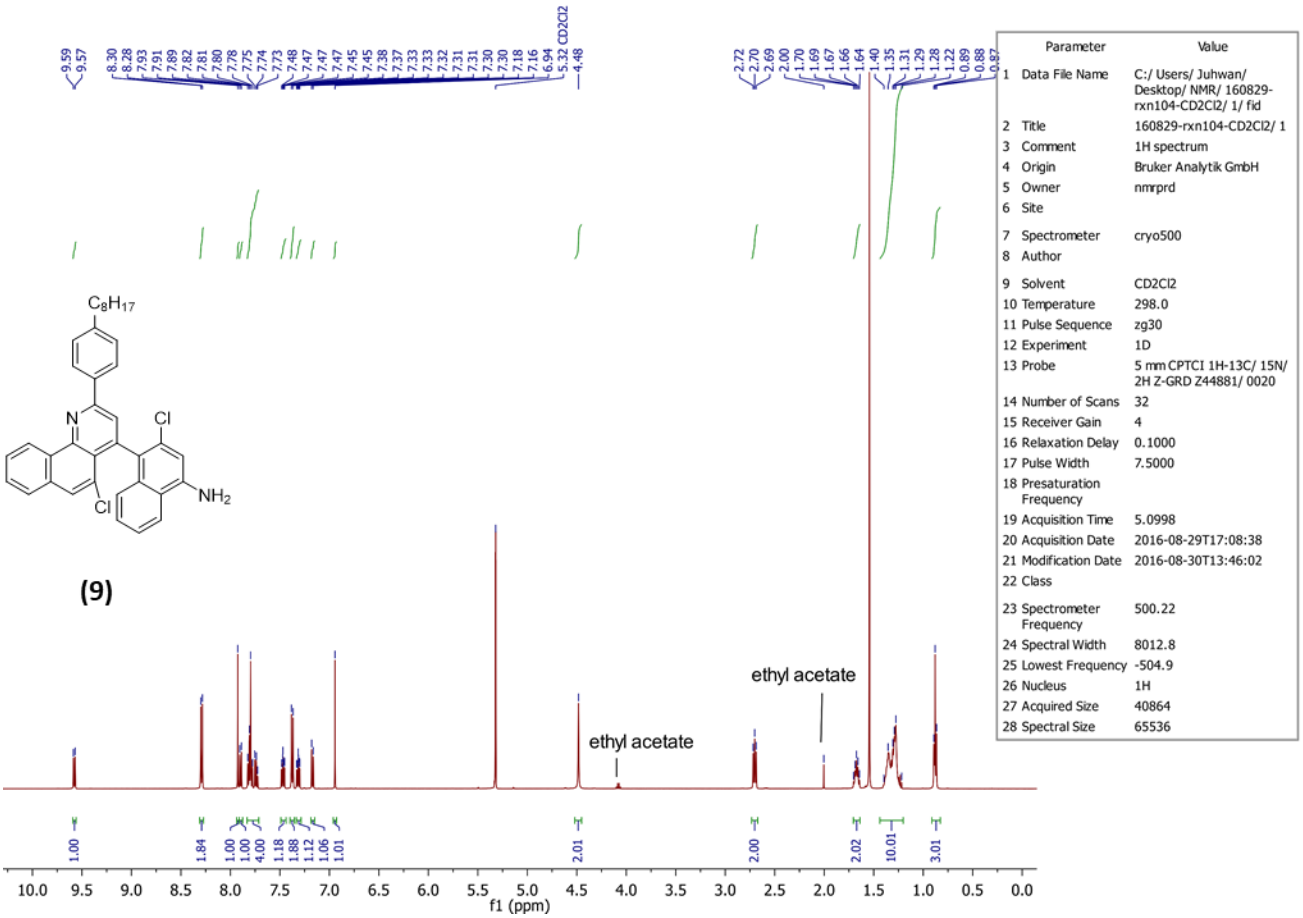

	Parameter	Value
1	Data File Name	C:/ Users/ Juhwan/ Desktop/ NMR/ 160829-rxn104-CD2Cl2/ 1/ fid
2	Title	160829-rxn104-CD2Cl2/ 1
3	Comment	1H spectrum
4	Origin	Bruker Analytik GmbH
5	Owner	nmrprd
6	Site	
7	Spectrometer	cryo500
8	Author	
9	Solvent	CD2Cl2
10	Temperature	298.0
11	Pulse Sequence	zg30
12	Experiment	1D
13	Probe	5 mm CPTCI 1H-13C/ 15N/ 2H Z-GRD Z44881/ 0020
14	Number of Scans	32
15	Receiver Gain	4
16	Relaxation Delay	0.1000
17	Pulse Width	7.5000
18	Presaturation Frequency	
19	Acquisition Time	5.0998
20	Acquisition Date	2016-08-29T17:08:38
21	Modification Date	2016-08-30T13:46:02
22	Class	
23	Spectrometer Frequency	500.22
24	Spectral Width	8012.8
25	Lowest Frequency	-504.9
26	Nucleus	1H
27	Acquired Size	40864
28	Spectral Size	65536

Figure S36. The ^{1}H NMR spectrum obtained for **9.**

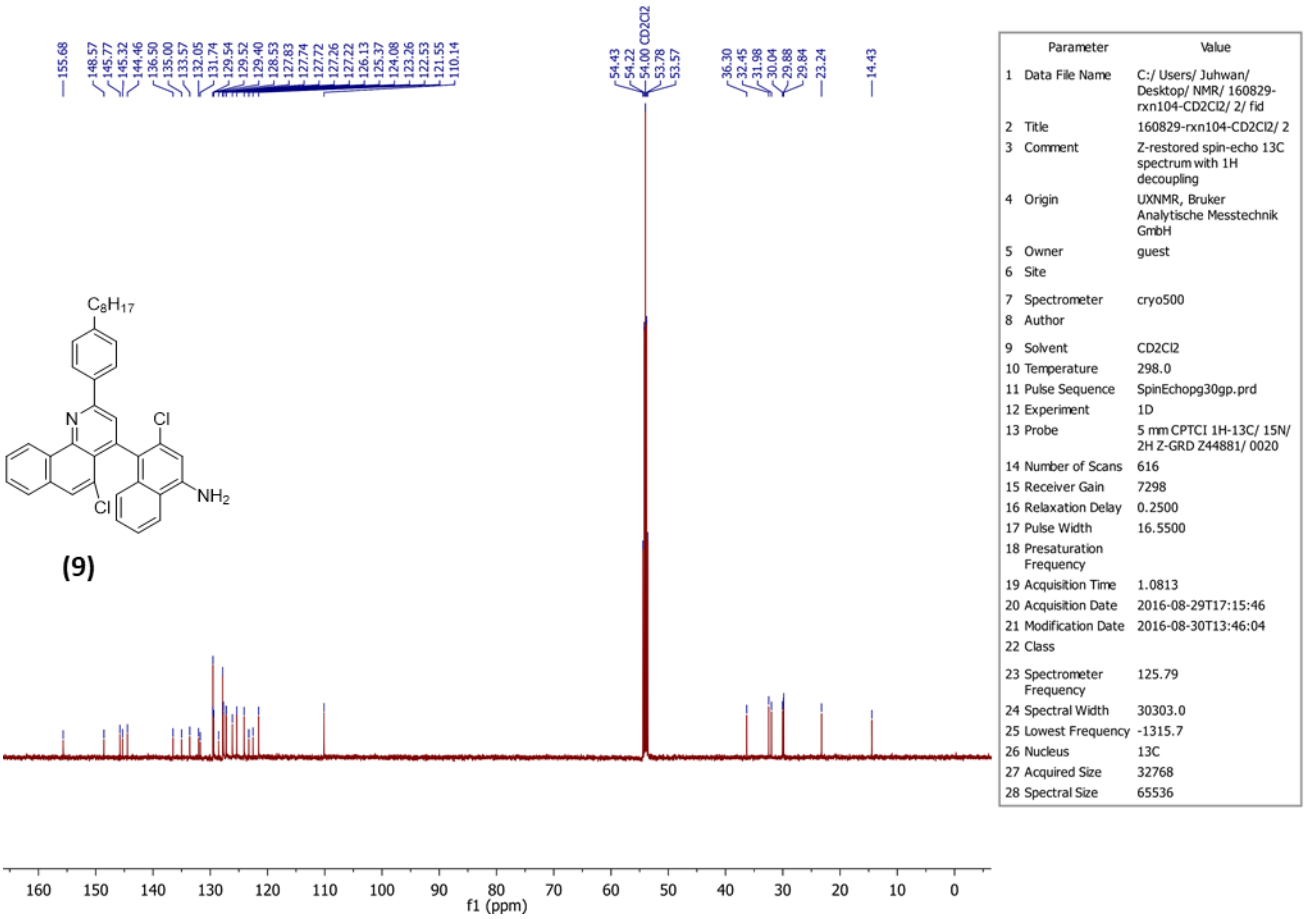

	Parameter	Value
1	Data File Name	C:/ Users/ Juhwan/ Desktop/ NMR/ 160829-rxn104-CD2Cl2/ 2/ fid
2	Title	160829-rxn104-CD2Cl2/ 2
3	Comment	Z-restored spin-echo 13C spectrum with 1H decoupling
4	Origin	UXNMR, Bruker Analytische Messtechnik GmbH
5	Owner	guest
6	Site	
7	Spectrometer	cryo500
8	Author	
9	Solvent	CD2Cl2
10	Temperature	298.0
11	Pulse Sequence	SpinEchopg30gp.prd
12	Experiment	1D
13	Probe	5 mm CPTCI 1H-13C/ 15N/ 2H Z-GRD Z44881/ 0020
14	Number of Scans	616
15	Receiver Gain	7298
16	Relaxation Delay	0.2500
17	Pulse Width	16.5500
18	Presaturation Frequency	
19	Acquisition Time	1.0813
20	Acquisition Date	2016-08-29T17:15:46
21	Modification Date	2016-08-30T13:46:04
22	Class	
23	Spectrometer Frequency	125.79
24	Spectral Width	30303.0
25	Lowest Frequency	-1315.7
26	Nucleus	13C
27	Acquired Size	32768
28	Spectral Size	65536

Figure S37. The ^{13}C NMR spectrum obtained for **9.**

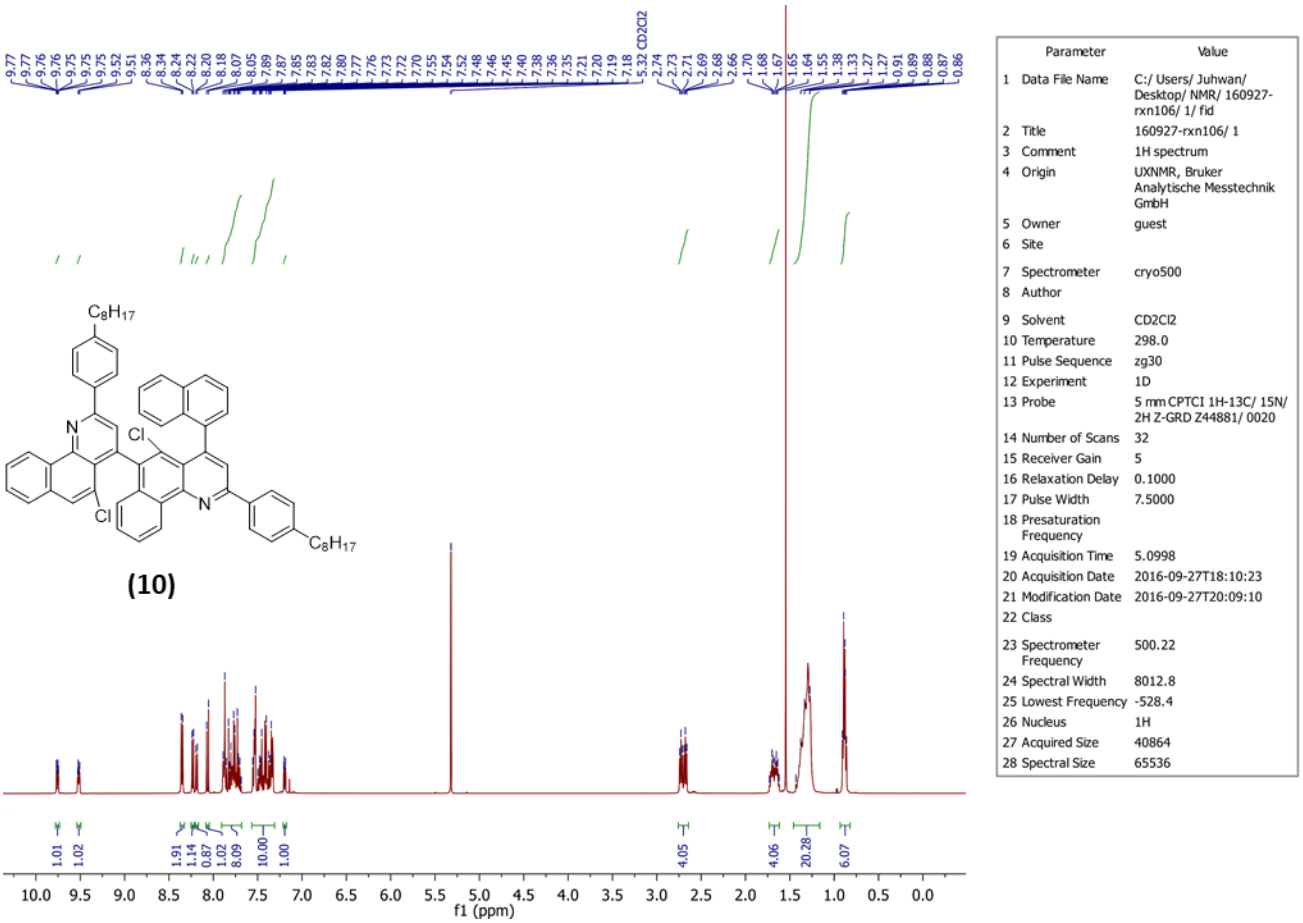

	Parameter	Value
1	Data File Name	C:/ Users/ Juhwan/ Desktop/ NMR/ 160927-rxn106/ 1/ fid
2	Title	160927-rxn106/ 1
3	Comment	1H spectrum
4	Origin	UXNMR, Bruker Analytische Messtechnik GmbH
5	Owner	guest
6	Site	
7	Spectrometer	cryo500
8	Author	
9	Solvent	CD2Cl2
10	Temperature	298.0
11	Pulse Sequence	zg30
12	Experiment	1D
13	Probe	5 mm CPTCI 1H-13C/ 15N/ 2H Z-GRD Z44881/ 0020
14	Number of Scans	32
15	Receiver Gain	5
16	Relaxation Delay	0.1000
17	Pulse Width	7.5000
18	Presaturation Frequency	
19	Acquisition Time	5.0998
20	Acquisition Date	2016-09-27T18:10:23
21	Modification Date	2016-09-27T20:09:10
22	Class	
23	Spectrometer Frequency	500.22
24	Spectral Width	8012.8
25	Lowest Frequency	-528.4
26	Nucleus	1H
27	Acquired Size	40864
28	Spectral Size	65536

Figure S38. The ^{1}H NMR spectrum obtained for **10.**

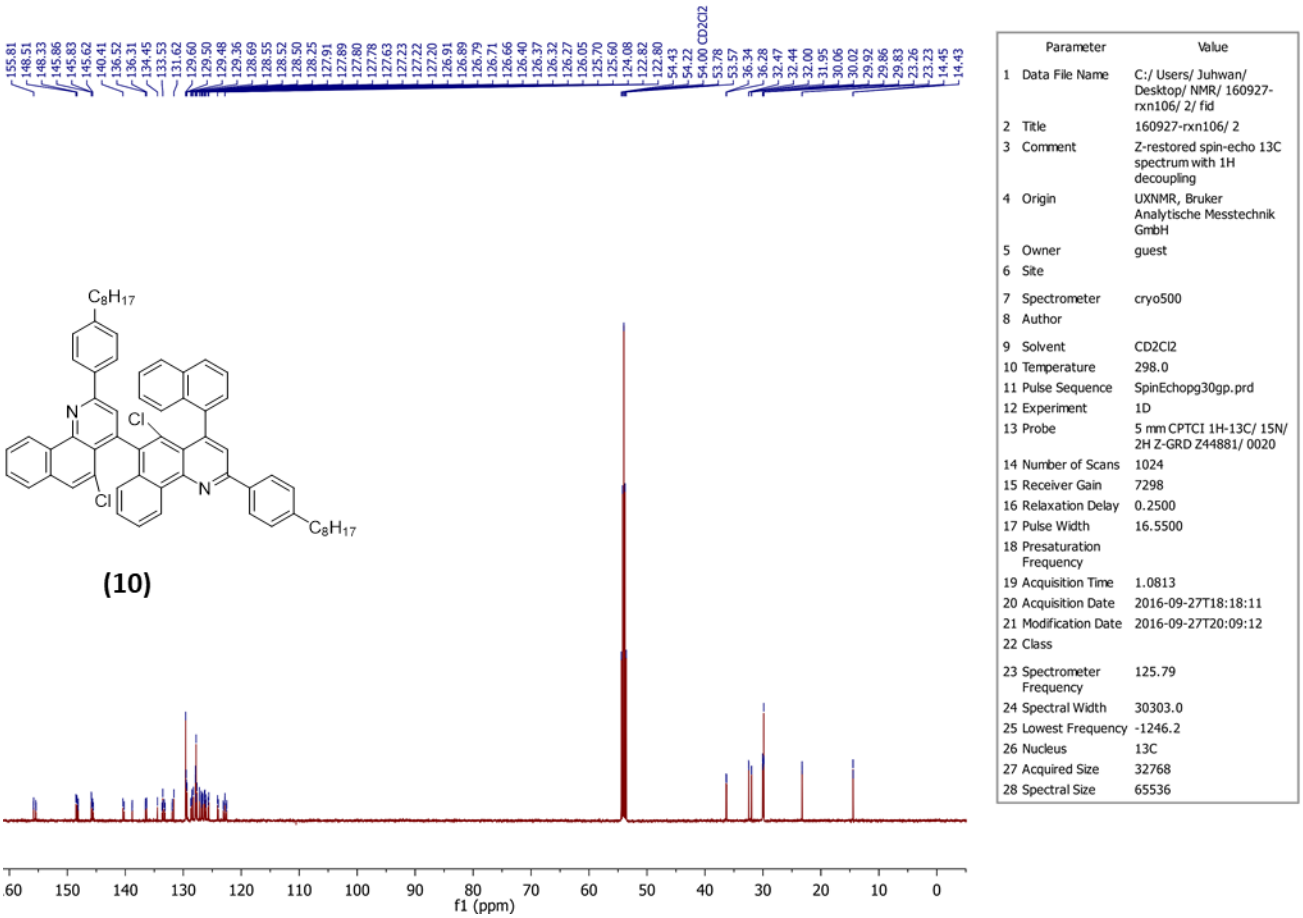

	Parameter	Value
1	Data File Name	C:/ Users/ Juhwan/ Desktop/ NMR/ 160927-rxn106/ 2/ fid
2	Title	160927-rxn106/ 2
3	Comment	Z-restored spin-echo 13C spectrum with 1H decoupling
4	Origin	UXNMR, Bruker Analytische Messtechnik GmbH
5	Owner	guest
6	Site	
7	Spectrometer	cryo500
8	Author	
9	Solvent	CD2Cl2
10	Temperature	298.0
11	Pulse Sequence	SpinEchopg30gp.prd
12	Experiment	1D
13	Probe	5 mm CPTCI 1H-13C/ 15N/ 2H Z-GRD Z44881/ 0020
14	Number of Scans	1024
15	Receiver Gain	7298
16	Relaxation Delay	0.2500
17	Pulse Width	16.5500
18	Presaturation Frequency	
19	Acquisition Time	1.0813
20	Acquisition Date	2016-09-27T18:18:11
21	Modification Date	2016-09-27T20:09:12
22	Class	
23	Spectrometer Frequency	125.79
24	Spectral Width	30303.0
25	Lowest Frequency	-1246.2
26	Nucleus	13C
27	Acquired Size	32768
28	Spectral Size	65536

Figure S39. The ^{13}C NMR spectrum obtained for **10.**

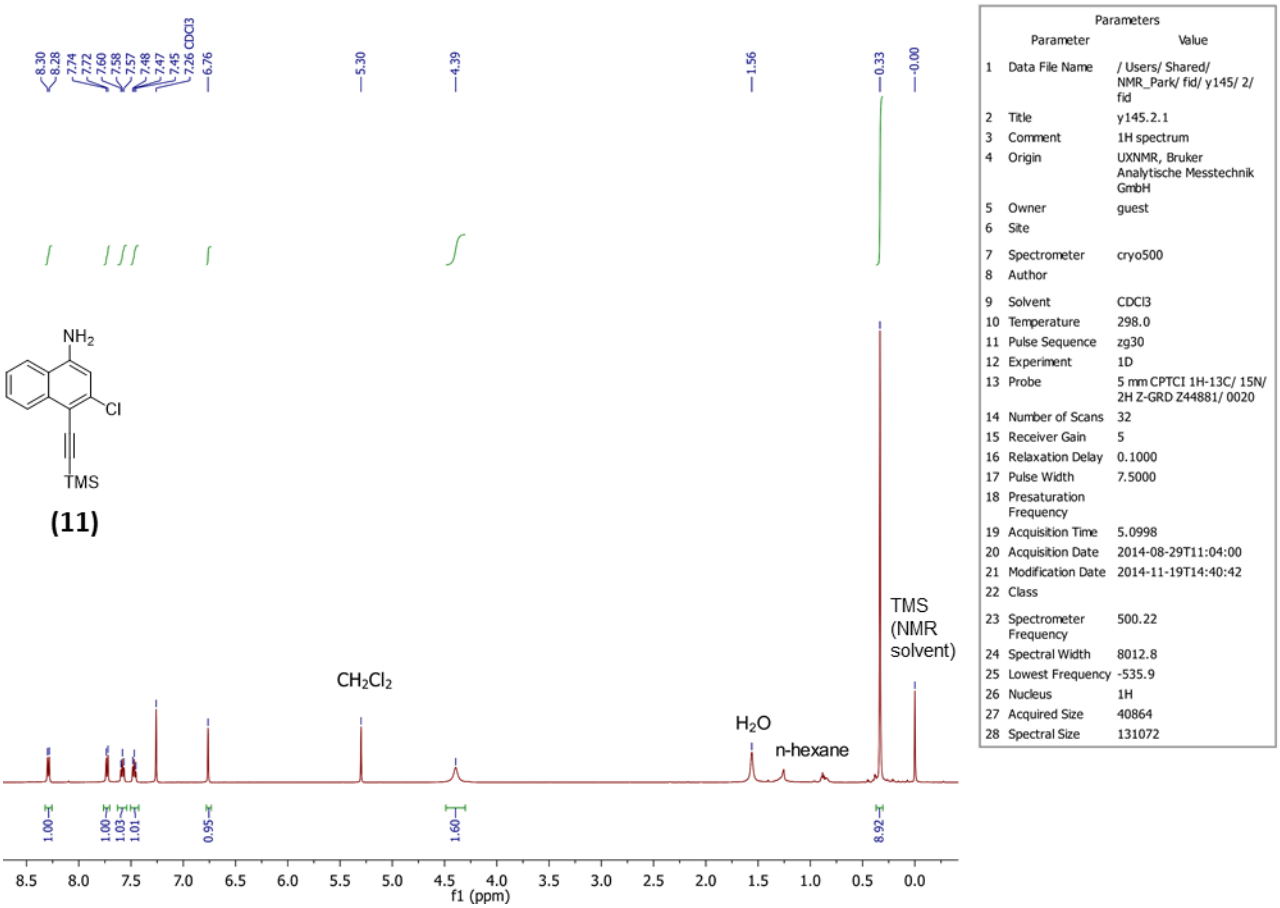

Parameters

	Parameter	Value
1	Data File Name	/ Users/ Shared/ NMR_Park/ fid/ y145/ 2/ fid
2	Title	y145.2.1
3	Comment	1H spectrum
4	Origin	UXNMR, Bruker Analytische Messtechnik GmbH
5	Owner	guest
6	Site	
7	Spectrometer	cryo500
8	Author	
9	Solvent	CDCl3
10	Temperature	298.0
11	Pulse Sequence	zg30
12	Experiment	1D
13	Probe	5 mm CPTCI 1H-13C/ 15N/ 2H Z-GRD Z44881/ 0020
14	Number of Scans	32
15	Receiver Gain	5
16	Relaxation Delay	0.1000
17	Pulse Width	7.5000
18	Presaturation Frequency	
19	Acquisition Time	5.0998
20	Acquisition Date	2014-08-29T11:04:00
21	Modification Date	2014-11-19T14:40:42
22	Class	
23	Spectrometer Frequency	500.22
24	Spectral Width	8012.8
25	Lowest Frequency	-535.9
26	Nucleus	1H
27	Acquired Size	40864
28	Spectral Size	131072

Figure S40. The ^{1}H NMR spectrum obtained for **11.**

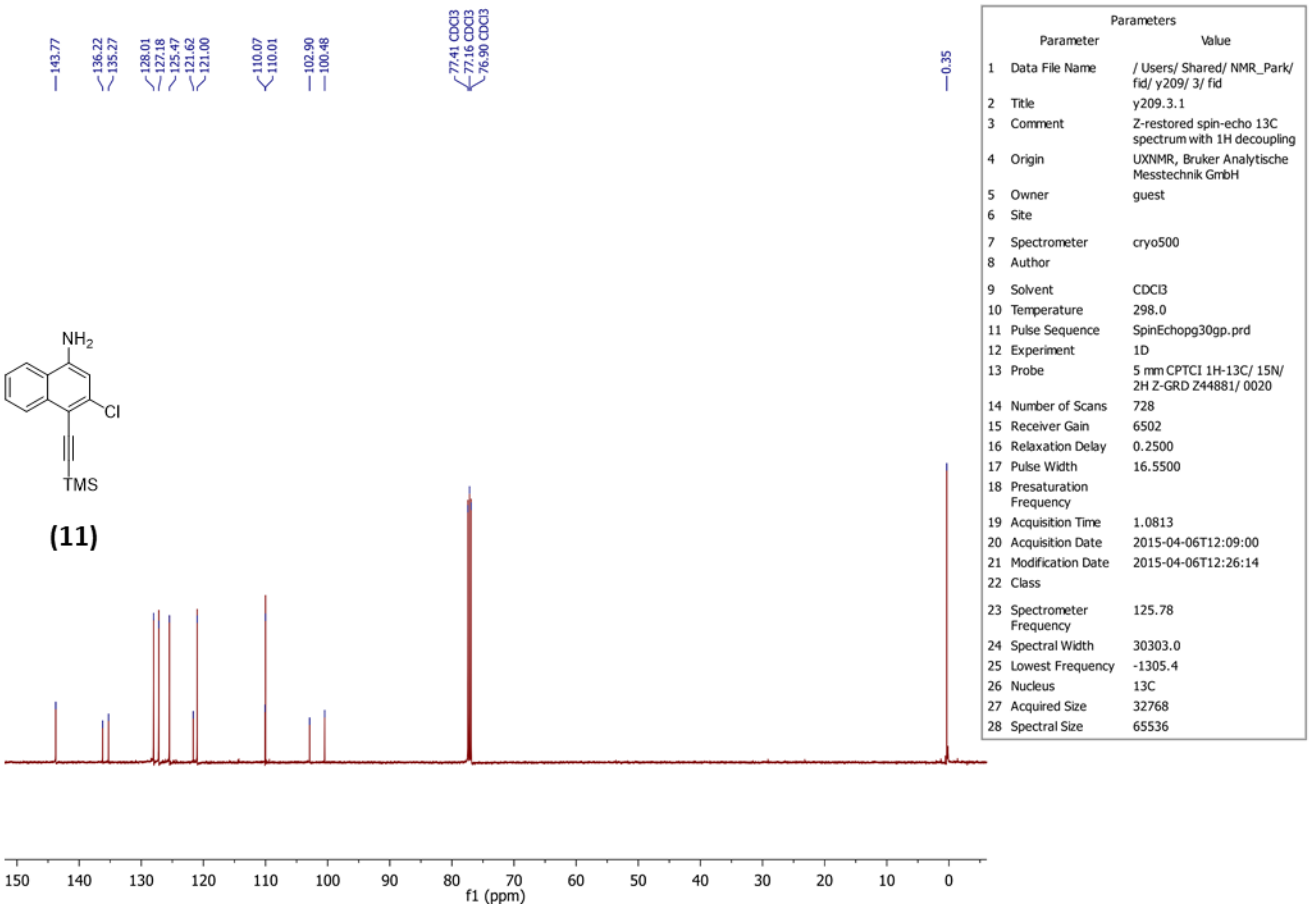

Parameters		
	Parameter	Value
1	Data File Name	/ Users/ Shared/ NMR_Park/ fid/ y209/ 3/ fid
2	Title	y209.3.1
3	Comment	Z-restored spin-echo 13C spectrum with 1H decoupling
4	Origin	UXNMR, Bruker Analytische Messtechnik GmbH
5	Owner	guest
6	Site	
7	Spectrometer	cryo500
8	Author	
9	Solvent	CDCl3
10	Temperature	298.0
11	Pulse Sequence	SpinEchopg30gp.prd
12	Experiment	1D
13	Probe	5 mm CPTCI 1H-13C/ 15N/ 2H Z-GRD Z44881/ 0020
14	Number of Scans	728
15	Receiver Gain	6502
16	Relaxation Delay	0.2500
17	Pulse Width	16.5500
18	Presaturation Frequency	
19	Acquisition Time	1.0813
20	Acquisition Date	2015-04-06T12:09:00
21	Modification Date	2015-04-06T12:26:14
22	Class	
23	Spectrometer Frequency	125.78
24	Spectral Width	30303.0
25	Lowest Frequency	-1305.4
26	Nucleus	13C
27	Acquired Size	32768
28	Spectral Size	65536

Figure S41. The ^{13}C NMR spectrum obtained for **11.**

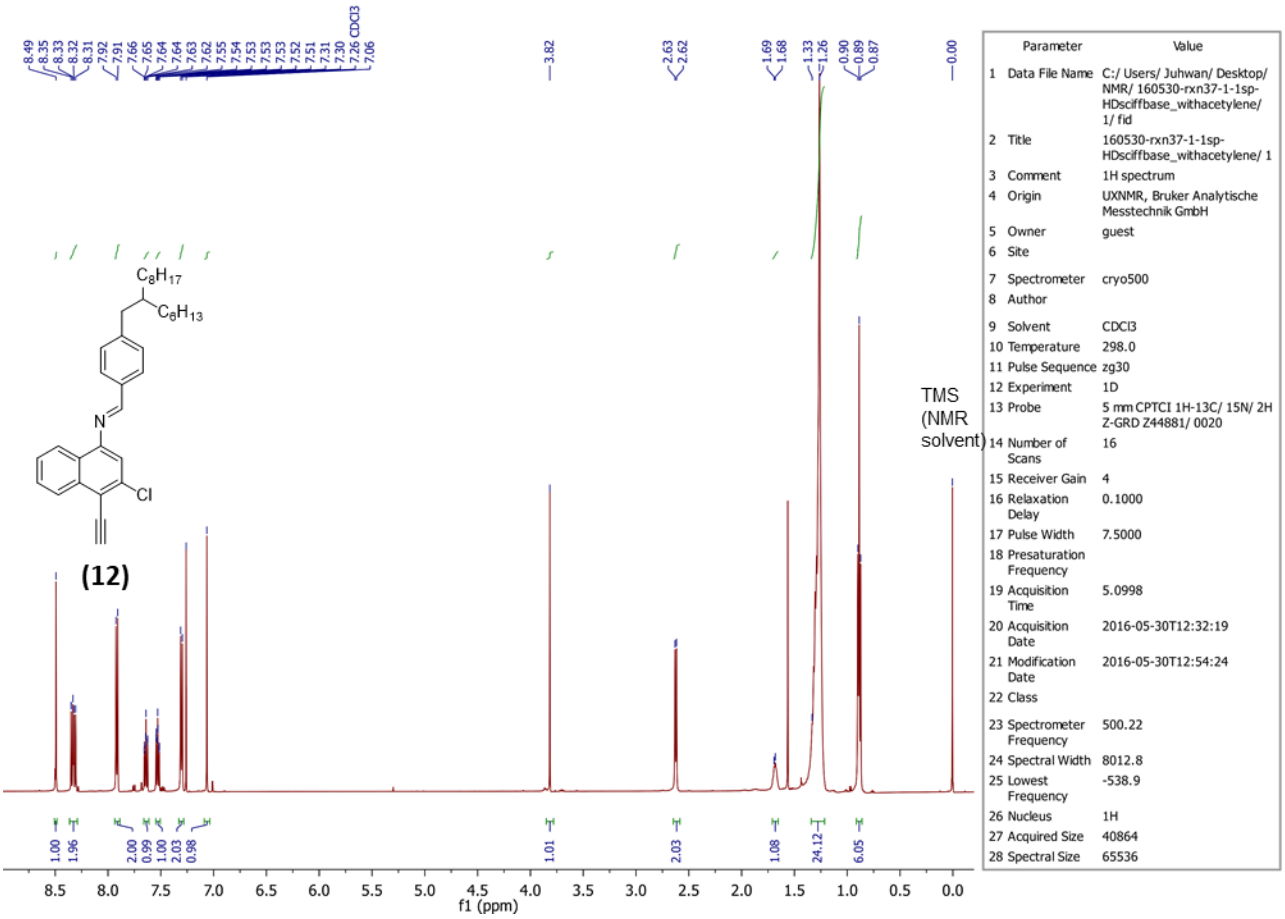

Figure S42. The ^{1}H NMR spectrum obtained for **12.**

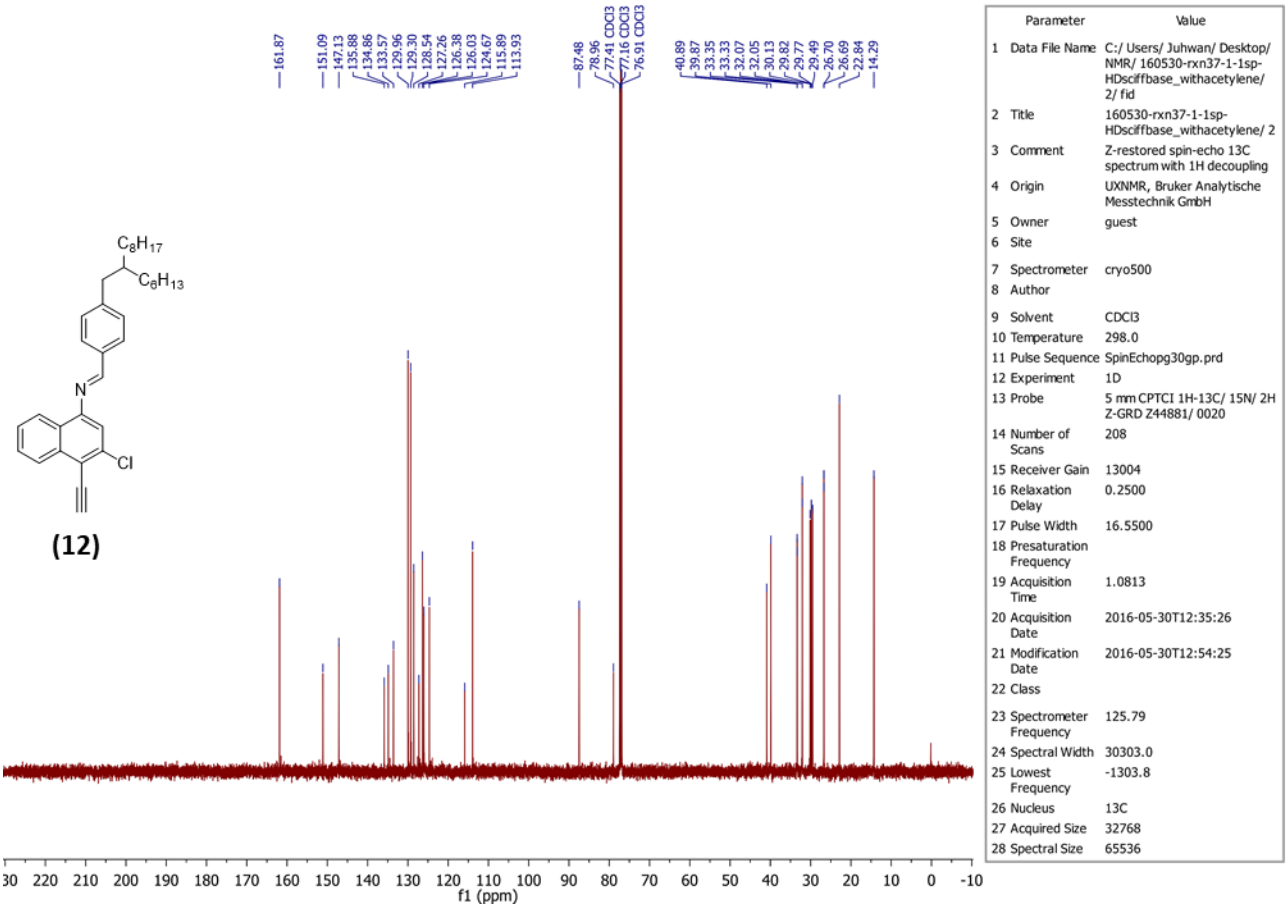

	Parameter	Value
1	Data File Name	C:/ Users/ Juhwan/ Desktop/ NMR/ 160530-rxn37-1-1sp-HDscIffbase_withacetylene/ 2/ fid
2	Title	160530-rxn37-1-1sp-HDscIffbase_withacetylene/ 2
3	Comment	Z-restored spin-echo 13C spectrum with 1H decoupling
4	Origin	UXNMR, Bruker Analytische Messtechnik GmbH
5	Owner	guest
6	Site	
7	Spectrometer	cryo500
8	Author	
9	Solvent	CDCl3
10	Temperature	298.0
11	Pulse Sequence	SpinEchopg30gp.prd
12	Experiment	1D
13	Probe	5 mm CPTCI 1H-13C/ 15N/ 2H Z-GRD Z44881/ 0020
14	Number of Scans	208
15	Receiver Gain	13004
16	Relaxation Delay	0.2500
17	Pulse Width	16.5500
18	Presaturation Frequency	
19	Acquisition Time	1.0813
20	Acquisition Date	2016-05-30T12:35:26
21	Modification Date	2016-05-30T12:54:25
22	Class	
23	Spectrometer Frequency	125.79
24	Spectral Width	30303.0
25	Lowest Frequency	-1303.8
26	Nucleus	13C
27	Acquired Size	32768
28	Spectral Size	65536

Figure S43. The ^{13}C NMR spectrum obtained for **12.**

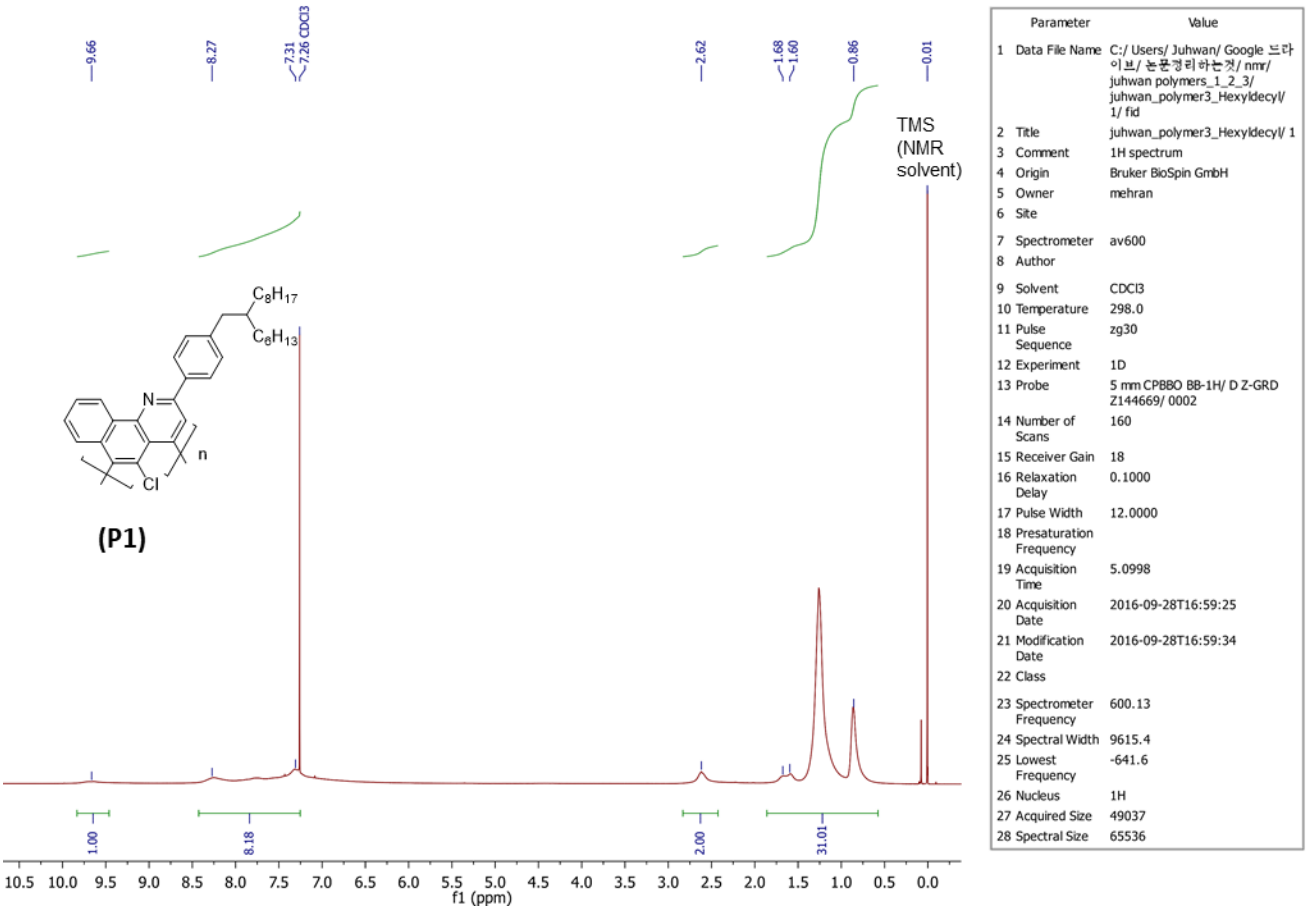

	Parameter	Value
1	Data File Name	C:/ Users/ Juhwan/ Google 드라이브/ 논문정리하는것/ nmr/ juhwan polymers_1_2_3/ juhwan_polymer3_Hexyldecyl/ 1/ fid
2	Title	juhwan_polymer3_Hexyldecyl/ 1
3	Comment	1H spectrum
4	Origin	Bruker BioSpin GmbH
5	Owner	mehran
6	Site	
7	Spectrometer	av600
8	Author	
9	Solvent	CDCl3
10	Temperature	298.0
11	Pulse Sequence	zg30
12	Experiment	1D
13	Probe	5 mm CPBBO BB-1H/ D Z-GRD Z144669/ 0002
14	Number of Scans	160
15	Receiver Gain	18
16	Relaxation Delay	0.1000
17	Pulse Width	12.0000
18	Presaturation Frequency	
19	Acquisition Time	5.0998
20	Acquisition Date	2016-09-28T16:59:25
21	Modification Date	2016-09-28T16:59:34
22	Class	
23	Spectrometer Frequency	600.13
24	Spectral Width	9615.4
25	Lowest Frequency	-641.6
26	Nucleus	1H
27	Acquired Size	49037
28	Spectral Size	65536

Figure S44. The ^{1}H NMR spectrum obtained for **P1.**